STUDIES OF CELLULAR QUIESCENCE IN PHOTOSYNTHETIC EUKARYOTES USING $CHLAMYDOMONAS\ REINHARDTII$ AS A REFERENCE MODEL

By

Chia-Hong Tsai

A DISSERTATION

Submitted to
Michigan State University
in partial fulfillment of the requirements
for the degree of

Plant Biology—Doctor of Philosophy

2014

ABSTRACT

STUDIES OF CELLULAR QUIESCENCE IN PHOTOSYNTHETIC EUKARYOTES USING CHLAMYDOMONAS REINHARDTII AS A REFERENCE MODEL

By

Chia-Hong Tsai

Cellular quiescence, defined as reversible cell cycle arrest, is a fundamental mechanism that organisms use to maintain tissue homeostasis or to overcome adverse conditions. In fact, most cells spend the majority of their life span in quiescence. Despite the importance, remarkably little is known about the regulation of quiescence. For photosynthetic organisms, it requires additional effort to maintain the state of quiescence, that is, to halt the photosynthetic machinery in a way that it can restart momentarily when conditions improve. Thus far, how plant cells exit quiescence, and regain competence to divide is entirely unknown.

The unicellular green alga *Chlamydomonas reinhardtii* was chosen as a reference model to study quiescence in photosynthetic eukaryotes for several reasons: First, quiescence and cell division can be discretely defined and controlled by manipulating nutrient availability. Second, microalgae tend to accumulate triacylglycerols only under the growth-limiting, quiescent state, which has long hampered efforts toward the efficient generation of biofuel feedstocks from microalgae. Mechanistic insights into the cellular quiescence hold great potential to uncouple this inverse relationship.

In this dissertation, I present the discovery of the protein Compromised Hydrolysis of Triacylglycerols 7 (CHT7), a repressor of cellular quiescence in Chlamydomonas that ensures the reversibility of quiescence. Moreover, I conducted comparative transcriptomics using the *cht7* mutant, which is unable to orderly progress from quiescence, to uncover the CHT7 regulon and transcriptional programs unique to the exit of quiescence. In addition, I found that lipid

droplets coordinate lipid and protein dynamics during quiescence and are important for the timeliness of quiescence exit. Overall, my findings make substantial progress towards the comprehensive understanding of cellular quiescence in photosynthetic cells, and promises to provide important insights into the regulation of cellular behavior in multicellular organisms as well.

TABLE OF CONTENTS

LIST OF TABLES	viii
LIST OF FIGURES	ix
CHAPTER 1 The Essence of Cellular Quiescence: a Literature Review	1
Introduction to quiescence	2
Mechanistic insights into cellular quiescence	
Signaling cascades that regulate the entry into quiescence	5
Microbes accumulate reducing compounds during quiescence	
Chlamydomonas reinhardtii as a reference model to study cellular quiescence	
Aims of the dissertation research.	
REFERENCES	
CHAPTER 2 Protein Compromised Hydrolysis of Triacylglycerols 7 (CHT7) A	Acts as a
Repressor of Cellular Quiescence in Chlamydomonas	
ABSTRACT	22
INTRODUCTION	23
MATERIALS AND METHODS	25
Strains, Genetic Analysis, and Growth Conditions	25
Generation of Antibodies, Immunoblotting, Subcellular Fractionation, and BN-I	PAGE26
Mutant Screen	
Confocal Microscopy and Construction of the CHT7-GFP Fusion	29
Phenotyping Assays	
Standard DNA and RNA Procedures	32
Illumina RNA Sequencing and Bioinformatics	37
RESULTS	
Isolation of compromised hydrolysis of triacylglycerols Mutants	39
CHT7 Encodes a CXC Domain DNA Binding Protein Present in the Nucleus	
Absence of CHT7 Affects the Exit from Quiescence but Not Cell Viability	
Absence of CHT7 Partially Derepresses Quiescence-Associated Transc	
Programs	
CHT7 Levels Remain Constant in Response to the N Supply, and CHT7 Is in	n a Large
Complex	
DISCUSSION	
REFERENCES	61
CHAPTER 3 Comparative Transcriptomic Analysis of Nitrogen Resupply	-induced
Modifications in a Chlamydomonas Quiescence-exit Mutant	71
ABSTRACT	72
INTRODUCTION	
MATERIALS AND METHODS	76
Strains and Growth Conditions	76

Illumina RNA Sequencing and Bioinformatics	76
Metabolite Measurements	76
Fatty Acid and Lipid Analysis	77
Standard RNA Techniques	78
RESULTS	79
Transcriptomes of Parental Line during different N regimes	79
Comparative Transcriptomics of cht7 and the Parental Line following N-resupp	
Metabolite Analyses Confirm the Effect of Transcriptional Changes on Lipid N	
	86
Two Classes of Lipases Affect TAG Accumulation in opposite ways	91
The cAMP-Dependent Protein Kinase A Pathway Is Involved in Quiescence Ex	
DISCUSSION	
The CHT7 regulon and possible influence of cAMP-PKA signaling	
REFERENCES	
CHAPTER 4 The Role of Lipid Droplet in Coordinating Lipid Dynamics to I	Ensure the
Reversibility of Cellular Quiescence in Chlamydomonas	106
ABSTRACT	
INTRODUCTION	108
MATERIALS AND METHODS	110
Strains and Growth Conditions	110
Fatty Acid and Lipid Analysis	110
Lipid Droplet Isolation, HDN-PAGE, and Co-immunoprecipitation	110
Immunofluorescence, Confocal, and Transmission Electronic Microscopy	
RESULTS	116
Transmission Electronic Microscopy Reveals Two Stages of LD Mobilization.	116
MLDP Recruits Different Sets of Proteins to LDs	
MLDP Is Indispensible for α-tubulin Association with LDs	122
The Surface of Lipid Droplet Has Unique Lipid and Fatty Acid Composition	124
Proper Surface Area of Lipid Droplet Ensures Orderly Progression out of Quies	scence.126
DISCUSSION	129
The role of lipid droplet in cellular quiescence	129
A new model of lipid droplet formation	131
REFERENCES	
CHAPTER 5 Conclusions and Perspectives	139
Regulatory processes by which CHT7 maintains the reversibility of quiescence	140
Potential modification of CHT7 activity during the entry into quiescence	
The regulatory logic underlying the CHT7 and Rb complexes to enable transition	ns between
quiescence and cell division	142
Functional interplay between CHT7 and other quiescence regulators	143
Lipid droplets are important for the survival during quiescence and for the quies	scence exit
	144
Biotechnological applications of cellular quiescence and lipid droplet biology	
REFERENCES	146

LIST OF TABLES

Table 2.1.	Oligonucleotide p	primers used in	this study	 	33

LIST OF FIGURES

Figure 1.1. Rb and cell cycle machinery
Figure 1.2. Suppression of irreversible routes
Figure 1.3. Chlamydomonas life cycles
Figure 2.1. Isolation of <i>cht</i> mutants
Figure 2.2. Phenotypes of <i>cht</i> 7
Figure 2.3. Meiotic progeny phenotyping and <i>cht7</i> complementation
Figure 2.4. CHT7 is a CXC domain-containing protein present in the nucleus
Figure 2.5. Nuclear localization of CHT7
Figure 2.6. Growth of <i>cht7</i> affected by different treatments
Figure 2.7. Growth, RNA, and protein of <i>cht7</i> affected by different treatments
Figure 2.8. Viability and colony formation of <i>cht7</i> during N deprivation50
Figure 2.9. Global gene expression comparison of N-replete and -deprived cells of PL <i>dw15</i> and <i>cht7</i>
Figure 2.10. Confirmation of transcriptional changes by qPCR and analysis of photosynthesis and flagellum-related genes
Figure 2.11. Abundance of CHT7 and hypothesis for CHT7 function

Figure 2.12. Immunodetection of CHT7 and 2D BN-SDS-PAGE
Figure 3.1. Cell Cycle and Proposed Functions for CHT7 in Quiescence
Figure 3.2. Experimental Design of RNA-Seq Experiments
Figure 3.3. Summary Scheme of Transcriptomic Analyses in the Parental Line80
Figure 3.4. Comparative Transcriptomics during Quiescence Exit83
Figure 3.5. Changes in Gene Expression and Metabolite of Tetrapyrrole Pathway and Peroxisomal Redox Homeostasis
Figure 3.6. Confirmation of Transcript Changes at Quiescence Exit
Figure 3.7. Changes in Gene Expression and Metabolite Levels Related to MGDG and Fatty Acid Syntheses
Figure 3.8. Detailed Lipid Analysis at Quiescence Exit
Figure 3.9. Changes in Gene Expression of Putative Lipases and β -oxidation93
Figure 3.10. Possible Role o cAMP-PKA Signaling in Quiescence Exit and Transcript Profiles of Related Genes
Figure 3.11. Fatty Acid Profiles of PKI-Treated Samples96
Figure 4.1. Ultrastructure of Cells during Quiescence Exit
Figure 4.2. Ultrastructure of Cells during Quiescence Exit
Figure 4.3. Ultrastructure of Cells during Ouiescence Exit

Figure 4.4. Lipid Droplet Localization and MLDP Complex Formation	122
Figure 4.5. Lipid Droplet Protein Quantification in the <i>MLDP</i> RNAi Lines	124
Figure 4.6. Lipid Profiles of Lipid Droplet Surface Membrane	126
Figure 4.7. Reduction of MLDP Affects Quiescence Exit, TAG Turnover, and Lipid Dro Homeostasis	-
Figure 4.8. A model for lipid droplet-specialized deacylation/reacylation cycle	131
Figure 4.9. A model for lipid droplet formation and deformation	133
Figure 5.1. Summary of pathways thought to control transitions between growth/division quiescence in <i>Chlamydomonas reinhardtii</i>	

CHAPTER 1

The Essence of Cellular Quiescence: a Literature Review

Introduction to quiescence

The eukaryotic cell cycle is divided into different phases: G1, characterized by cell growth; S, during which synthesis of DNA occurs; G2, when cells prepare for division; and M, which is defined by mitosis. Other types of cell cycle control, especially the ability to temporarily withdraw from cell division, are essential for survival during adverse conditions, particularly in unicellular organisms, and for the maintenance of tissue homeostasis in multicellular organisms. This non-dividing state is called quiescence, and is distinguished from senescence or terminal differentiation by its reversibility (Gray et al., 2004; Valcourt et al., 2012). Whether prokaryotic or eukaryotic, unicellular or multicellular, virtually all cells are capable of entering quiescence in order to ensure the continuity of life. Nevertheless, the signals that promote quiescence vary across different cell types. For example, bacteria and yeast enter stationary phase when their carbon source is exhausted or in response to the deprivation of specific nutrients, e.g. nitrogen (N), sulfur, or phosphate (Thevelein et al., 2000). In mammals, quiescence is seldom induced by starvation because to maintain homeostasis cells are continuously supplied with glucose, amino acids and other nutrients provided by nearby capillaries (Longo, 1999). Cells such as fibroblasts, lymphocytes, and stem cells, typically quiesce, unless they are exposed to proliferative signaling molecules or situational cues (Valcourt et al., 2012). Quiescence also occurs in the context of development. In the Arabidopsis root meristem, stem cells surround a small group of organizing cells, referred to as the quiescent center (Wildwater et al., 2005). Despite these differences, many quiescent responses appear to be universal, including the changes in transcriptional and translational regulations, in metabolic states, as well as in other physiological aspects (Gray et al., 2004; Wu et al., 2004; Coller et al., 2006; Miller et al., 2010; Valcourt et al., 2012; Gifford et al., 2013). Quiescence is relevant to many fields of study ranging from stem cell and cancer research

to stress biology in photosynthetic organisms. A more in-depth understanding of the conserved mechanisms underlying the entry into, maintenance of, and exit from quiescence promises to provide important insights into the developments of anticancer therapies and the optimization of algal biofuel feedstocks. This chapter will summarize current knowledge about quiescence, with a special focus on unicellular organism as it is more closely related to my work on *Chlamydomonas reinhardtii*.

Mechanistic insights into cellular quiescence

Cell cycle arrest and reversibility comprises cellular quiescence. On the molecular level, cell cycle arrest is established through a complex interplay between proteins. The human Rb tumor suppressor protein and its homologs, also referred to as pocket proteins, are components of multiprotein transcriptional complexes in most eukaryotic organisms with fundamental roles in regulating cell cycle progression (Figure 1.1) (Knudsen and Knudsen, 2006; Burkhart and Sage, 2008). Briefly, Rb interacts with DNA-binding proteins such as E2F and DP to repress gene expressions required for cell cycle progression. Acute mutation of Rb gene function in mouse embryo fibroblasts is sufficient to reverse cell cycle arrest (Sage et al., 2003). The transition from quiescence is stimulated by mitogenic signals, following through the sequestration of cyclindependent kinase (CDK) inhibitors p21 and p27, and the activation of CDK4 and CDK6, allowing consecutive phosphorylation of Rb. The hyperphosphorylated Rb dissociates from E2F transcription factors and releases them to activate respective genes (DeGregori et al., 1995). Although yeast cells are lacking in Rb and E2F proteins (Ohtani and Nevins, 1994), they employ a similar regulatory process. A cell size regulator WHI5 inhibits the G1/S transcription by binding to the transcription factors SBF/MBF on the cis-regulatory elements. This inhibition can

be reversed by CDK-dependent phosphorylation of WHI5 when the CDK inhibitor SIC1 is withdrawn (Costanzo et al., 2004). Deletion of WHI5 promotes cell cycle progression without the upstream activation of SBF/MBF.

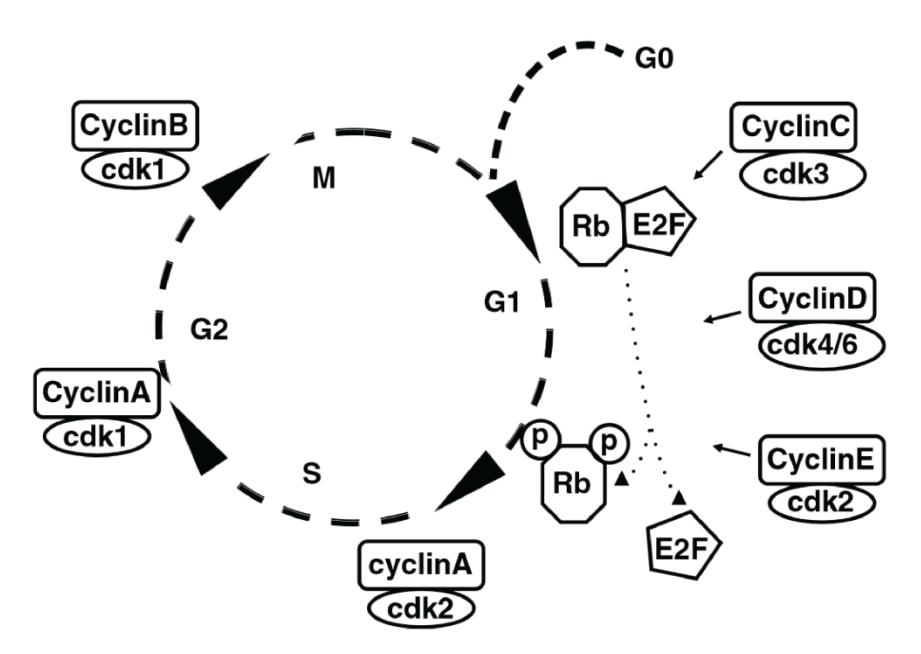


Figure 1.1. Rb and cell cycle machinery. Rb and Rb-p represent the unphosphorylated and the phosphorylated forms of the retinoblastoma protein. In G0 and early G1, Rb physically associates with E2F factors and blocks their transactivation domain. In late G1, Rb-p releases E2F, allowing the expression of genes that encode products necessary for S-phase progression (Giacinti and Giordano, 2006).

Reversibility is the defining nature of cellular quiescence. In contrast to other arrested states such as senescence, apoptosis, and terminal differentiation, only in quiescence this block to proliferation can be reversed (Coller, 2011). One mechanism by which the reversibility is insured is the suppression of irreversible cell fates. Transcriptional profiling of quiescent human fibroblasts uncovered the regulation of genes that inhibit apoptosis or cellular differentiations (Coller et al., 2006). Later on, it became known that a transcriptional repressor HES1 blocks the alternative routes to premature senescence and myogenic differentiation in quiescent fibroblasts by modifying histone tails and thus affecting chromatin conformation (Sang et al., 2008; Sang

and Coller, 2009). In some cancers, the HES1 pathway is hijacked, thus allowing cancer cells to escape from irreversible cell cycle arrest and undergo tumorigenesis (Figure 1.2).

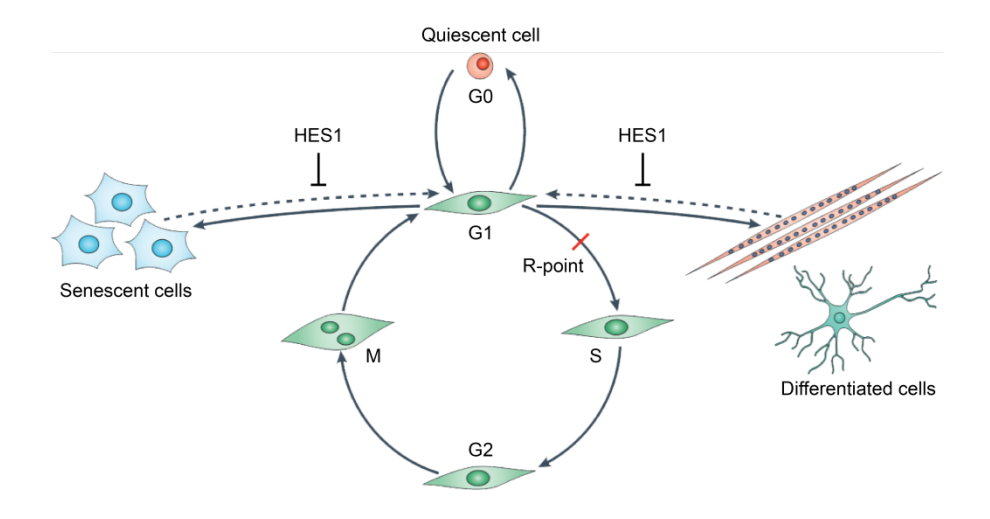


Figure 1.2. Suppression of irreversible routes. Irreversible routes to senescence and terminal differentiation are suppressed by HES1 in quiescent cell. (Modified from Cheung and Rando, 2013).

Signaling cascades that regulate the entry into quiescence

The immunosuppressant rapamycin has provided a great tool in the discovery of the mechanisms that control the entry into quiescence. Treatment of rapamycin inhibits growth and division in both yeast and mammalian cells. Rapamycin-treated cells acquire many features characteristic of quiescence: G1 phase DNA content, repression of ribosomal protein genes and induction of genes encoding protein chaperones, reduced rates of protein synthesis, and high levels of autophagy (Barbet et al., 1996; Noda and Ohsumi, 1998). In addition, rapamycin-treated yeast accumulates storage compounds such as glycogen and trehalose. The target of rapamycin, namely TOR, and its directly and indirectly interacting proteins translate extracellular nutrient signals into information that helps decide the extent of cell growth (Rohde and Cardenas, 2004). When nutrients are abundant, TOR kinases, in association with its cooperating enzymes,

phosphorylate downstream targets that enhance protein synthesis and cell growth. When the cellular AMP/ATP ratio is high or amino acids are scarce, the TOR pathway is suppressed, thus, allowing the activation of autophagy to reclaim metabolites, to spare ATP, and to eliminate degraded proteins and organelles. In yeast, there are two TOR kinase proteins, TOR1 and TOR2, but only the TOR1 complex is sensitive to rapamycin. Disruption of the TOR1 complex mimics rapamycin treatment and a quiescence-like state (Loewith et al., 2002). Therefore, the TOR pathway has generally been considered to be a negative regulator of the transition into quiescence. The TOR kinases were first identified in *Saccharomyces cerevisiae*, and are highly conserved in animals and plants (Zhang et al., 2000; Russell et al., 2011; Xiong et al., 2013). Components of the TOR pathway have also been identified in Chlamydomonas by screening mutants insensitive to rapamycin as well as by in silico studies (Perez-Perez et al., 2010). Intriguingly, the growth of Chlamydomonas cells is not completely abolished by rapamycin as is the case for yeast. Even using a saturated concentration of rapamycin, Chlamydomonas cells can still grow albeit they take twice as long to reach the same density.

The cyclic AMP (cAMP)-dependent protein kinase A (PKA) pathway is well-studied in yeast, and in spite of some unanswered questions, it is presumably another element that prevents the entry into quiescence. The enzyme adenylyl cyclase catalyzes the conversion of ATP into cAMP and pyrophosphate. When cAMP concentration increases, for example in the presence of high glucose, cAMP binds to the inhibitory domains of PKA which results in the dissociation and activation of the catalytic domains. Yeast cells deficient in basal cAMP synthesis gradually enter the quiescent state; this can be rescued by providing external cAMP (Boutelet et al., 1985; van Aelst et al., 1991). Subcellular localization of PKA in yeast is under nutritional control, as it shuttles from nucleus to cytoplasm when entering quiescence (Griffioen et al., 2000). The

nuclear targets of PKA are the nutrient-regulated transcription factors MSN2 and MSN4 (Smith et al., 1998; Beck and Hall, 1999). Interestingly, PKA activity is dispensable in the *msn2 msn4* double mutant, suggesting that in proliferative cells, MSN2 and MSN4 counteract PKA-dependent growth by stimulating gene expression that inhibits growth, consistent with the fact that MSN2/MSN4 activity is required for expression of YAK1, previously shown to antagonize PKA-dependent growth (Garrett and Broach, 1989). MSN2 and MSN4 are also targets of the TOR pathway (Beck and Hall, 1999), providing evidence that signaling pathways thought to prevent entry into quiescence comprise an interconnecting network.

Activators of quiescence are inherently required for the establishment of viable quiescent cells; without them, cells frequently die rapidly after the transition. The yeast protein kinase C encoded by *PKC1* is one such regulator. The *pkc1* mutant undergoes cell lysis on carbon or N deprivation due to a deficiency in cell wall construction—a unique feature of quiescent yeast—and thus is vulnerable to osmotic changes (Levin and Bartlett-Heubusch, 1992). A mitogenactivated protein (MAP) kinase cascade involving the MAP kinase MPK1 is thought to mediate the signaling by PKC1. Mutants defective in MPK1, and its targets MKK1, MKK2 (MAP kinase kinase), and BCK1 (encoding MAP kinase kinase kinase) all show a similar phenotype as *pkc1* (Lee and Levin, 1992; Irie et al., 1993; Lee et al., 1993). The PKC1 pathway is transiently activated by the inhibition of TOR to remodel the cell surface and to ensure viability during the entry into quiescence. The *pkc1* and the related mutants in the pathway die in rapamycincontaining, nutrient-replete medium, therefore, the PKC1 pathway seems not act as a nutrient sensor (Krause and Gray, 2002).

Microbes accumulate reducing compounds during quiescence

A myriad of metabolic adjustments takes place to meet the changing demands of cells during quiescence (Gray et al., 2004; Valcourt et al., 2012). The rule of thumb is: a lower anabolism such as the shift away from TCA (tricarboxylic acid) cycle to protect against the superoxide produced by oxidative phosphorylation, and a higher catabolism that includes, for example, the increased abundance of glycolysis enzymes. A remarkable exception in microbial quiescence is the accumulation of carbon stores, even though the chemical structure of the storage differs. Quiescent yeast cells accumulate glycogen, a disaccharide trehalose, and triacylglycerols (TAGs) as the main forms of metabolizable carbon storage (Lillie and Pringle, 1980; Hosaka and Yamashita, 1984). The bacterial pathogen Vibrio cholera produces glycogen when living in nutrient-poor aquatic environments (Bourassa and Camilli, 2009). Mycobacterium tuberculosis stores TAGs and wax esters in large cytosolic inclusions in preparation for a dormancy-like state (Daniel et al., 2004; Sirakova et al., 2012). For bacteria living in soil and the rhizosphere, intracellular deposition of polyhydroxyalkanoates, a group of bioplastic carbon polymers, is critical for enduring suboptimal conditions (Kadouri et al., 2005). In addition, C. reinhardtii accumulates starch granules and TAGs during starvation for N, phosphorus, sulfur, zinc or iron, and in response to high salt or heat stress (Hu et al., 2008; Matthew et al., 2009; Kropat et al., 2011; Siaut et al., 2011; Hemme et al., 2014).

The importance of storage compounds to quiescence is an unresolved question. In yeast, trehalose and glycogen decrease slowly with time during long-term stationary phase. However, these carbohydrates are probably not metabolized for energy, at least not during quiescence, as they do not always correlate with viability (Sillje et al., 1999). The primary function of trehalose is thought to protect proteins from damage by oxygen radicals, and to act as a chemical chaperone to assist protein folding (Singer and Lindquist, 1998; Benaroudj et al., 2001). Mutants

unable to synthesize trehalose exit quiescence much more slowly (Sillje et al., 1999; Shi et al., 2010). Hydrolyzing one molecule of trehalose releases two molecules of glucose, whereas cleavage of a single glycosidic bond in glycogen produces just one, making trehalose the obvious carbohydrate of choice to fuel quiescence exit. However, trehalose is more osmotically active than glycogen, which could be a problem. TAG has the highest energy output per weight of material in cellular metabolism, and is rapidly hydrolyzed when supplemented with fresh medium (Kurat et al., 2006). TGL3 and TGL4 are the major TAG lipases in yeast; the tgl3 tgl4 double mutant completely loses lipolytic activity and exhibits delayed daughter cell formation and cell cycle progression (Kurat et al., 2006; Kurat et al., 2009). In Chlamydomonas, TAGs accumulated during quiescence function at least in part as energy sink to accommodate the reducing power generated by the photosynthetic machinery (Li et al., 2012). A mutant producing less than half of the wild-type TAG content loses viability during the N deprivation-induced quiescence, likely due to a detrimental overreduction of the photosynthetic electron transport chain. It bleaches during N deprivation, a phenotype reversed by inhibition of the photosynthetic electron transport chain (Li et al., 2012).

Notably, there is an inverse relationship between growth and TAG production. Growth-limiting stresses in Mycobacterium, e.g. antibiotic treatment, lead to the induction of TAG biosynthesis. Mycobacterium mutants whose dominant TAG synthase is disrupted are unable to arrest their growth and continue to proliferate in the conditions that normally induce quiescence (Baek et al., 2011). It appears to result from redirecting the acetyl-CoA from the TCA cycle, where it is used to generate chemical energy during aerobic respiration, to the synthesis of fatty acids, which are subsequently stored in TAGs. The growth-limiting effect is not restricted to Mycobacterium. For example, yeast mutants unable to produce glycogen or trehalose persist with

high TCA fluxes during stationary phase (Sillje et al., 1999). This inverse relationship is also well known for microalgae, and has long been hampering the progress in developing microalgae into sustainable biofuel feedstocks. The almost universal propensity of microorganisms to channel acetyl-CoA into TAG storage in response to quiescence may act as a common strategy for reducing growth and altering the metabolic state.

Chlamydomonas reinhardtii as a reference model to study cellular quiescence

The unicellular green alga *Chlamydomonas reinhardtii* has a short life cycle, a sequenced genome (Merchant et al., 2007), and a growing molecular toolbox for forward and reverse genetic studies, including insertional mutagenesis (Kindle, 1990), gene silencing (Kim and Cerutti, 2009; Molnar et al., 2009), and fluorescent protein-tag (Rasala et al., 2013). In addition, a genome-wide mutant library is under construction and will offer a powerful resource comparable to the Arabidopsis collections. Among the principle areas using this model system are eukaryotic flagellar structure and function, basal bodies (centrioles), cell-cell recognition, cell cycle control, chloroplast biogenesis, phototaxis, nonphotochemical quenching, and especially photosynthesis for Chlamydomonas can grow in the dark on an organic carbon (e.g. acetate), and thus provides advantages over land plants (Harris, 2001; Peers et al., 2009).

The cell size of *C. reinhardtii* ranges between 5 to 10 µm; intracellular space is mostly occupied by a single chloroplast. The life cycle of *C. reinhardtii* is very simple. Under vegetative growth cells maintain haploidy; when N levels fall below threshold, they differentiate into sexually active gametes. Contact between opposite mating types (mt⁺ and mt⁻) initiates a rapid fertilization and formation of a diploid zygote that is astonishingly resistant to environmental insults. When conditions improve, the dormant zygote undergoes meiosis and gives rise to four

recombinant haploid products (Sager and Granick, 1954; Goodenough et al., 2007). The cell cycle of *C. reinhardtii* is a variation of the eukaryotic cell cycle, with additional rapid cell divisions bypassing G1 until a specific daughter cell size has been reached (Figure 1.3) (Bisova et al., 2005).

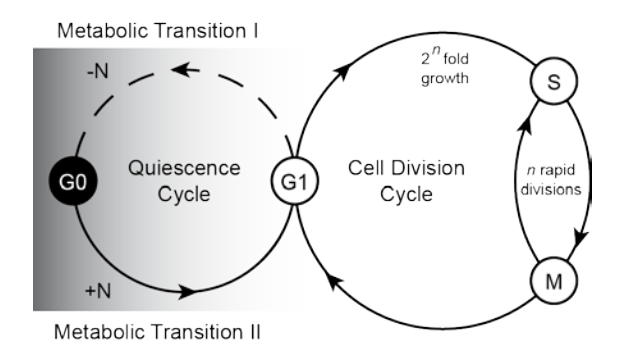


Figure 1.3. Chlamydomonas life cycles. The cell division cycle with G1, S, G2, and M phases, and the quiescence cycle (G0) are depicted. -N, N deprivation, +N, N resupply.

The unicellular green alga Chlamydomonas reinhardtii was chosen as a reference model organism to investigate life cycle transitions in photosynthetic eukaryotes for several reasons: First, the two life cycle states of interest—quiescence and cell division—can be discretely defined and controlled. Second, an extensive number of system-level studies of N deprivation has been completed in recent years in Chlamydomonas, and mutants with unique phenotypes during N-deprivation are available, setting a solid foundation for investigating cellular quiescence in the context of N deprivation (Bolling and Fiehn, 2005; Li et al., 2010; Miller et al., 2010; Moellering and Benning, 2010; Work et al., 2010; Nguyen et al., 2011; Li et al., 2012; Blaby et al., 2013; Schmollinger et al., 2014).

Aims of the dissertation research

The research of this dissertation is dedicated to the understanding of cellular quiescence in photosynthetic organism, using *C. reinhardtii* as a reference model. Chapter 2 describes the

discovery of CHT7, a repressor of cellular quiescence. Chapter 3 presents the transcriptomic regulation of the quiescence cycle. Chapter 4 reports the role of lipid droplets in coordinating lipid dynamics to ensure the reversibility of quiescence.

REFERENCES

REFERENCES

- **Baek, S.H., Li, A.H., and Sassetti, C.M.** (2011). Metabolic regulation of mycobacterial growth and antibiotic sensitivity. PLoS biology **9,** e1001065.
- Barbet, N.C., Schneider, U., Helliwell, S.B., Stansfield, I., Tuite, M.F., and Hall, M.N. (1996). TOR controls translation initiation and early G1 progression in yeast. Molecular biology of the cell **7**, 25-42.
- **Beck, T., and Hall, M.N.** (1999). The TOR signalling pathway controls nuclear localization of nutrient-regulated transcription factors. Nature **402**, 689-692.
- **Benaroudj, N., Lee, D.H., and Goldberg, A.L.** (2001). Trehalose accumulation during cellular stress protects cells and cellular proteins from damage by oxygen radicals. The Journal of biological chemistry **276**, 24261-24267.
- **Bisova, K., Krylov, D.M., and Umen, J.G.** (2005). Genome-wide annotation and expression profiling of cell cycle regulatory genes in Chlamydomonas reinhardtii. Plant physiology **137,** 475-491.
- Blaby, I.K., Glaesener, A.G., Mettler, T., Fitz-Gibbon, S.T., Gallaher, S.D., Liu, B., Boyle, N.R., Kropat, J., Stitt, M., Johnson, S., Benning, C., Pellegrini, M., Casero, D., and Merchant, S.S. (2013). Systems-level analysis of nitrogen starvation-induced modifications of carbon metabolism in a Chlamydomonas reinhardtii starchless mutant. The Plant cell **25**, 4305-4323.
- **Bolling, C., and Fiehn, O.** (2005). Metabolite profiling of Chlamydomonas reinhardtii under nutrient deprivation. Plant physiology **139,** 1995-2005.
- **Bourassa, L., and Camilli, A.** (2009). Glycogen contributes to the environmental persistence and transmission of Vibrio cholerae. Molecular microbiology **72,** 124-138.
- **Boutelet, F., Petitjean, A., and Hilger, F.** (1985). Yeast cdc35 mutants are defective in adenylate cyclase and are allelic with cyr1 mutants while CAS1, a new gene, is involved in the regulation of adenylate cyclase. The EMBO journal **4,** 2635-2641.
- **Burkhart, D.L., and Sage, J.** (2008). Cellular mechanisms of tumour suppression by the retinoblastoma gene. Nature reviews. Cancer **8,** 671-682.
- Coller, H.A. (2011). Cell biology. The essence of quiescence. Science 334, 1074-1075.
- **Cheung, T.H., and Rando. T.A.** (2013). Molecular regulation of stem cell quiescence. Nature Reviews. Molecular Cell Biology **14,** 329-340.

- **Coller, H.A., Sang, L., and Roberts, J.M.** (2006). A new description of cellular quiescence. PLoS biology **4,** e83.
- Costanzo, M., Nishikawa, J.L., Tang, X., Millman, J.S., Schub, O., Breitkreuz, K., Dewar, D., Rupes, I., Andrews, B., and Tyers, M. (2004). CDK activity antagonizes Whi5, an inhibitor of G1/S transcription in yeast. Cell 117, 899-913.
- Daniel, J., Deb, C., Dubey, V.S., Sirakova, T.D., Abomoelak, B., Morbidoni, H.R., and Kolattukudy, P.E. (2004). Induction of a novel class of diacylglycerol acyltransferases and triacylglycerol accumulation in Mycobacterium tuberculosis as it goes into a dormancy-like state in culture. Journal of bacteriology **186**, 5017-5030.
- **DeGregori, J., Kowalik, T., and Nevins, J.R.** (1995). Cellular targets for activation by the E2F1 transcription factor include DNA synthesis- and G1/S-regulatory genes. Molecular and cellular biology **15,** 4215-4224.
- Giacinti C., and Giordano, A. (2006). RB and cell cycle progression. Oncogne 25, 5220-5227.
- **Garrett, S., and Broach, J.** (1989). Loss of Ras activity in Saccharomyces cerevisiae is suppressed by disruptions of a new kinase gene, YAKI, whose product may act downstream of the cAMP-dependent protein kinase. Genes & development **3,** 1336-1348.
- Gifford, C.A., Ziller, M.J., Gu, H., Trapnell, C., Donaghey, J., Tsankov, A., Shalek, A.K., Kelley, D.R., Shishkin, A.A., Issner, R., Zhang, X., Coyne, M., Fostel, J.L., Holmes, L., Meldrim, J., Guttman, M., Epstein, C., Park, H., Kohlbacher, O., Rinn, J., Gnirke, A., Lander, E.S., Bernstein, B.E., and Meissner, A. (2013). Transcriptional and epigenetic dynamics during specification of human embryonic stem cells. Cell 153, 1149-1163.
- **Goodenough, U., Lin, H., and Lee, J.H.** (2007). Sex determination in Chlamydomonas. Seminars in cell & developmental biology **18,** 350-361.
- Gray, J.V., Petsko, G.A., Johnston, G.C., Ringe, D., Singer, R.A., and Werner-Washburne, M. (2004). "Sleeping beauty": quiescence in Saccharomyces cerevisiae. Microbiology and molecular biology reviews: MMBR 68, 187-206.
- **Griffioen, G., Anghileri, P., Imre, E., Baroni, M.D., and Ruis, H.** (2000). Nutritional control of nucleocytoplasmic localization of cAMP-dependent protein kinase catalytic and regulatory subunits in Saccharomyces cerevisiae. The Journal of biological chemistry **275**, 1449-1456.
- **Harris, E.H.** (2001). Chlamydomonas as a Model Organism. Annual review of plant physiology and plant molecular biology **52**, 363-406.
- Hemme, D., Veyel, D., Muhlhaus, T., Sommer, F., Juppner, J., Unger, A.K., Sandmann, M., Fehrle, I., Schonfelder, S., Steup, M., Geimer, S., Kopka, J., Giavalisco, P., and Schroda, M. (2014). Systems-Wide Analysis of Acclimation Responses to Long-Term

- Heat Stress and Recovery in the Photosynthetic Model Organism Chlamydomonas reinhardtii. The Plant cell.
- **Hosaka, K., and Yamashita, S.** (1984). Regulatory role of phosphatidate phosphatase in triacylglycerol synthesis of Saccharomyces cerevisiae. Biochimica et biophysica acta **796**, 110-117.
- Hu, Q., Sommerfeld, M., Jarvis, E., Ghirardi, M., Posewitz, M., Seibert, M., and Darzins, A. (2008). Microalgal triacylglycerols as feedstocks for biofuel production: perspectives and advances. The Plant journal: for cell and molecular biology **54**, 621-639.
- Irie, K., Takase, M., Lee, K.S., Levin, D.E., Araki, H., Matsumoto, K., and Oshima, Y. (1993). MKK1 and MKK2, which encode Saccharomyces cerevisiae mitogen-activated protein kinase-kinase homologs, function in the pathway mediated by protein kinase C. Molecular and cellular biology 13, 3076-3083.
- **Kadouri, D., Jurkevitch, E., Okon, Y., and Castro-Sowinski, S.** (2005). Ecological and agricultural significance of bacterial polyhydroxyalkanoates. Critical reviews in microbiology **31**, 55-67.
- **Kim, E.J., and Cerutti, H.** (2009). Targeted gene silencing by RNA interference in Chlamydomonas. Methods in cell biology **93,** 99-110.
- **Kindle, K.L.** (1990). High-frequency nuclear transformation of Chlamydomonas reinhardtii. Proceedings of the National Academy of Sciences of the United States of America **87**, 1228-1232.
- **Knudsen, E.S., and Knudsen, K.E.** (2006). Retinoblastoma tumor suppressor: where cancer meets the cell cycle. Experimental biology and medicine **231**, 1271-1281.
- **Krause, S.A., and Gray, J.V.** (2002). The protein kinase C pathway is required for viability in quiescence in Saccharomyces cerevisiae. Current biology: CB **12**, 588-593.
- Kropat, J., Hong-Hermesdorf, A., Casero, D., Ent, P., Castruita, M., Pellegrini, M., Merchant, S.S., and Malasarn, D. (2011). A revised mineral nutrient supplement increases biomass and growth rate in Chlamydomonas reinhardtii. The Plant journal: for cell and molecular biology **66**, 770-780.
- Kurat, C.F., Wolinski, H., Petschnigg, J., Kaluarachchi, S., Andrews, B., Natter, K., and Kohlwein, S.D. (2009). Cdk1/Cdc28-dependent activation of the major triacylglycerol lipase Tgl4 in yeast links lipolysis to cell-cycle progression. Molecular cell **33**, 53-63.
- Kurat, C.F., Natter, K., Petschnigg, J., Wolinski, H., Scheuringer, K., Scholz, H., Zimmermann, R., Leber, R., Zechner, R., and Kohlwein, S.D. (2006). Obese yeast: triglyceride lipolysis is functionally conserved from mammals to yeast. The Journal of biological chemistry 281, 491-500.

- **Lee, K.S., and Levin, D.E.** (1992). Dominant mutations in a gene encoding a putative protein kinase (BCK1) bypass the requirement for a Saccharomyces cerevisiae protein kinase C homolog. Molecular and cellular biology **12,** 172-182.
- Lee, K.S., Irie, K., Gotoh, Y., Watanabe, Y., Araki, H., Nishida, E., Matsumoto, K., and Levin, D.E. (1993). A yeast mitogen-activated protein kinase homolog (Mpk1p) mediates signalling by protein kinase C. Molecular and cellular biology 13, 3067-3075.
- **Levin, D.E., and Bartlett-Heubusch, E.** (1992). Mutants in the S. cerevisiae PKC1 gene display a cell cycle-specific osmotic stability defect. The Journal of cell biology **116,** 1221-1229.
- Li, X., Moellering, E.R., Liu, B., Johnny, C., Fedewa, M., Sears, B.B., Kuo, M.H., and Benning, C. (2012). A galactoglycerolipid lipase is required for triacylglycerol accumulation and survival following nitrogen deprivation in Chlamydomonas reinhardtii. The Plant cell **24**, 4670-4686.
- Li, Y., Han, D., Hu, G., Dauvillee, D., Sommerfeld, M., Ball, S., and Hu, Q. (2010). Chlamydomonas starchless mutant defective in ADP-glucose pyrophosphorylase hyperaccumulates triacylglycerol. Metabolic engineering 12, 387-391.
- **Lillie, S.H., and Pringle, J.R.** (1980). Reserve carbohydrate metabolism in Saccharomyces cerevisiae: responses to nutrient limitation. Journal of bacteriology **143,** 1384-1394.
- Loewith, R., Jacinto, E., Wullschleger, S., Lorberg, A., Crespo, J.L., Bonenfant, D., Oppliger, W., Jenoe, P., and Hall, M.N. (2002). Two TOR complexes, only one of which is rapamycin sensitive, have distinct roles in cell growth control. Molecular cell 10, 457-468.
- **Longo, V.D.** (1999). Mutations in signal transduction proteins increase stress resistance and longevity in yeast, nematodes, fruit flies, and mammalian neuronal cells. Neurobiology of aging **20**, 479-486.
- Matthew, T., Zhou, W., Rupprecht, J., Lim, L., Thomas-Hall, S.R., Doebbe, A., Kruse, O., Hankamer, B., Marx, U.C., Smith, S.M., and Schenk, P.M. (2009). The metabolome of Chlamydomonas reinhardtii following induction of anaerobic H2 production by sulfur depletion. The Journal of biological chemistry **284**, 23415-23425.
- Merchant, S.S., Prochnik, S.E., Vallon, O., Harris, E.H., Karpowicz, S.J., Witman, G.B., Terry, A., Salamov, A., Fritz-Laylin, L.K., Marechal-Drouard, L., Marshall, W.F., Qu, L.H., Nelson, D.R., Sanderfoot, A.A., Spalding, M.H., Kapitonov, V.V., Ren, Q., Ferris, P., Lindquist, E., Shapiro, H., Lucas, S.M., Grimwood, J., Schmutz, J., Cardol, P., Cerutti, H., Chanfreau, G., Chen, C.L., Cognat, V., Croft, M.T., Dent, R., Dutcher, S., Fernandez, E., Fukuzawa, H., Gonzalez-Ballester, D., Gonzalez-Halphen, D., Hallmann, A., Hanikenne, M., Hippler, M., Inwood, W., Jabbari, K., Kalanon, M., Kuras, R., Lefebvre, P.A., Lemaire, S.D., Lobanov, A.V., Lohr, M., Manuell, A., Meier, I., Mets, L., Mittag, M., Mittelmeier, T., Moroney, J.V., Moseley, J., Napoli, C., Nedelcu, A.M., Niyogi, K., Novoselov, S.V., Paulsen, I.T., Pazour, G.,

- Purton, S., Ral, J.P., Riano-Pachon, D.M., Riekhof, W., Rymarquis, L., Schroda, M., Stern, D., Umen, J., Willows, R., Wilson, N., Zimmer, S.L., Allmer, J., Balk, J., Bisova, K., Chen, C.J., Elias, M., Gendler, K., Hauser, C., Lamb, M.R., Ledford, H., Long, J.C., Minagawa, J., Page, M.D., Pan, J., Pootakham, W., Roje, S., Rose, A., Stahlberg, E., Terauchi, A.M., Yang, P., Ball, S., Bowler, C., Dieckmann, C.L., Gladyshev, V.N., Green, P., Jorgensen, R., Mayfield, S., Mueller-Roeber, B., Rajamani, S., Sayre, R.T., Brokstein, P., Dubchak, I., Goodstein, D., Hornick, L., Huang, Y.W., Jhaveri, J., Luo, Y., Martinez, D., Ngau, W.C., Otillar, B., Poliakov, A., Porter, A., Szajkowski, L., Werner, G., Zhou, K., Grigoriev, I.V., Rokhsar, D.S., and Grossman, A.R. (2007). The Chlamydomonas genome reveals the evolution of key animal and plant functions. Science 318, 245-250.
- Miller, R., Wu, G., Deshpande, R.R., Vieler, A., Gartner, K., Li, X., Moellering, E.R., Zauner, S., Cornish, A.J., Liu, B., Bullard, B., Sears, B.B., Kuo, M.H., Hegg, E.L., Shachar-Hill, Y., Shiu, S.H., and Benning, C. (2010). Changes in transcript abundance in Chlamydomonas reinhardtii following nitrogen deprivation predict diversion of metabolism. Plant physiology 154, 1737-1752.
- **Moellering, E.R., and Benning, C.** (2010). RNA interference silencing of a major lipid droplet protein affects lipid droplet size in Chlamydomonas reinhardtii. Eukaryotic cell **9,** 97-106.
- Molnar, A., Bassett, A., Thuenemann, E., Schwach, F., Karkare, S., Ossowski, S., Weigel, D., and Baulcombe, D. (2009). Highly specific gene silencing by artificial microRNAs in the unicellular alga Chlamydomonas reinhardtii. The Plant journal: for cell and molecular biology 58, 165-174.
- Nguyen, H.M., Baudet, M., Cuine, S., Adriano, J.M., Barthe, D., Billon, E., Bruley, C., Beisson, F., Peltier, G., Ferro, M., and Li-Beisson, Y. (2011). Proteomic profiling of oil bodies isolated from the unicellular green microalga Chlamydomonas reinhardtii: with focus on proteins involved in lipid metabolism. Proteomics 11, 4266-4273.
- **Noda, T., and Ohsumi, Y.** (1998). Tor, a phosphatidylinositol kinase homologue, controls autophagy in yeast. The Journal of biological chemistry **273**, 3963-3966.
- **Ohtani, K., and Nevins, J.R.** (1994). Functional properties of a Drosophila homolog of the E2F1 gene. Molecular and cellular biology **14**, 1603-1612.
- Peers, G., Truong, T.B., Ostendorf, E., Busch, A., Elrad, D., Grossman, A.R., Hippler, M., and Niyogi, K.K. (2009). An ancient light-harvesting protein is critical for the regulation of algal photosynthesis. Nature **462**, 518-521.
- **Perez-Perez, M.E., Florencio, F.J., and Crespo, J.L.** (2010). Inhibition of target of rapamycin signaling and stress activate autophagy in Chlamydomonas reinhardtii. Plant physiology **152,** 1874-1888.
- Rasala, B.A., Barrera, D.J., Ng, J., Plucinak, T.M., Rosenberg, J.N., Weeks, D.P., Oyler, G.A., Peterson, T.C., Haerizadeh, F., and Mayfield, S.P. (2013). Expanding the

- spectral palette of fluorescent proteins for the green microalga Chlamydomonas reinhardtii. The Plant journal : for cell and molecular biology **74**, 545-556.
- **Rohde, J.R., and Cardenas, M.E.** (2004). Nutrient signaling through TOR kinases controls gene expression and cellular differentiation in fungi. Current topics in microbiology and immunology **279**, 53-72.
- **Russell, R.C., Fang, C., and Guan, K.L.** (2011). An emerging role for TOR signaling in mammalian tissue and stem cell physiology. Development **138**, 3343-3356.
- Sage, J., Miller, A.L., Perez-Mancera, P.A., Wysocki, J.M., and Jacks, T. (2003). Acute mutation of retinoblastoma gene function is sufficient for cell cycle re-entry. Nature 424, 223-228.
- **Sager, R., and Granick, S.** (1954). Nutritional control of sexuality in Chlamydomonas reinhardi. The Journal of general physiology **37**, 729-742.
- **Sang, L., and Coller, H.A.** (2009). Fear of commitment: Hes1 protects quiescent fibroblasts from irreversible cellular fates. Cell cycle **8,** 2161-2167.
- Sang, L., Coller, H.A., and Roberts, J.M. (2008). Control of the reversibility of cellular quiescence by the transcriptional repressor HES1. Science 321, 1095-1100.
- Schmollinger, S., Muhlhaus, T., Boyle, N.R., Blaby, I.K., Casero, D., Mettler, T., Moseley, J.L., Kropat, J., Sommer, F., Strenkert, D., Hemme, D., Pellegrini, M., Grossman, A.R., Stitt, M., Schroda, M., and Merchant, S.S. (2014). Nitrogen-Sparing Mechanisms in Chlamydomonas Affect the Transcriptome, the Proteome, and Photosynthetic Metabolism. The Plant cell **26**, 1410-1435.
- **Shi, L., Sutter, B.M., Ye, X., and Tu, B.P.** (2010). Trehalose is a key determinant of the quiescent metabolic state that fuels cell cycle progression upon return to growth. Molecular biology of the cell **21,** 1982-1990.
- Siaut, M., Cuine, S., Cagnon, C., Fessler, B., Nguyen, M., Carrier, P., Beyly, A., Beisson, F., Triantaphylides, C., Li-Beisson, Y., and Peltier, G. (2011). Oil accumulation in the model green alga Chlamydomonas reinhardtii: characterization, variability between common laboratory strains and relationship with starch reserves. BMC biotechnology 11, 7.
- Sillje, H.H., Paalman, J.W., ter Schure, E.G., Olsthoorn, S.Q., Verkleij, A.J., Boonstra, J., and Verrips, C.T. (1999). Function of trehalose and glycogen in cell cycle progression and cell viability in Saccharomyces cerevisiae. Journal of bacteriology 181, 396-400.
- **Singer, M.A., and Lindquist, S.** (1998). Thermotolerance in Saccharomyces cerevisiae: the Yin and Yang of trehalose. Trends in biotechnology **16,** 460-468.

- Sirakova, T.D., Deb, C., Daniel, J., Singh, H.D., Maamar, H., Dubey, V.S., and Kolattukudy, P.E. (2012). Wax ester synthesis is required for Mycobacterium tuberculosis to enter in vitro dormancy. PloS one 7, e51641.
- Smith, A., Ward, M.P., and Garrett, S. (1998). Yeast PKA represses Msn2p/Msn4p-dependent gene expression to regulate growth, stress response and glycogen accumulation. The EMBO journal 17, 3556-3564.
- Thevelein, J.M., Cauwenberg, L., Colombo, S., De Winde, J.H., Donation, M., Dumortier, F., Kraakman, L., Lemaire, K., Ma, P., Nauwelaers, D., Rolland, F., Teunissen, A., Van Dijck, P., Versele, M., Wera, S., and Winderickx, J. (2000). Nutrient-induced signal transduction through the protein kinase A pathway and its role in the control of metabolism, stress resistance, and growth in yeast. Enzyme and microbial technology 26, 819-825.
- Valcourt, J.R., Lemons, J.M., Haley, E.M., Kojima, M., Demuren, O.O., and Coller, H.A. (2012). Staying alive: metabolic adaptations to quiescence. Cell cycle 11, 1680-1696.
- van Aelst, L., Jans, A.W., and Thevelein, J.M. (1991). Involvement of the CDC25 gene product in the signal transmission pathway of the glucose-induced RAS-mediated cAMP signal in the yeast Saccharomyces cerevisiae. Journal of general microbiology 137, 341-349.
- Wildwater, M., Campilho, A., Perez-Perez, J.M., Heidstra, R., Blilou, I., Korthout, H., Chatterjee, J., Mariconti, L., Gruissem, W., and Scheres, B. (2005). The RETINOBLASTOMA-RELATED gene regulates stem cell maintenance in Arabidopsis roots. Cell **123**, 1337-1349.
- Work, V.H., Radakovits, R., Jinkerson, R.E., Meuser, J.E., Elliott, L.G., Vinyard, D.J., Laurens, L.M., Dismukes, G.C., and Posewitz, M.C. (2010). Increased lipid accumulation in the Chlamydomonas reinhardtii sta7-10 starchless isoamylase mutant and increased carbohydrate synthesis in complemented strains. Eukaryotic cell 9, 1251-1261.
- Wu, J., Zhang, N., Hayes, A., Panoutsopoulou, K., and Oliver, S.G. (2004). Global analysis of nutrient control of gene expression in Saccharomyces cerevisiae during growth and starvation. Proceedings of the National Academy of Sciences of the United States of America 101, 3148-3153.
- Xiong, Y., McCormack, M., Li, L., Hall, Q., Xiang, C., and Sheen, J. (2013). Glucose-TOR signalling reprograms the transcriptome and activates meristems. Nature **496**, 181-186.
- Zhang, H., Stallock, J.P., Ng, J.C., Reinhard, C., and Neufeld, T.P. (2000). Regulation of cellular growth by the Drosophila target of rapamycin dTOR. Genes & development 14, 2712-2724.

CHAPTER 2

Protein Compromised Hydrolysis of Triacylglycerols 7 (CHT7) Acts as a Repressor of Cellular Quiescence in Chlamydomonas¹

¹This research was published in: Tsai, C.H., Warakanont, J., Takeuchi, T., Sears, B.B., Moellering, E.R., and Benning, C. (2014). The protein Compromised Hydrolysis of Triacylglycerols 7 (CHT7) acts as a repressor of cellular quiescence in Chlamydomonas. Proc. Natl. Acad. Sci. U S A. 111, 15833-15838. I contributed to the data shown in all of the figures.

ABSTRACT

Microalgae are prolific photosynthetic organisms that have the potential to sustainably produce high-value chemical feedstocks. However, an industry based on microalgal biomass still is faced with challenges. For example, microalgae tend to accumulate valuable compounds, such as triacylglycerols, only under stress conditions that limit growth. To investigate the fundamental mechanisms at the base of this conundrum—the inverse relationship between biomass production and storage compound accumulation—I applied a combination of cell biological and genetic approaches. Conceptually, nutrient deprivation, which commonly is used to induce the accumulation of triacylglycerol in microalgae, leads to a state of cellular quiescence defined by a halt of cell divisions that is reversible upon nutrient resupply. To identify factors that govern cellular quiescence, we screened for mutants of the model alga Chlamydomonas reinhardtii that, in contrast to wildtype cells placed under conditions of nitrogen deprivation, were unable to degrade triacylglycerols following nitrogen resupply. One of the mutants described here in detail, compromised hydrolysis of triacylglycerols 7 (cht7), was severely impaired in regrowth following removal of different conditions inducing cellular quiescence. The mutant carries a deletion affecting four genes, only one of which rescued the quiescence phenotype when reintroduced. It encodes a protein with similarity to mammalian and plant DNA binding proteins. Comparison of transcriptomes indicated a partial derepression of quiescence-related transcriptional programs in the mutant under conditions favorable to growth. Thus, CHT7 likely is a repressor of cellular quiescence and provides a possible target for the engineering of highbiomass/high-triacylglycerol microalgae.

INTRODUCTION

Nutrient deprivation of microalgal cultures provides a facile experimental tool to induce and study triacylglycerol (TAG) accumulation in lipid droplets and is used in biotechnological settings for the production of high-value oils (Hu et al., 2008; Liu and Benning, 2013). In particular, responses to the withdrawal of nitrogen (N) have been studied widely in the model unicellular green alga *Chlamydomonas reinhardtii*, and a comprehensive picture of N-sparing mechanisms during N deprivation is emerging through integrated global analysis of transcripts, proteins, and metabolites (Miller et al., 2010; Blaby et al., 2013; Schmollinger et al., 2014). Mechanisms of lipid droplet formation following N deprivation and proteins associated with lipid droplets are being explored (Moellering and Benning, 2010; Goodson et al., 2011; Nguyen et al., 2011), and mutants have become available that provide mechanistic insights in vivo into specific aspects of the lipid biosynthetic machinery of *C. reinhardtii* required for TAG accumulation (Boyle et al., 2012; Li et al., 2012; Nguyen et al., 2013).

From a cell biological viewpoint, N deprivation induces cellular quiescence, a reversible state of the cell cycle during which cell divisions temporarily cease and cells are reprogrammed to adjust metabolism for survival of the adverse condition (Valcourt et al., 2012). In *C. reinhardtii*, metabolic changes during N deprivation-induced quiescence include the partial degradation and reorganization of the photosynthetic apparatus and the protein biosynthetic machinery, induction of lipase and autophagy genes, and accumulation of carbon storage compounds (Miller et al., 2010; Blaby et al., 2013; Schmollinger et al., 2014). N deprivation also induces gametogenesis (Beck and Acker, 1992), allowing cells of opposite mating types to fuse and form thick-walled zygospores that can survive temporary harsh conditions. The goal of this study was to gain mechanistic insights into the regulation of N deprivation-induced quiescence in

C. reinhardtii and to answer the question of how changes in the metabolic status of the algal cell induced by N deprivation affect progression through the cell cycle or the entry and exit into and out of quiescence. Toward this end, I searched for mutants of C. reinhardtii unable to rapidly exit quiescence, readjust their metabolism, and resume growth following N resupply after a period of N deprivation. As proxy for the metabolic status of the cell, I focused on TAG degradation following N resupply and identified a mutant and corresponding protein that met the criteria for a repressor of quiescence in C. reinhardtii.

MATERIALS AND METHODS

Strains, Genetic Analysis, and Growth Conditions

Chlamydomonas reinhardtii cell wall-less strain dw15 (cw15, nit1, mt+) was obtained from A. Grossman, Department of Plant Biology, Carnegie Institution for Science, Stanford, CA, and is referred to as the wild type (with regard to CHT7) parental line (PL) throughout. CC-198 (er-u-37, str-u-2-60, mt-) and CC-110 (spr-u-1-6-2 mt+) were obtained from the Chlamydomonas Resource Center (www. chlamycollection.org). CC-198 was crossed to cht7 as described previously (Li et al., 2012). Progeny were analyzed for the hygromycin B resistance marker aph7, mating type, and cell wall traits. A hygromycin-resistant, mt-, cw+ meiotic product (2-5-1) was selected and crossed to CC-110, producing zygospores that were used for tetrad analysis to test for cosegregation of the aph7 marker and the cht7 phenotypes.

Complemented *cht7* lines were generated with two similar methods. In method 1, cotransformation, a 7,873-bp genomic fragment containing the intact CHT7 gene with 1-kb flanking sequences on both ends was excised from BAC 21K10 (Clemson University Genomics Institute) by using EcoRI and HindIII. Plasmid pMN24 (Fernandez et al., 1989) carrying the *C. reinhardtii* nitrate reductase gene NIT1 as selection marker was linearized with EcoRV. Both DNA fragments were cotransformed into *cht7*. In each transformation, 0.5 µg of linearized pMN24 and 0.5 µg gel-purified BAC fragment were used. In method 2, transformation of the selectable marker linked to the BAC fragment, the 7,873-bp fragment was inserted into the EcoRI and HindIII sites of pBR322. The construct then was digested by EcoRV and SspI to release an 8,220-bp fragment that included the 7,873-bp fragment. The 8,220-bp fragment was inserted into EcoRV-linearized pMN24 to produce pMN24-CHT7. EcoRV-linearized pMN24-CHT7 was used for transformation of the *cht7* mutant. TAP plates (see below) containing 10 mM

nitrate instead of 10 mM ammonium were used for selection. Colonies were picked into 96-well plates and grown N deprived and N resupplied following the same protocol described below. Cell growth after N resupply was measured with a FLUOstar Optima 96-well plate reader (BMG Labtech). Those able to resume growth after N resupply likely were complemented. Strains having pMN24 alone were used as empty vector control. Complementation lines C1 and C2 were produced by method 1; C3 and C4 were by method 2. Primers of APH7-F and APH7-R and primers of CHT7-F and CHT7-R were used to validate the retention of the aph7 insertion and the reintroduction of CHT7 gene, respectively (Figure 2.3). All primer sequences are listed in Table 2.1.

In general, cells were grown in TAP medium (Harris, 1989) under continuous light (70–80 μmol·m–2·s–1) at 22 °C or ambient room temperature (~22 °C) for solid media, which contained 0.8% agar (Phytoblend; Caisson Labs). Concentration of cells was monitored with a Z2 Coulter Counter (Beckman Coulter) or a hemocytometer.

Generation of Antibodies, Immunoblotting, Subcellular Fractionation, and BN-PAGE

To generate antibodies against MLDP, the full-length coding sequence of MLDP was amplified using primers (MLDPcds-F/MLDPcds-R) and total cDNA as the template, and was inserted into the BamHI and XhoI sites of pET28B(+) (Novagen EMD Chemicals). For the development of antibodies against CHT7, the full-length coding sequence of CHT7 was synthesized (Life Technologies) with codons optimized for expression in *Escherichia coli*. The synthesized CHT7 sequence was inserted into the EcoRI and HindIII sites of pET28B(+). Both constructs were introduced into E. coli BL21 (DE3). Recombinant proteins (6xHis-MLDP and 6xHis-CHT7) were purified using Ni-nitrilotriacetic acid agarose (Qiagen) and separated by SDSPAGE to

examine their purity. Few other proteins were copurified with 6xHis MLDP, yielding a fairly clean substrate for the generation of antibodies. In contrast, the elution of 6xHis-CHT7 contained many other proteins. 6xHis-CHT7 was excised from the SDS-PAGE gel and eluted. Roughly 2 mg of each protein was sent for antibody production in rabbits by Cocalico Biologicals, Inc. Immunoblots using MLDP antiserum are shown in Figure 2.1A; those using CHT7 antiserum are shown in Figure 2.12A.

For immunoblot analysis, SDS-PAGE gels were blotted onto PVDF membranes in transfer buffer [25 mM Tris, 192 mM Gly, and 10% (vol/vol) methanol] for 60 min at 100 V. Membranes were blocked for 60 min in TBST [50 mM Tris, 150 mM NaCl, 0.05% (vol/vol) Tween 20, pH 7.6] with 5% (wt/vol) nonfat dry milk and probed with primary antibodies overnight at 4 °C. The primary antibodies (MLDP antiserum and CHT7 antiserum) were used at 1:1,000 dilutions. Goat anti-rabbit secondary antibodies coupled to horseradish peroxidase were used at 1:10,000 dilution and incubated with blots at room temperature for 30 min. Blots then were washed six times with TBST at room temperature for 10 min each. Antigen was detected by chemiluminescence (Bio-Rad Clarity Western ECL substrate) using a charge-coupled device (CCD) imaging system. For samples containing detergent or reducing agent, the RC DC Protein Assay Kit (Bio-Rad) was used for protein quantification.

C. reinhardtii nuclei were isolated as described previously (Winck et al., 2011) using a CelLytic PN kit (Sigma-Aldrich). Chloroplast fractions were prepared according to (Mason et al., 2006). Organelle pellets were solubilized in $2 \times$ SDS sample buffer, boiled at 95 °C for 5 min, and centrifuged at $20,000 \times g$ for 10 min to remove insoluble portions. Supernatants were collected and tested for the enrichment of CHT7 protein.

For BN-PAGE analysis, 50 mL of cells were pelleted and resuspended in PBS with protease inhibitor (P9599; Sigma-Aldrich) and phosphatase inhibitor (Thermo Scientific) at a concentration of 109 cells/mL and then lysed by sonication on ice with 0.6 s on and 0.5 s off for 20 s per cycle with 20 cycles and 20 s between each cycle. The sonication was repeated 20 times. Insoluble materials were removed by centrifugation at 20,000 × g for 30 min at 4 °C. Protein content in this case was determined using the Quick Start Bradford protein assay (Bio-Rad). Supernatants containing 25 µg of proteins were loaded onto each lane of BN-PAGE Novex 4–16% (wt/vol) Bis-Tris gels (Life Technologies), and BN electrophoresis was performed as described (Wittig et al., 2006). After denaturation, gels were either blotted directly or run in a second dimension on a 10% (wt/vol) SDS-PAGE gel followed by immunoblotting.

Mutant Screen

Insertional mutagenesis was done as described previously (Li et al., 2012) except for the use of a shorter, 2,012-bp PvuII fragment of the pHyg3 plasmid that contains only the hygromycin B resistance gene *aph7*. Hygromycin B-resistant colonies were picked into 96-well cell culture plates (Corning) with 200 μL of TAP medium and grown for 3 d. The plates were replicated before the cultures were subjected to 48 h N deprivation followed by 24 h N resupply as described above. For processing, the cultures were transferred to a 96-well PCR plate (Life Technologies) and centrifuged at 2,000 × g. The cell pellets were resuspended with 50 μL of 2× SDS sample buffer [0.1 M Tris, pH 6.8; 2.75% (wt/vol) SDS; and 5% (vol/vol) β-mercaptoethanol] and boiled at 95 °C for 5 min in a Bio-Rad iCycler thermocycler. Lysates from each well then were blotted onto an Amersham Hybond-ECL nitrocellulose membrane (GE Healthcare) placed on top of one layer of Whatman filter paper by using a MilliBlot- D 96-well

filtering system (Sigma-Aldrich). Immunodetection of MLDP was done as described above. During the primary screen of 1,760 insertional lines, 13 putative mutants were selected for secondary (standard immunoblot) and tertiary tests (lipid analysis), which led to the confirmation of eight mutants with the *cht* phenotype.

Confocal Microscopy and Construction of the CHT7-GFP Fusion

For the detection of lipid droplets stained by Nile red, cultures of cells were incubated with the fluorescent dye Nile red in the dark at a final concentration of 2.5 µg/mL (from a stock of 50 µg/mL in methanol). Cells were immobilized by spotting on poly-L-lysine–coated slides (Electron Microscopy Sciences). Images were captured with a FluoView FV10i confocal microscope (Olympus America). The 488-nm argon laser was used in combination with a 560–615-nm filter; for chlorophyll autofluorescence, a filter for far-red was used.

To observe subcellular localization of CHT7, pMN24-CHT7- GFP was constructed to express the translational fusion under the control of the endogenous promoter and terminator. Plasmid pMN24-CHT7 was digested with AvrII to remove a 2,829-bp fragment containing the 3' end of CHT7 genomic sequence. The 2,829-bp fragment was inserted into pBR322 linearized with NheI to obtain pBR322-2829. *C. reinhardtii* codon-optimized EGFP was amplified by Phusion DNA polymerase (New England BioLabs) from pJR38 (Neupert et al., 2009) using primers GFP-F (SmaI cut site) and GFP-R (SpeI cut site), which also introduced an N-terminal linker (GAAAAAAAA). This PCR product was inserted into pPCR-Blunt using the Zero Blunt PCR Cloning Kit (Life Technologies) to produce pPCRBlunt-GFP and sequenced. The GFP fragment was excised by SmaI and SpeI and inserted into the PmII and SpeI sites of pBR322-2829 to obtain pBR322- GFP, which then was digested with FseI and SpeI to obtain a 1,486-bp

fragment. This fragment is composed of the last 701 bp of the CHT7 gene (before the stop codon), glycine/alanine linker, GFP, and the first 44 bp of CHT7 3' UTR. The larger DNA product (~25 kb) from the Fsel/Spel double digestion of pMN24-CHT7 was gel purified with the QIAEX II Gel Extraction Kit (Qiagen) and served as the vector for the 1,486-bp insert to complete pMN24-CHT7-GFP. The insert from this plasmid was sequenced to confirm that GFP was in frame with CHT7. Confocal images were collected sequentially with the Olympus FluoView 1000 Confocal Laser Scanning Microscope (Olympus America) using a 100× UPlanSApo oil objective (N.A. 1.4). Hoechst 33342 fluorescence was excited with the 405-nm diode laser while the fluorescence emission was collected from 430 to 470 nm. GFP fluorescence was excited with a 488-nm argon gas laser while the fluorescence emission was collected from 500 to 530 nm. Far-red autofluorescence was excited with a 559-nm solid-state laser while the fluorescence emission was collected at 655–755 nm.

Phenotyping Assays

To induce N deprivation, midlog-phase cells grown in TAP were collected by centrifugation $(2,000 \times g, 4 \, ^{\circ}\text{C}, 2 \, \text{min})$, washed twice with TAP-N (NH4Cl omitted from TAP), and resuspended in TAP-N at 0.3 OD550. N was resupplied with either of two methods that gave the same outcome in all of the physiological and biochemical experiments tested. In method 1, after 48 h of N deprivation, cells were pelleted by centrifugation $(2,000 \times g, 4 \, ^{\circ}\text{C}, 2 \, \text{min})$ and resuspended with the same volume of TAP. In method 2, 1% culture volume of 1 M NH4Cl $(100\times)$ was added to the N-deprived culture. Except for the primary mutant screen, method 2 was used to avoid physical damage to cells during centrifugation. To conduct P deprivation or

rapamycin treatment, cells were washed and resuspended in medium without phosphate or with 1 μM rapamycin. Conditions were reversed by washing and resuspending cells in regular TAP.

Cell viability was assessed by using SYTOX Green (Molecular Probes Inc.), to which living cells are impermeable but which binds the nucleic acids of dead cells, yielding intense fluorescence. Cells were grown in TAP-N. At the times indicated (Figure 2.8B), 1 µL of 5 mM SYTOX Green was added to 1 mL culture and incubated for 5 min in the dark. The cells were observed by fluorescence microscopy (Leica DRMA2) with excitation at 488 nm using a FITC filter for SYTOX Green and a Texas Red filter for chlorophyll autofluorescence. Data were collected with FV1000 ASW software (Olympus).

To assess the ability of cells to divide, a set volume of culture deprived of N for the time indicated (Figure 2.8C) was diluted in warm TAP medium with 0.4% agar (PhytoBlend) that was not yet solidified and poured evenly over the solid TAP medium. Colony-forming units (CFUs) and the diameter of individual colonies were measured 11 d later. CFUs were monitored for another 2 wk, with few additional colonies forming. Cells from a second aliquot were counted with a hemocytometer to provide a denominator to calculate the fraction (%) of CFUs per cells plated.

For lipid analysis, extraction, TLC of neutral lipids, fatty acid methyl ester (FAME) preparation, and gas-liquid chromatography were conducted as previously described in (Moellering and Benning, 2010). Cell pellets were extracted into methanol and chloroform (2:1 vol/vol). To the extract, 0.5 volume of 0.9% KCl was added and mixed, followed by phase separation at low-speed centrifugation. For TAG quantification, lipids were resolved by TLC on Silica G60 plates (EMD Chemicals) developed in petroleum ether-diethyl ether-acetic acid (80:20:1 by volume). After visualization by brief iodine staining, FAME of each lipid or total

cellular lipid was processed and quantified by gas chromatography as previously described (Rossak et al., 1997).

Standard DNA and RNA Procedures

C. reinhardtii genomic DNA was isolated as previously described (Newman et al., 1990). For Southern blotting, DNA digested with BamHI was separated by agarose gel electrophoresis (10 µg DNA per lane). DNA was transferred to a nylon membrane (Amersham Hybond-N+; GE Healthcare) and UV cross-linked. The probe was labeled by digoxigenin through PCR amplification of a 234-bp region within the hygromycin B resistance cassette with primers S-F and S-R. Prehybridization, hybridization, and chemiluminescent detection were performed using a kit from Roche following the manufacturer's instructions.

To identify the locus disrupted by insertional mutagenesis, SiteFinding-PCR (Tan et al., 2005) was used with minor modifications and with primers designed for the pHyg3 plasmid. The primers used for finding the insertion in *cht7* were SiteFinder1 in combination with GSP3-3 and GSP3-4 and SiteFinder3 in combination with GSP8-02 and GSP8-0. In addition, nested primers SFP1 and SFP2 were used for both combinations. To confirm the results of SiteFinding-PCR, standard PCR was performed using primers amplifying regions across the ends of the insertion and the flanking sequences (CHT7-1-F/CHT7-1-R; CHT7-2-F/CHT7-2-R; CHT7-3-F/CHT7-3-R; CHT7-4-F/CHT7-4-R). All primers may be found in Table 2.1.

Table 2.1. Oligonucleotide primers used in this study

Name	Sequence			
MLDPcds-F	GGATTCATGGCCGAGTCTGCTGGAAA			
MLDPcds-R	CTCGAGGCATCATAGCACAAGGCATT			
S-F	ACCAACATCTTCGTGGACCT			
S-R	CTCCTCGAACACCTCGAAGT			
SiteFinder1	CACGACACGCTACTCAACACACCACCTCGCACAGCGTCCTCAAGCGG			
	CCGCNNNNNGCCT			
Ci4-Ei-1-2	CACGACACGCTACTCAACACACCACCTCGCACAGCGTCCTCAAGCG			
SiteFinder3	GCCGCNNNNNNGCCG			
SFP1	CACGACACGCTACTCAACAC			
SFP2	ACTCAACACCACCTCGCACAGC			
GSP3-3	ACTGCTCGCCTTCACCTTCC			
GSP3-4	CTGGATCTCTCCGGCTTCAC			
GSP8-0	CGCCCTACCTTTTGCTGGA			
GSP8-02	GGTCGAAGCATCATCGGTGT			
CHT7-1-F	ACACTTAGACCCGTGGCTTC			
CHT7-1-R	TGGAAGTGTCATAGCGCAAG			
CHT7-2-F	AAACCATGCAAAAGGTGCAC			
CHT7-2-R	CGCTCACAATTCCACACAAC			
CHT7-3-F	CTCAAGTGCTGAAGCGGTAG			
CHT7-3-R	TGGTGGTCGACAAACTCTTG			
CHT7-4-F	TTTACAACGTCGTGACTGGG			
CHT7-4-R	CATGAGGTATGGTGGTCGAC			
γ-tubulin -F	CGCCAAGTACATCTCCATCC			
γ-tubulin -R	TAGGGGCTCTTCTTGGACAG			
Gene1-F	TTCTCGGGTCAGATATTGGG			
Gene1-R	TTGAGGCAGAACGACTTCTTG			
Gene2-F	GTGTCCTACACAGTTCGA			
Gene2-R	GTAGTACACCTTGCTTCG			
Gene3-F	AATTCTCAAGTAAG			

Table 2.1 (cont'd)

Gene3-R	TATATACAAAACAACGAATA
Gene4-F	TATTCCTCTCAAAGTCGATT
Gene4-R	TTGCATCTTTGATGTAGAAC
APH7-F	CTCAAGTGCTGAAGCGGTAG
APH7-R	TGGTGGTCGACAAACTCTTG
CHT7-F	TTCTCGGGTCAGATATTGGG
CHT7-R	TTGAGGCAGAACGACTTCTTG
GFP-F	CCCGGGAGCGGCAGCGGCAGCAGCCGCGATGGCCAAGGGC
	GAGGAGCT
GFP-R	ACTAGTTTACTTGTACAGCTCGTCCA

Gene Name	Gene ID ^a	qPCR Primer Sequence (Forward / Reverse)
CBLP	g6364	GCCACACCGAGTGGGTGTCGTGCG /
		CCTTGCCGCCCGAGGCGCACAGCG
CHT7	Cre11.g481800	TCGCGGTGTCTAAAATTGTACTG /
		GGTTGTTAAAGCACTGCATGCA
APG3	Cre02.g102350	GACGACATTCCCGACATCACT /
		GCCGCAGCCTCATCATCT
APG8	Cre16.g689650	ACCCCGACATTCAAGCA / TGCGGCCTCCGCTTT
LHCA3	g11502	GGGTGTGTCGTGCTTGCA / CGCACGCAGGCACAGA
LHCB4	Cre17.g720250	CGTGGTGATTGGCGTTGAC /
		GACGGAGCCCTTGTTGTTCTT
LHCBM1	g1276	CCAAGTTCACCCCCAGTAA /
		TGCATCCCTATTGGTACATCAAA
LHCBM4	Cre06.g283950	GAAACCCCGCAGAAGTGAAG /
		CACGGTAAGGGCCATTTGC
NAB1	Cre06.g268600	CGACTGGTGCCCACGACTA /
		CACATACACTCCTCCTGCATTTTC
PSAD	g5492	TTGCGACCCCGCAGTT /
		CACGCACACGCTAACATCTACA

Table 2.1 (cont'd)

MCA1	Cre08.g358250	CCGGTTGCGCATCGA /
		AAAACCAAGCATTAACCGATCAA
PSBS1/	Cre01.g016600/	TGTGCAACACCCTTCAAAATG /
PSBS2	Cre01.g016750	GCGCTGGGCGAAAGC
FAP113	Cre07.g321400	GCGGAGGCATGTCATATGG /
		CTGTCTCTGCAAATGTATGTCAGTGT
FAP138	Cre14.g632350	CGCATGCACCGAGAACAC / CACGCCCGGGCCTAA
FAP139	g9599	GCCGCGGAGATGGCTAA /
		CTTATTGCACGAGGCTAACCAA
E A D202	Cre03.g162850	TGGCTGCGCCATGGTT /
FAP292		GAGTCCTGCGGTCAGGGTAA
IFT46	g5332	CCAGCTGCGCCTAGAGATG /
IF140		TGGCCCCTCGTCCATGT
IET57	Cre10.g467000	TGAGGCAGGCATA /
IFT57		GGATACCGCTGCCTTT
E A 1	Cre06.g257600	TCTTGGCTTTCTGCTGTGTAC /
FA1		GTGCACAAGACCGGTCCTTT
EAO	Cre07.g351150	GGCGATTGACGGACTATGAAC /
FA2		TTAAAGACCGCGCCAAAGG
CIII D	Cre05.g242000	CGAGCTCAAGAAGATTTGGTTGA /
CHLD		CCGAAGATGCAAGCCATAATATG
CITY IC	Cre12.g510800	CATGTGTTGCGGTGTGCTTT /
CHLI2		TCCCACCCGCTCAGTCA
CPX1	Cre02.g085450	TGGTCGTCGACTTCCTGTGTAA /
		ATGGGTACGCAGGACAGTAACA
CPX2	Cre02.g092600	TACGGCGGTGGCTGTGA /
		ACTGCGAGTCCTCCACGTCTA
POR	Cre01.g015350	GCTGCTGGATGACCTGAAGAA /
		TGATGGAGCCGACGATGAT

Table 2.1 (cont'd)

UROD1	Cre11.g467700	CGCTTCGGCTGAGTGTTTAGA /
		AGGCTCCCGTCCATCA
BCC1	Cre17.g715250	CCACAGTCGCGAATCACAAT /
		GGTGGCGCACTT
BCC2	Cre01.g037850	CTGGTGGTGCTGCTGACT /
		CGGCTCAGAACCTGAATAACAA
BCR1	Cre08.g359350	AACCGCGTGCTGATCAATG /
		TGAAAGTGCCCTAAAACCAAACA
HAD1	Cre03.g208050	CTGACCCACATGAGACATGACA /
		GCGGCGCATTCGTTGT
KAS2	Cre07.g335300	TGGGCCGGCTGTACGA /
KAS2		CTCAGCTGTATCGAAGCTTTAAGATC
MCT1	Cre14.g621650	GGTGTCTAGGCGCATCACTTTT /
MCTT		TGAGCATGGTGGCCATCTT
APX2	g10003	CTGCGCGAGGTGTTTGG /
AI A2		GCGCCACAATGTCCTTGTC
CAT1	Cre09.g417150	GGAGGCTGCAGGAAAACTGA /
CAII		TCTCCAGCCTGGGCTACCT
HPR1	Cre06.g295450	TGCATCTTGCATTGGTTACATG /
пгкі		CGCGTTCCCTGGCTCAT
MAS1	g2904	${\tt GCCCCTTGTGCCATATGC/CCCCGATGCTGTCA}$
MDH2	Cre10.g423250	GAACCGCATTCAAAAGATTGC /
		TGAACTTCCGCGGTTTCG
PXN1	Cre07.g353300	GCTGCAAATGCATTGGATCA /
		CCGGCGTGAGTTAAGAACCA

^aCorresponding to the version 5.3.1 genome. All primer sequences are written 5' to 3'. N indicates a random nucleotide. Except CBLP, all other qPCR primers were designed by Primer Express Version 3.0 (Life Technologies).

To produce cDNA templates used for qPCR, total RNA was purified with the RNeasy PlantMini Kit (Qiagen) including the oncolumn DNase digestion and then subjected to reverse transcription by using SuperScript III reverse transcriptase (Life Technologies). qPCR was performed on an ABI Prism 7000 (Applied Biosystems) using SYBR Green PCR Master Mix (Life Technologies) with an equivalent cDNA template and 0.25 μM of each primer. The amount of cDNA input was optimized after serial dilutions. In all qPCR experiments, expression of the target gene was normalized to the endogenous reference gene CBLP, a gene commonly used for normalization in *C. reinhardtii* (Allen et al., 2007), using the cycle threshold (CT) 2–ΔΔCT method. All experiments were done using at least two biological replicates, and each reaction was run with technical replicates. qPCR procedures and analysis followed the minimum information for publication of quantitative real-time PCR experiment guidelines (Bustin et al., 2009). For quantification, TRIzol reagent (Life Technologies) was used for RNA isolation, and the concentration of RNA was measured with a NanoDrop instrument (Thermo Scientific). qPCR primers are listed in Table 2.1.

Illumina RNA Sequencing and Bioinformatics

For Illumina RNA sequencing, total RNA was isolated by using the Qiagen RNeasy Plant Mini Kit including the on-column DNase digestion. RNA integrity was examined with a 2100 Bioanalyzer (Agilent Technologies), and every sample had an RNA integrity number greater than 7.0. Three biologically independent sets of samples were prepared at different times and submitted directly to the Michigan State University Research Technologies Service Facility (rtsf.natsci.msu.edu/) for sequencing on an Illumina Genome Analyzer II (Illumina). The cDNA libraries were prepared for single-end sequencing. Default parameters were used to pass reads by

using Illumina quality control tools. The filtered sequence data were deposited at the National Center for Biotechnology Information Sequence Read Archive (www.ncbi.nlm.nih.gov/Traces/sra/) with the BioProject ID PRJNA241455 for the Illumina dataset.

RNA abundance in the samples was computed using the CLC Genomics Workbench (www.clcbio.com/corporate/about-clcbio/), version 5.5.1. Reads were trimmed and filtered based quality with Trim Sequences algorithm (www.clcsupport.com/ the on clcgenomicsworkbench/650/index.php?manual=Trimming.html; Maximum Limit: 0.05. ambiguities: 2). Genome sequence and annotations were downloaded from JGI (www.phytozome.net/ chlamy.php). C. reinhardtii version 5.3.1 was used. Differential expression was determined by using the numbers of mapped reads overlapping with annotated C. reinhardtii genes as inputs to DESeq, version 1.10.1 (Anders and Huber, 2010). GO analysis of RNA-Seq data was performed using Goseq, version 1.10.1 (Young et al., 2010). I used the default Wallenius approximation to calculate the over- and underrepresented GO categories among differentially expressed genes using a P value of 0.05. The hierarchical clustering and heat maps were calculated and drawn using Qlucore Omics Explorer (qlucore.com/).

RESULTS

Isolation of compromised hydrolysis of triacylglycerols Mutants

The amount of TAG in C. reinhardtii coincides with the abundance of the major lipid dropletassociated protein (MLDP) (Moellering and Benning, 2010) (Figure 2.1A). This correlation was used to identify mutants of C. reinhardtii with altered TAG degradation after the resupply of N to N-deprived cells. An immuno-dot blot-based assay for MLDP allowed us to screen indirectly for TAG abundance in a mutant population generated by random insertion of a selectable marker (Figure 2.1B). Insertion lines were cultured in N-replete medium for 48 h, followed by 48 h of N deprivation, and then resupplied with N. Typically, 24 h after N resupply, most of the TAG accumulated during N deprivation was hydrolyzed and MLDP was degraded in the parental line (PL), dw15 (Figure 2.2A). Putative mutants with a persistent MLDP immunosignal after 24 h N resupply were designated compromised hydrolysis of triacylglycerols (cht). Among the initial 1,760 insertion lines, eight putative *cht* mutants were identified, with *cht7* showing the greatest delay in MLDP degradation (Figure 2.2A). Importantly, TAG content also decreased with a severe delay in response to N resupply in cht7 (Figure 2.2B). Lipid droplets observed following Nile red staining of cells of the PL started to decrease in size after 12 h of N resupply, and by 24 h, these cells were virtually devoid of lipid droplets (Figure 2.2C). In contrast, cht7 cells retained lipid droplets even after 24 h.

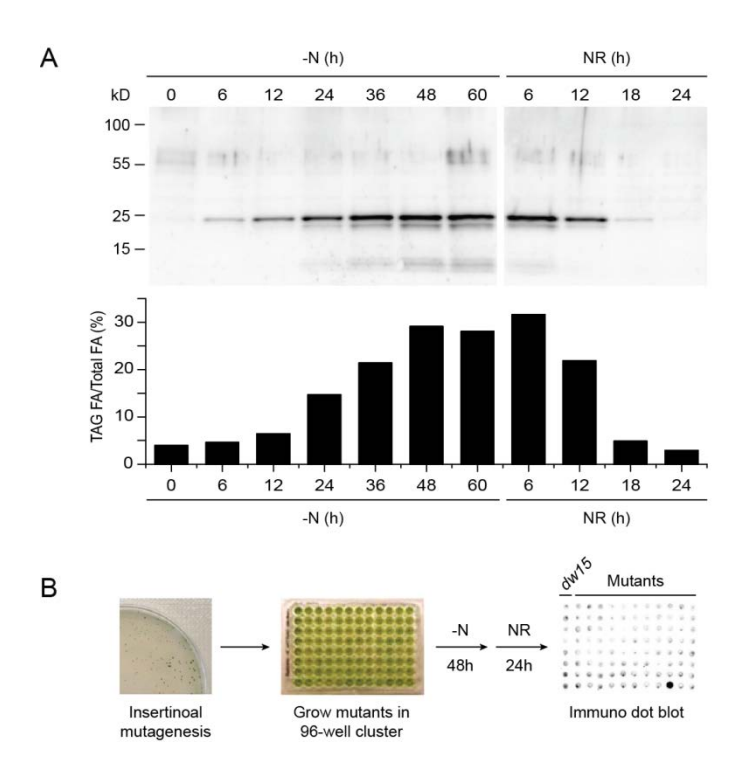


Figure 2.1. Isolation of *cht* **mutants.** (A) Immunoblot quantification of MLDP (top panel) and TAG accumulation (Bottom) in *dw15* [depicted as the ratio of TAG fatty acids (FA) over total FAs] after N deprivation (–N) followed by N resupply (NR) for the indicated times (hours). (B) Overview of the mutant isolation procedure using immunodot blots with MLDP antibodies.

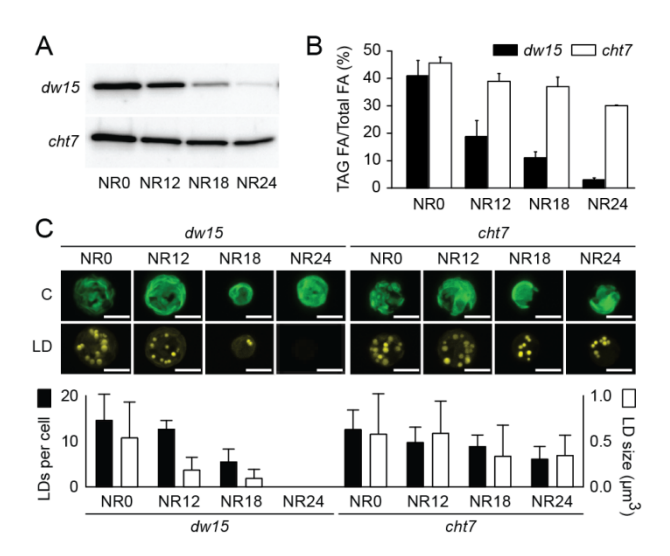


Figure 2.2. Phenotypes of *cht7*. (A) Immunoblot of MLDP in the PL (*dw15*) and *cht7* mutant following N resupply (NR) at times indicated (hours). (B) TAG degradation in *dw15* and *cht7* following N resupply. (C) Confocal microscopy images (Top) and lipid droplet quantification (Bottom) of Nile red-stained *dw15* and *cht7* cells following N resupply. Chlorophyll fluorescence (C) and Nile red fluorescence of lipid droplets (LD); scale bar, 5 μm. Lipid droplets of 5–20 cells, depending on the sample, were counted and their area was quantified with imaging software and their volume calculated. No lipid droplets were observed in *dw15* cells at NR24. SD is indicated.

CHT7 Encodes a CXC Domain DNA Binding Protein Present in the Nucleus

The *cht7* mutant was crossed to a line of the opposite mating type. Abundance of TAG in meiotic progeny following N resupply cosegregated with the antibiotic marker, suggesting that a single nuclear mutation was responsible for the lipid phenotype (Figure 2.3A). DNA/DNA hybridization blots confirmed the presence of a single insertion (Figure 2.3B). With SiteFinding-PCR (Tan et al., 2005), the flanking sequences on both ends of the inserted hygromycin B marker were mapped and a 18,087-bp deletion affecting four predicted genes was discovered (Figure 2.4A). Complementation of the defect was accomplished following transformation with a genomic fragment containing gene 1 bracketed by 1,000 bp on either side (Figure 2.3 C and D). Expression of this gene in the complemented lines was confirmed by the presence of the CHT7

protein (Figure 2.5B). Therefore, loss of gene 1 (Cre11.g481800, *C. reinhardtii* genome v5.3.1; CHT7) is the cause for the delayed TAG degradation following N resupply in *cht7*.

The predicted CHT7 protein contains two cysteine-rich motifs comprising CXC domains (Pfam 03638) (Punta et al., 2012), initially defined in human tesmin (Sugihara et al., 1999) and Arabidopsis TSO1 (Hauser et al., 2000) (Figure 2.4B). TSO1 and other CXC proteins, e.g., soybean CPP1 (Cvitanich et al., 2000), human LIN54 (Schmit et al., 2009), and Caenorhabditis elegans Lin54 (Tabuchi et al., 2011), have been shown to bind zinc (Andersen et al., 2007) and specific DNA sequences through their CXC domains. To determine whether CHT7 is located in the nucleus, I added a C-terminal green fluorescent protein (GFP) to CHT7, thereby increasing its size by 30 kDa, and introduced it into the cht7 background (Figure 2.5B). Phenotypes of cht7 were rescued in CHT7-GFP:cht7 transgenic lines (Figure 2.5C), indicating that CHT7-GFP is functional and present in its correct location. The nucleus was visualized using the DNA-binding dye Hoechst 33342 (Figure 2.4C, yellow arrows; Figure 2.5A). Aside from strong chlorophyll fluorescence delineating the chloroplast, in N-replete CHT7- GFP:cht7 transgenic lines I observed only GFP-specific signals associated with the nucleus (Figure 2.4C, white arrows). After 48 h of N deprivation, the cells were lysed when exposed to the Hoechst dye. Therefore, I examined the location of CHT7 in N-deprived cells without nuclear staining. GFP signal still was observed in the nucleus (Figure 2.4C). Because of the ambiguities related to chlorophyll fluorescence, I used cell fractionation in combination with markers and confirmed the nuclear location of CHT7 and its absence from chloroplasts (Figure 2.4D).

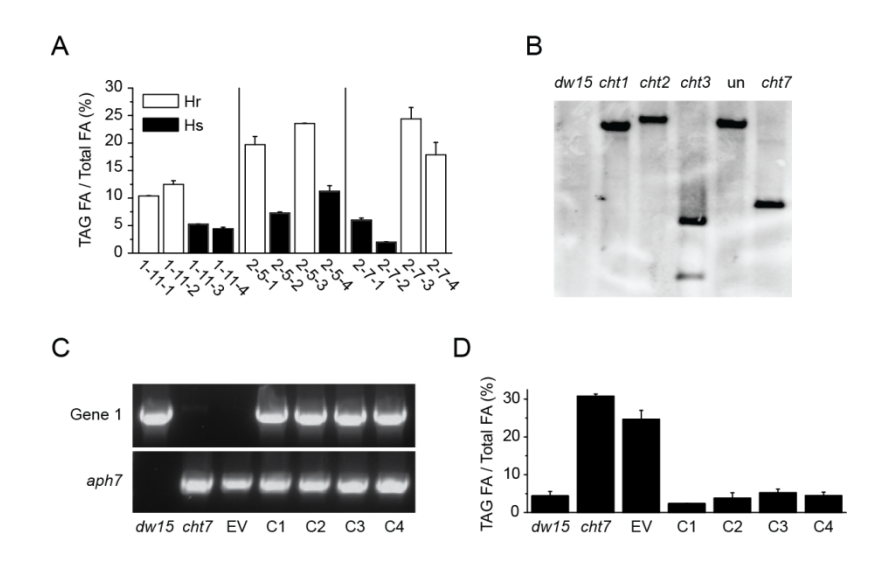


Figure 2.3. Meiotic progeny phenotyping and *cht7* **complementation.** (A) TAG content of three complete meiotic tetrads (1–11, 2–5, 2–7) after 24 h N resupply. Hr and Hs indicate hygromycin B-resistant and -sensitive lines, respectively. The ratio of fatty acids (FA) in TAGs over total FAs in the lipid extracts is shown. (B) Southern blot probed against the pHyg3 insertion indicates single insertion in the genome of *cht7*. *cht1*, *cht2* and *cht3*, mutants isolated in the same mutant screen; *dw15*, the parental line; un, unrelated mutant. (C) Genetic background of complementation lines. (Top) Amplicon targeting genomic fragment of gene 1 (refer to Fig. 2A). (Bottom) Amplicon targeting the *aph7* gene of the pHyg3 insertion. C1–4, complemented *cht7* mutant lines; EV, empty vector control. (D) Restoration of TAG degradation in four independent transgenic *cht7* lines carrying a genomic wild-type copy of gene 1. Cells were N deprived for 48 h, followed by 24 h N resupply. Averages (n = 3) and SDs are given.

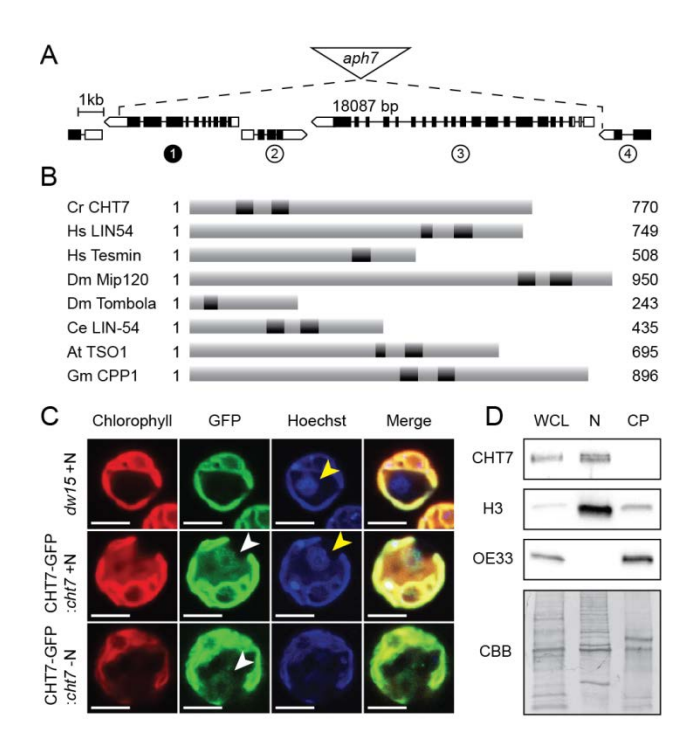


Figure 2.4. CHT7 is a CXC domain-containing protein present in the nucleus. (A) Structure of the *cht7* genomic locus with gene 1 corresponding to CHT7. Black boxes, exons; white boxes, untranslated regions; arrow points, 3'-ends of ORFs. (B) Different CXC-domain proteins from different species: At, *Arabidopsis thaliana*; Ce, *Caenorhabditis elegans*; Cr, *C. reinhardtii*; Dm, *Drosophila melanogaster*; Gm, *Glycine max*; Hs, *Homo sapiens*. Black boxes, CXC domains. (C) Nuclear localization of CHT7-GFP by confocal microscopy in N-replete (+N) or N-deprived (-N) cells. The PL (*dw15*) and a transgenic line expressing EGFP-tagged CHT7 under the regulation of the endogenous CHT7 promoter in the *cht7* mutant background (CHT7-GFP:*cht7*) are shown. The nuclear CHT7-GFP signal is marked by white arrows. The nuclei were stained with Hoechst 33342 (marked by yellow arrows). (D) Enrichment of CHT7 in nuclear extracts shown by immunoblot. Five micrograms of protein was loaded into each well. Markers: chloroplast (CP), OE33; nucleus (N), histone 3 (H3). CBB, Coomassie Brilliant Blue; WCL, whole-cell lysate.

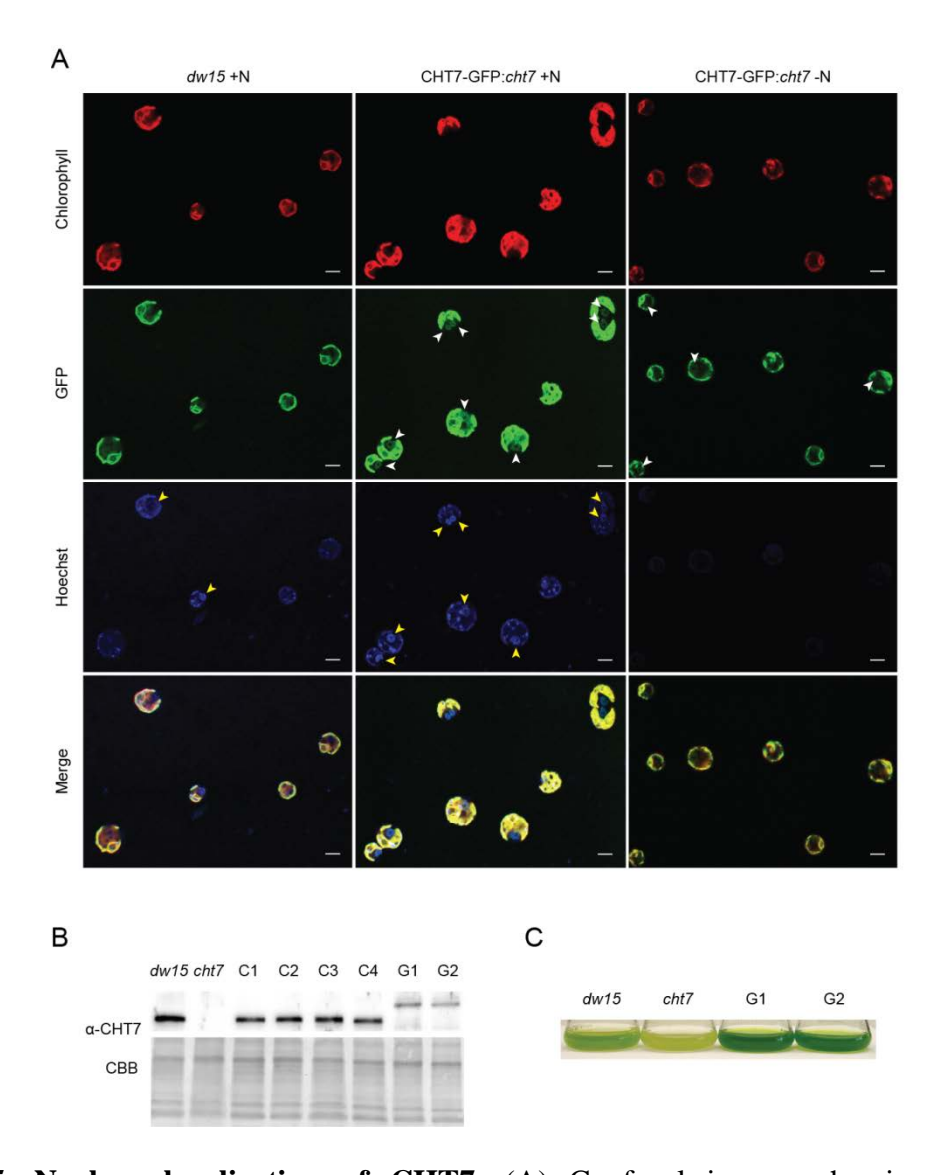


Figure 2.5. Nuclear localization of CHT7. (A) Confocal images showing the nuclear localization of CHT7 in N replete (+N) or N deprived (-N) cells. Fluorescence was detected in the parental line (dw15) and a transgenic line expressing EGFP-tagged CHT7 under the regulation of the endogenous CHT7 promoter in the cht7 mutant background (CHT7-GFP:cht7). The nuclear CHT7-GFP signal is marked by white arrows. The nuclei were stained with Hoechst 33342 (marked by yellow arrows). (B) CHT7 protein levels at midlog growth detected by immunoblot using CHT7 antiserum (α-CHT7). Equal total protein was loaded as shown by Coomassie Brilliant Blue (CBB) staining. G1 and G2, two independent lines of CHT7-GFP:cht7. (C) Restoration of the growth phenotype of two cht7 lines producing a CHT7-GFP fusion. Cells were N deprived for 48 h, followed by 24 h of N resupply.

Absence of CHT7 Affects the Exit from Quiescence but Not Cell Viability

Growth of the cht7 mutant was normal in N-replete medium under standard conditions (Figure 2.6A). However, when cht7 cells in liquid cultures had been deprived of N, which then was resupplied, growth was severely delayed (Figure 2.6B). This delay in growth and the delay in TAG degradation following N resupply (Figure 2.2B) suggested that the *cht*7 mutant struggles to reverse quiescence either because of its inability to correctly perceive the N status of cells during resupply of N, because cht7 cells simply lose viability following N deprivation, or because of a general defect in the regulation of quiescence. To rule out the possibility of a specific N-sensing defect in cht7, I tested induction of quiescence by phosphate deprivation (Figure 2.6C and Figure 2.7A). The cht7 mutant also showed delayed regrowth when phosphate was resupplied to a deprived culture, suggesting a more general defect than N sensing. In yeast and many other organisms, the nutrient status of the cell to a large extent is integrated with progression through the cell cycle by the TOR (target of rapamycin) signaling pathway (Gray et al., 2004). Typically, rapamycin treatment induces quiescence, and I tested the effect of its removal in cht7. A saturating concentration of rapamycin (1 µM) as established for C. reinhardtii (Perez-Perez et al., 2010) doubled the time needed for division of the PL (23.9 h) and slightly more so for cht7 (30.1 h) (Figure 2.7B). A striking difference was seen when rapamycin was removed: the *cht7* mutant was much slower to regrow, similar to the effect of nutrient resupply (Figure 2.6D and Figure 2.7C). Thus, the defect in *cht7* affects the ability of cells to exit quiescence, regardless of how it is induced.

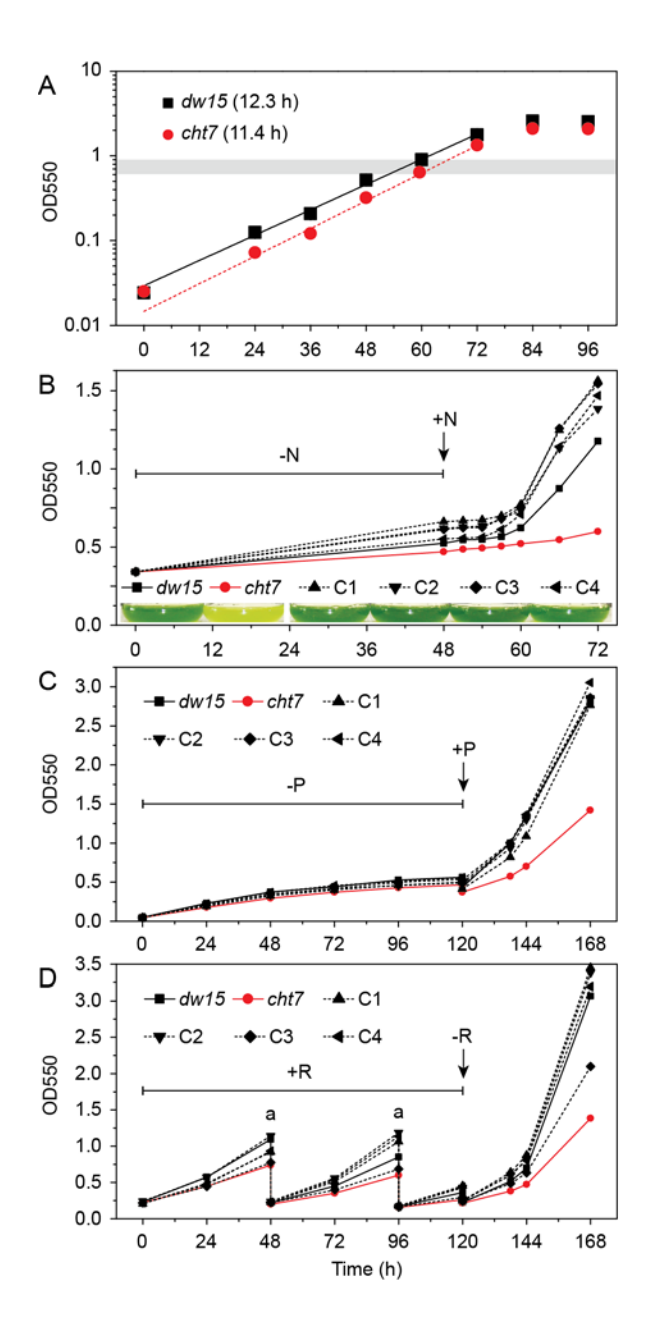


Figure 2.6. Growth of *cht7* **affected by different treatments.** (A) Growth of *cht7* and PL (*dw15*) on N-replete medium (OD at 550 nm). Doubling times are given in parentheses. The gray bar indicates the OD at which N-replete samples were taken for all experiments in this study. Averages of three biological replicates are given, with SDs for all points being smaller than 3%. (B) Growth of *dw15*, *cht7*, and four independent complementation lines (C1–4) during N deprivation (-N) followed by N resupply (+N) measured at the times indicted. (Inset) Cultures at 24 h following N resupply. (C) Growth during phosphate deprivation (-P) followed by P resupply (+P). (D) Growth in the medium with 1 μM rapamycin (+R) followed by the removal of rapamycin (-R). Cultures were diluted twice (a) with medium containing 1 μM rapamycin to avoid reaching stationary phase.

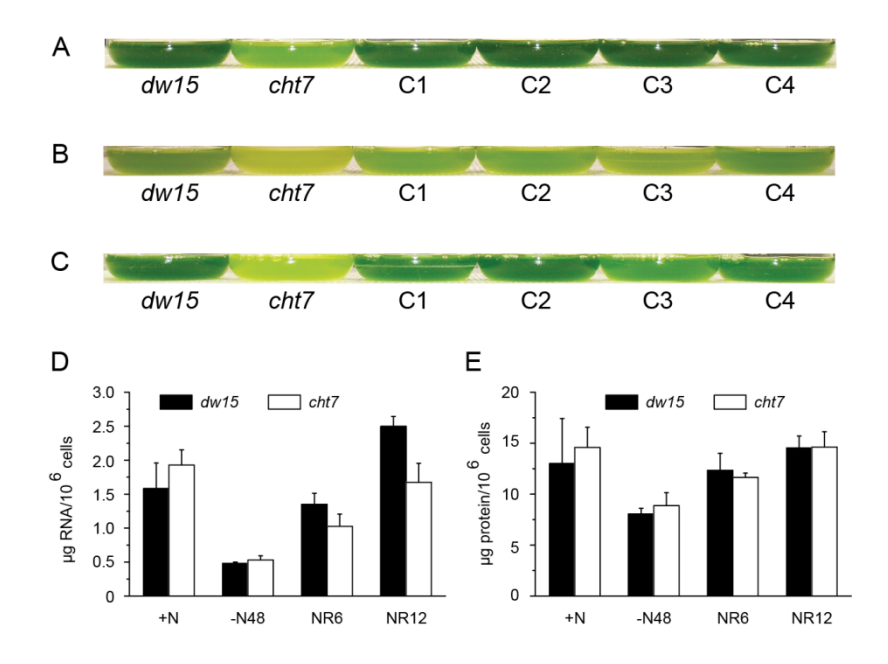


Figure 2.7. Growth, RNA, and protein of *cht7* affected by different treatments. (A) Cultures of dw15, cht7, and four complementation lines (C1–4) at 48 h following P resupply. (B) Cultures after 120 h of rapamycin treatment. (C) Cultures at 48 h following the removal of rapamycin. (D and E) RNA (D) and protein (E) contents of dw15 and cht7 cells in the presence (+N) and absence (-N) of N or following N resupply (NR) at the times (hours) indicated. For all quantitative data, averages (n = 3) and SD are indicated.

One trivial explanation for the growth phenotype is that most *cht7* cells cannot survive N deprivation. The number and integrity of cells were assessed by using a hemocytometer and SYTOX Green, which does not penetrate living cells but stains the nuclear DNA of nonviable or partially lysed cells (Sato et al., 2004). Parallel cultures of PL and *cht7* had a similar number of intact cells (Figure 2.8A), and cells were similarly viable (Figure 2.8B) during the 5 d following N deprivation. Moreover, following N deprivation, *cht7* cells changed their metabolism to accumulate TAG (Figure 2.2, NR0) and they decreased RNA and protein synthesis (Figure 2.7 D and E). In addition, *cht7* cells increased RNA and protein synthesis following N resupply in parallel to the PL (Figure 2.7 D and E). It should also be noted that *cht7* cells were capable of normal mating following N deprivation. Therefore, the mutant had no defect in gametogenesis. Thus, I concluded that *cht7* cells had not lysed, were viable, and were metabolically active and

mating competent following N deprivation. However, when plated on agar-solidified N-replete medium at different times of N deprivation, the efficiency of *cht7* colony formation (observed 11 d after plating and again after an additional 14 d with no further increase in numbers) decreased during the first 24 h following N deprivation to ~20%, compared with 80% for the PL (Figure 2.8C), and remained there. Presumably, during the first 24 h as *cht7* cells become increasingly N-deprived, they enter quiescence, after which only 20% of the cells pass an apparent threshold or checkpoint, allowing for colony formation. These *cht7* colonies had a decreased diameter (Figure 2.8D) consistent with a delay in resumption of cell division. When the *cht7* colonies were transferred to N-replete liquid medium, they grew at a rate similar to that of PL but again showed a delay in regrowth after N deprivation followed by resupply, recapitulating the original *cht7* phenotype (Figure 2.8C, Inset). Together, these observations are consistent with a regulatory defect in *cht7* preventing most *cht7* cells from orderly progression out of quiescence to resume normal growth, even though they are viable and metabolically active during N deprivation.

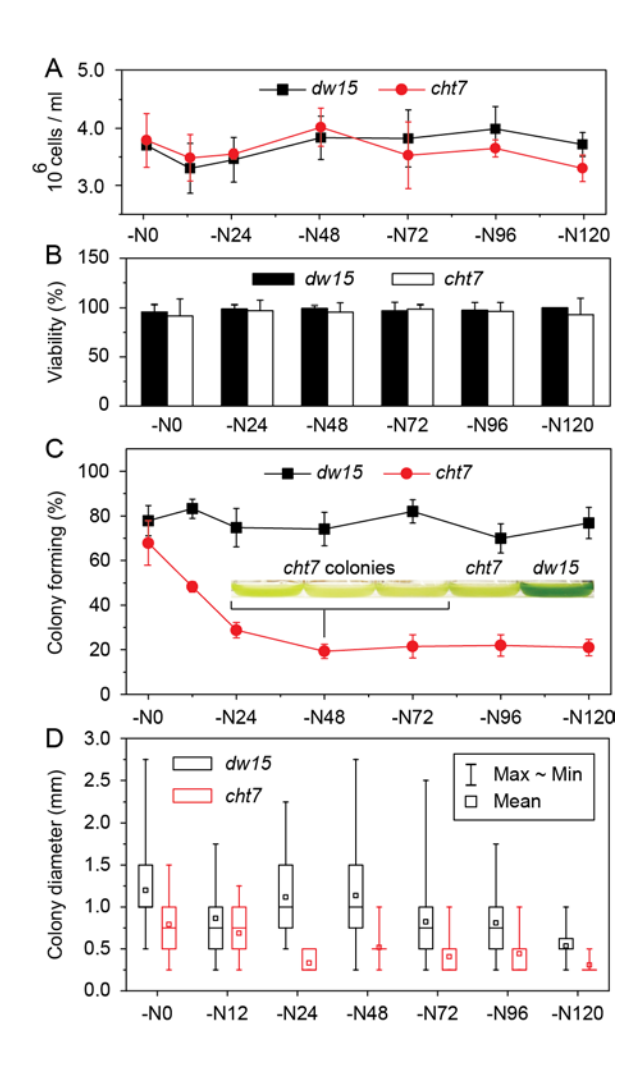


Figure 2.8. Viability and colony formation of *cht7* during N deprivation. (A) Cell concentration of PL *dw15* and *cht7* during N deprivation (-N) at times (h) indicated, determined by using a hemocytometer. The averages of three to six measurements and SDs are indicated. (B) SYTOX Green viability staining of *dw15* and *cht7* cells shown in A at times indicated. Approximately 10–20 images showing 5–10 cells each were examined and averaged per time point. SD between images is indicated. (C) Colony formation of N-deprived (-N) *dw15* and *cht7* plated on N-replete solid medium at times indicated and incubated for 11 d. The average percentage of plated cells forming a colony on three plates is given. SD is indicated. (Inset) Three liquid cultures derived from *cht7* colonies from this experiment (-N48), the original *cht7* mutant, and *dw15* PL first grown in N-replete medium then N deprived, followed by N resupply and growth for 24 h, recapitulating the original phenotype. (D) Size of the colonies formed by the N-deprived cells after plating on N-replete medium. All colonies on one plate were analyzed, with n ranging from 6 to 70 (usually fewer for *cht7*). Mean, maximum, minimum, and quartile values are indicated. Data points in all panels (A–D) were obtained in the same experiment.

Absence of CHT7 Partially Derepresses Quiescence-Associated Transcriptional Programs

Because CHT7 resembles known DNA binding proteins, I asked whether a change in global transcriptional profiles during or even before entering quiescence might explain the observed phenotypes of *cht7*. Global transcript profiles of *cht7* and the PL were compared by RNA sequencing (RNA-Seq) during midlog phase of an N-replete culture and after 48 h of N deprivation [Figure 2.10A; for complete data sets and enriched Gene Ontology (GO) categories, refer to Online Supplemental Data Sets 1 and 2]. To confirm the findings obtained by RNA-Seq and to test for effects specific to the loss of CHT7, the expression of selected genes was tested by quantitative PCR (qPCR) in the PL, *cht7*, and multiple complementation lines. The expression of selected genes observed by RNA-Seq (three independent biological repeats) was comparable to that measured by qPCR (correlation coefficient R2 = 0.8065; Figure 2.10B).

In line with previously reported transcriptional changes for *C. reinhardtii* (Miller et al., 2010; Blaby et al., 2013; Schmollinger et al., 2014) following N deprivation, 2,647 genes were upregulated and 3,346 down-regulated in PL (*dw15*) N-deprived cells compared with PL N-replete cells (Figure 2.9A, blue circles; twofold cutoff, P < 0.05). Comparing *cht7* N-replete with PL N-replete cells, 1,477 genes were found up-regulated and 1,491 down-regulated in *cht7* (Figure 2.9A, yellow circles). Most strikingly, there was a substantial overlap in genes upregulated (573) and down-regulated (894) between the two comparisons (Figure 2.9A, intersecting blue and yellow circles; Online Supplemental Data Set 3). In other words, a subset of genes, i.e., 49% of all genes that were misregulated in *cht7* during N-replete conditions, were expressed as if the cells had already entered quiescence. Examples are genes involved in photosynthesis, such as *PSBS1*, *MCA1*, *NAB1*, and *LHCBM4*, and genes related to flagellum assembly, such as *FA1*, *FA2*, *FAP139*, and *IFT46* (Figure 2.9B; Figure 2.10 C–E for qPCR

confirmation). Autophagy is a hallmark of quiescence, and autophagy markers APG8 (Cre16.g689650) (Perez-Perez et al., 2010; Klionsky et al., 2012) and APG3 (Cre02. g102350) were constitutively expressed in cht7, although at lower levels than in the PL following N deprivation. To further explore this pattern of transcriptional alterations in N-replete cht7, I asked whether these misregulated genes represent meaningful biological functions. In the PL Ndeprived versus PL N-replete comparison (Figure 2.9A, blue circles), differentially expressed genes were enriched in 68 GO categories, with 18 GO categories associated with flagellum assembly and 21 with photosynthesis (Online Supplemental Data Set 2). Differentially expressed genes in the cht7 N-replete versus PL N-replete comparison (Figure 2.9A, yellow circles) fell into six enriched GO categories, one of which was associated with flagellum assembly and two with photosynthesis. Indeed, virtually every gene involved in photosynthesis and 171 of 320 genes associated with flagellum assembly tended to be differentially regulated in the same manner in both comparisons (Figure 2.10 A, F, and G), but not necessarily to the same extent. In most cases, differential gene expression was less pronounced in the cht7 N-replete versus PL Nreplete comparison than in the PL N-deprived versus PL N-replete comparison (Figure 2.9B; Figure 2.10 A, F, and G; and Online Supplemental Data Set 3).

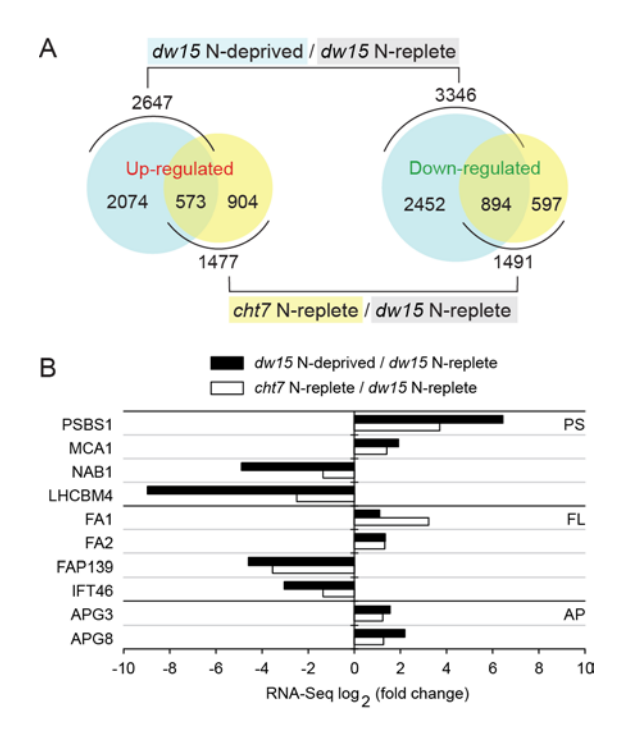


Figure 2.9. Global gene expression comparison of N-replete and -deprived cells of PL *dw15* **and** *cht7*. (A) Large circles: total number of genes changed in expression in a comparison of *dw15* N deprived for 48 h and *dw15* N replete (never deprived of N). Small circles: total number of genes changed in expression in a comparison of the *cht7* mutant N replete and *dw15* N replete. Circle size is proportional to the number of genes. (B) RNA-Seq log2 (fold change) of representative genes encoding the indicated proteins related to photosynthesis (PS), flagellum (FL), or autophagy (AP).

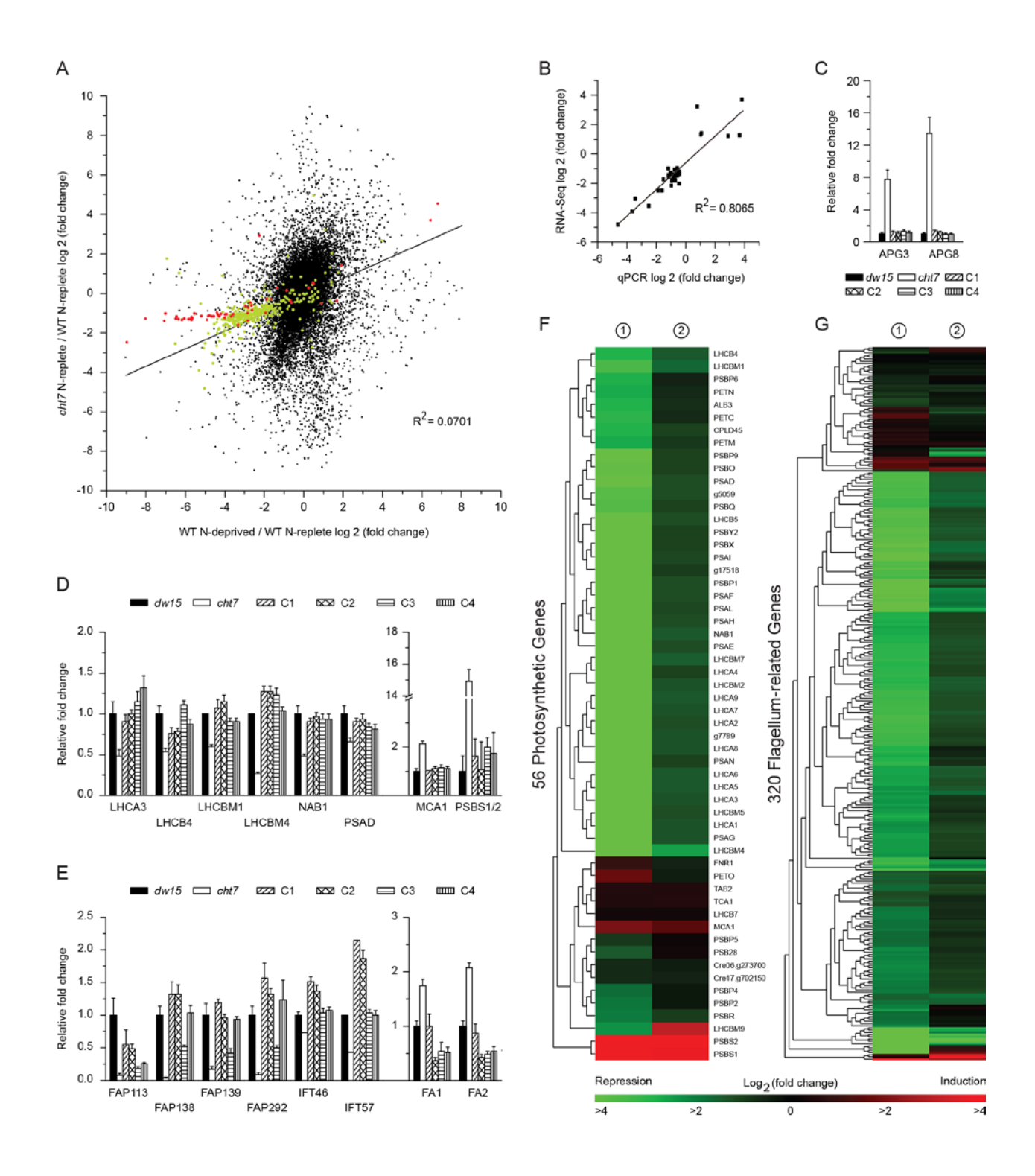


Figure 2.10. Confirmation of transcriptional changes by qPCR and analysis of photosynthesis and flagellum-related genes. (A) Scatter plot of all genes in the RNASeq comparisons (dw15 N-deprived/dw15 N-replete against cht7 N-replete/dw15 N-replete). Genes involved in photosynthesis are shown in red, those involved in flagellum assembly in green. (B) Comparison of fold change in abundance of transcripts for the comparison cht7 N-replete and dw15 N-replete obtained by quantification of RNA levels by qPCR analysis (x-axis) or RNA-Seq

Figure 2.10 (cont'd)

experiments (y-axis). (C) qPCR analysis of autophagy marker genes (APG, autophagy-related protein; dw15, parental line; cht7 mutant; C1–4, complemented cht7 mutant lines) in N-replete medium. Averages and SD are indicated. At least two biological replicates were included in the analysis. (D and E) qPCR analysis of selected photosynthetic genes (D) and flagellum-related genes (E) in N-replete medium. Genes down-regulated in cht7 are shown in the left graph, genes up-regulated in cht7 in the right graph. Averages and SD are indicated. At least two biological replicates were included in the analysis. (F and G) Cluster analysis showing transcript profiles of photosynthetic genes (F) and flagellum-related genes (G). The set of genes was clustered hierarchically into groups on the basis of the similarity of their expression profiles. The expression pattern of each gene is displayed here as a heat map according to the color scale at the bottom. Heat map beneath "1" represents the ratio of mRNA levels in N-deprived dw15 to N-replete dw15. Heat map beneath "2" represents the ratio of mRNA levels in N-replete cht7 to N-replete dw15. Included here are all relevant genes, including those that fall below the twofold threshold.

CHT7 Levels Remain Constant in Response to the N Supply, and CHT7 Is in a Large Complex

One may hypothesize that to exert its effects on gene expression related to quiescence, CHT7 abundance changes in response to the N supply. However, immunoblotting indicated that CHT7 protein abundance (see Figure 2.12A for purity of CHT7 antiserum) was relatively constant during the conditions tested, which included N deprivation and several time points following resupply of N (Figure 2.11A). Using blue native (BN) gel electrophoresis, I also determined that CHT7 is part of a larger protein complex that does not change in apparent size or abundance following N deprivation (Figure 2.11B; see Figure 2.12B for 2D electrophoresis).

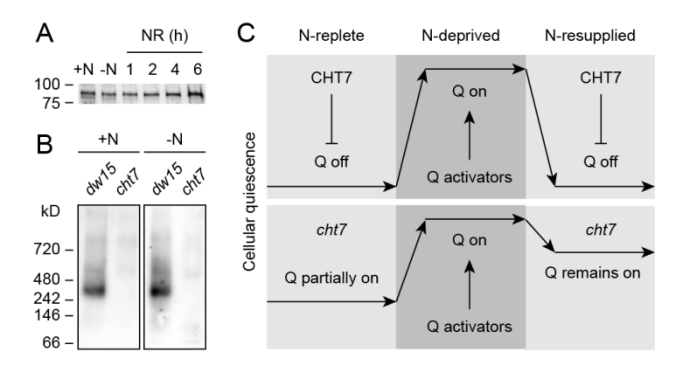


Figure 2.11. Abundance of CHT7 and hypothesis for CHT7 function. (A) Anti-CHT7 immunoblot showing CHT7 protein levels in the presence (+N) and absence of N (-N) or after N resupply (NR) at times (hours) indicated. Equal amounts of protein were loaded. (B) Immunodetection of a high molecular weight CHT7 complex by BN-PAGE. Whole-cell lysates were loaded at equal protein, and *cht7* was used as a negative control to discriminate against nonspecific signals. *dw15*, PL of *cht7*; +N, N replete; –N, N deprived. (C) We hypothesize that CHT7 acts as a repressor in safeguarding against the premature activation of global transcriptional changes associated with quiescence (Q) during N-replete growth and also to fully revert quiescence after N resupply. Activators of quiescence are postulated to fully turn on quiescence following N deprivation, but their inactivation after N resupply is insufficient in the absence of CHT7 to restore growth.

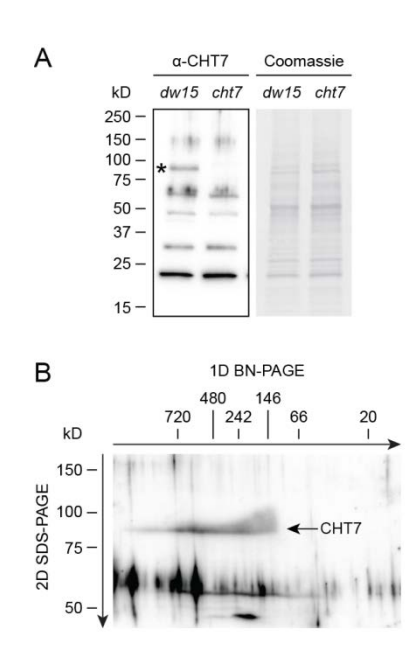


Figure 2.12. Immunodetection of CHT7 and 2D BN-SDS-PAGE. (A) Immunoblot of whole-cell lysates from parental line dw15 or cht7 mutant probed with CHT7 antibodies (α -CHT7). The migration of CHT7 at its predicted molecular weight is indicated by an asterisk. Nonspecific binding to other proteins recognized by the antibodies is shown but did not interfere with specific

Figure 2.12 (cont'd)

CHT7 detection, as the CHT7 signal is missing in *cht7* extracts. (B) Cell lysates of N-replete parental line *dw15* were analyzed in the first dimension by BN-PAGE (1D BN-PAGE, marker at top) and then denatured and run on SDS-PAGE in the second dimension (2D SDS-PAGE, marker at left) followed by anti-CHT7 immunoblot. CHT7 is indicated by the arrow.

DISCUSSION

Regulatory proteins that participate in the integration of the metabolic status of the cell with cell cycle activity are of fundamental biological importance and also are potential targets to maximize algal biomass and its TAG content by engineering. The unicellular alga C. reinhardtii provides an excellent genetic model for a photosynthetic eukaryotic cell, in which nutrient status may be manipulated readily to induce and reverse cellular quiescence. Hence, I isolated a mutant, cht7, affected in the reversal of N deprivation-induced quiescence, i.e., the degradation of lipid droplet protein MLDP and TAG, and the regrowth of algal mutant cultures when N is resupplied. I have ruled out several trivial explanations for this phenotype, including loss of viability of the mutant during N deprivation or a specific deficiency in an N-signaling pathway. The delay in regrowth in response to phosphate refeeding and after removal of rapamycin-induced quiescence of cht7 (Figure 2.6 C and D) points to a more general defect in cht7 in the integration of the nutrient status of the cell with the cell cycle. CHT7 likely is localized in the nucleus and contains a putative CXC DNA binding motif (Figure 2.4) consistent with its possible role as a regulator of gene expression. Thus, I hypothesized and subsequently showed that CHT7 affects transcriptional programs associated with N deprivation-induced quiescence. A subset of genes normally up- or down-regulated is misregulated in cht7 under N-replete conditions, consistent with a partial derepression of transcriptional programs characteristic for quiescence. The extent of these changes in the expression of individual genes, as well as the number of genes affected, is smaller than observed following full induction of quiescence in response to N deprivation in the PL, which may explain the apparent lack of a growth phenotype of cht7 under the N-replete conditions tested (Figure 2.6A). Thus, although quiescence programs are fully off under Nreplete conditions in the PL, they are partially on in cht7, as summarized in the model in Figure

2.11C. Based on this observation, CHT7 appears to act as a repressor of a subfraction of the transcriptional program associated with quiescence. During N deprivation, activators likely come into play to establish full quiescence to the same extent in *cht7* and the PL, as they behave similarly: for example, accumulating TAG and ceasing to divide without loss of viability. However, the delayed growth of *cht7* following N resupply suggests that CHT7 is needed to turn off quiescence-associated programs to reestablish growth rapidly (Figure 2.11C). One may postulate that any number of repressors and activators of quiescence have to be balanced out during quiescence exit and that the absence of CHT7 in the mutant shifts this balance. Assuming the involvement of multiple inputs and regulatory components besides CHT7 to govern quiescence, the apparent threshold phenomenon documented in the ability of ~20% of N-deprived *cht7* cells to "escape deep quiescence" (Figure 2.8C) seems plausible.

The delay in regrowth of the *cht7* mutant when resupplied with N following deprivation is similar to the phenotype of the *mat3* mutant (Armbrust et al., 1995). MAT3 is a *C. reinhardtii* ortholog of the mammalian retinoblastoma tumor suppressor protein (Rb) (Sadasivam and DeCaprio, 2013). Both CHT7 and Rb/MAT3 are present in the *C. reinhardtii* nucleus throughout the cell cycle (Olson et al., 2010). However, the absence of Rb/MAT3 leads to drastically reduced cell size, an essential cue in *C. reinhardtii* for decisions made during cell cycle progression, whereas *cht7* cell size is normal (Figure 2.4C and Figure 2.5A). In general, Rb interacts directly with DNA-binding proteins, such as members of the E2F and DP protein families, to repress genes required for cell cycle progression during quiescence (Olson et al., 2010; Sadasivam and DeCaprio, 2013). CXC domain proteins in animals have been found in large multiprotein complexes involved in transcriptional regulation that also contain Rb (Sadasivam and DeCaprio, 2013). Thus, the fact that CHT7 is a CXC domain protein present in a

large complex (Figure 2.11B) leads to intriguing questions regarding the precise regulatory function of CHT7, such as whether CHT7 and Rb/MAT3 might cooperate in the regulation of quiescence.

The persistence of CHT7 before, during, and after quiescence (Figure 2.11A) suggests that fluctuation of its abundance likely is not part of the regulatory mechanism determining entry and exit into and out of quiescence. Changes in abundance or size of the CHT7 complex during quiescence also were not observed (Figure 2.11B). Movement of CHT7 in and out of the nucleus also seems an unlikely mechanism to modulate CHT7, as I observed the protein in the nucleus before and during N deprivation (Figure 2.4C). However, I currently cannot rule out posttranslational modifications of CHT7 depending on the nutritional status of the cell that may modulate its possible DNA binding preferences.

As summarized in Figure 2.11C, all current data point toward a role of CHT7 as a repressor of a subset of transcriptional programs associated with nutrient deprivation-induced quiescence. Its activity likely is balanced by other regulatory factors, such as activators of quiescence. Its loss causes partial derepression of quiescence-associated transcriptional programs during N-replete conditions; CHT7 apparently is not needed for full establishment of quiescence during N deprivation, but its absence prevents the orderly and rapid exit from quiescence following N refeeding. As such, CHT7 is a candidate regulatory factor involved in the integration of the metabolic status of the cell and cell division, and its discovery provides a unique entry point for a more in-depth study of the regulation of cellular quiescence and the discovery of additional factors involved.

REFERENCES

REFERENCES

- Allen, M.D., Kropat, J., Tottey, S., Del Campo, J.A., and Merchant, S.S. (2007). Manganese deficiency in Chlamydomonas results in loss of photosystem II and MnSOD function, sensitivity to peroxides, and secondary phosphorus and iron deficiency. Plant physiology 143, 263-277.
- **Anders, S., and Huber, W.** (2010). Differential expression analysis for sequence count data. Genome biology **11**, R106.
- Andersen, S.U., Algreen-Petersen, R.G., Hoedl, M., Jurkiewicz, A., Cvitanich, C., Braunschweig, U., Schauser, L., Oh, S.A., Twell, D., and Jensen, E.O. (2007). The conserved cysteine-rich domain of a tesmin/TSO1-like protein binds zinc in vitro and TSO1 is required for both male and female fertility in Arabidopsis thaliana. Journal of experimental botany 58, 3657-3670.
- **Armbrust, E.V., Ibrahim, A., and Goodenough, U.W.** (1995). A mating type-linked mutation that disrupts the uniparental inheritance of chloroplast DNA also disrupts cell-size control in Chlamydomonas. Molecular biology of the cell **6,** 1807-1818.
- **Beck, C.F., and Acker, A.** (1992). Gametic Differentiation of Chlamydomonas reinhardtii: Control by Nitrogen and Light. Plant physiology **98,** 822-826.
- Blaby, I.K., Glaesener, A.G., Mettler, T., Fitz-Gibbon, S.T., Gallaher, S.D., Liu, B., Boyle, N.R., Kropat, J., Stitt, M., Johnson, S., Benning, C., Pellegrini, M., Casero, D., and Merchant, S.S. (2013). Systems-level analysis of nitrogen starvation-induced modifications of carbon metabolism in a Chlamydomonas reinhardtii starchless mutant. The Plant cell **25**, 4305-4323.
- Boyle, N.R., Page, M.D., Liu, B., Blaby, I.K., Casero, D., Kropat, J., Cokus, S.J., Hong-Hermesdorf, A., Shaw, J., Karpowicz, S.J., Gallaher, S.D., Johnson, S., Benning, C., Pellegrini, M., Grossman, A., and Merchant, S.S. (2012). Three acyltransferases and nitrogen-responsive regulator are implicated in nitrogen starvation-induced triacylglycerol accumulation in Chlamydomonas. The Journal of biological chemistry 287, 15811-15825.
- Bustin, S.A., Benes, V., Garson, J.A., Hellemans, J., Huggett, J., Kubista, M., Mueller, R., Nolan, T., Pfaffl, M.W., Shipley, G.L., Vandesompele, J., and Wittwer, C.T. (2009). The MIQE guidelines: minimum information for publication of quantitative real-time PCR experiments. Clinical chemistry 55, 611-622.
- Cvitanich, C., Pallisgaard, N., Nielsen, K.A., Hansen, A.C., Larsen, K., Pihakaski-Maunsbach, K., Marcker, K.A., and Jensen, E.O. (2000). CPP1, a DNA-binding

- protein involved in the expression of a soybean leghemoglobin c3 gene. Proceedings of the National Academy of Sciences of the United States of America **97**, 8163-8168.
- Fernandez, E., Schnell, R., Ranum, L.P., Hussey, S.C., Silflow, C.D., and Lefebvre, P.A. (1989). Isolation and characterization of the nitrate reductase structural gene of Chlamydomonas reinhardtii. Proceedings of the National Academy of Sciences of the United States of America 86, 6449-6453.
- Goodson, C., Roth, R., Wang, Z.T., and Goodenough, U. (2011). Structural correlates of cytoplasmic and chloroplast lipid body synthesis in Chlamydomonas reinhardtii and stimulation of lipid body production with acetate boost. Eukaryotic cell 10, 1592-1606.
- Gray, J.V., Petsko, G.A., Johnston, G.C., Ringe, D., Singer, R.A., and Werner-Washburne, M. (2004). "Sleeping beauty": quiescence in Saccharomyces cerevisiae. Microbiology and molecular biology reviews: MMBR 68, 187-206.
- **Harris, E.H.** (1989). Chlamydomonas Sourcebook. (New York: Academic Press: New York: Academic Press).
- Hauser, B.A., He, J.Q., Park, S.O., and Gasser, C.S. (2000). TSO1 is a novel protein that modulates cytokinesis and cell expansion in Arabidopsis. Development 127, 2219-2226.
- Hu, Q., Sommerfeld, M., Jarvis, E., Ghirardi, M., Posewitz, M., Seibert, M., and Darzins, A. (2008). Microalgal triacylglycerols as feedstocks for biofuel production: perspectives and advances. The Plant journal: for cell and molecular biology **54**, 621-639.
- Klionsky, D.J., Abdalla, F.C., Abeliovich, H., Abraham, R.T., Acevedo-Arozena, A., Adeli, K., Agholme, L., Agnello, M., Agostinis, P., Aguirre-Ghiso, J.A., Ahn, H.J., Ait-Mohamed, O., Ait-Si-Ali, S., Akematsu, T., Akira, S., Al-Younes, H.M., Al-Zeer, M.A., Albert, M.L., Albin, R.L., Alegre-Abarrategui, J., Aleo, M.F., Alirezaei, M., Almasan, A., Almonte-Becerril, M., Amano, A., Amaravadi, R., Amarnath, S., Amer, A.O., Andrieu-Abadie, N., Anantharam, V., Ann, D.K., Anoopkumar-Dukie, S., Aoki, H., Apostolova, N., Arancia, G., Aris, J.P., Asanuma, K., Asare, N.Y., Ashida, H., Askanas, V., Askew, D.S., Auberger, P., Baba, M., Backues, S.K., Baehrecke, E.H., Bahr, B.A., Bai, X.Y., Bailly, Y., Baiocchi, R., Baldini, G., Balduini, W., Ballabio, A., Bamber, B.A., Bampton, E.T., Banhegyi, G., Bartholomew, C.R., Bassham, D.C., Bast, R.C., Jr., Batoko, H., Bay, B.H., Beau, I., Bechet, D.M., Begley, T.J., Behl, C., Behrends, C., Bekri, S., Bellaire, B., Bendall, L.J., Benetti, L., Berliocchi, L., Bernardi, H., Bernassola, F., Besteiro, S., Bhatia-Kissova, I., Bi, X., Biard-Piechaczyk, M., Blum, J.S., Boise, L.H., Bonaldo, P., Boone, D.L., Bornhauser, B.C., Bortoluci, K.R., Bossis, I., Bost, F., Bourquin, J.P., Boya, P., Boyer-Guittaut, M., Bozhkov, P.V., Brady, N.R., Brancolini, C., Brech, A., Brenman, J.E., Brennand, A., Bresnick, E.H., Brest, P., Bridges, D., Bristol, M.L., Brookes, P.S., Brown, E.J., Brumell, J.H., Brunetti-Pierri, N., Brunk, U.T., Bulman, D.E., Bultman, S.J., Bultynck, G., Burbulla, L.F., Bursch, W., Butchar, J.P., Buzgariu, W., Bydlowski, S.P., Cadwell, K., Cahova, M., Cai, D., Cai, J., Cai, Q., Calabretta, B., Calvo-Garrido, J., Camougrand, N., Campanella, M., Campos-Salinas, J., Candi, E., Cao,

L., Caplan, A.B., Carding, S.R., Cardoso, S.M., Carew, J.S., Carlin, C.R., Carmignac, V., Carneiro, L.A., Carra, S., Caruso, R.A., Casari, G., Casas, C., Castino, R., Cebollero, E., Cecconi, F., Celli, J., Chaachouay, H., Chae, H.J., Chai, C.Y., Chan, D.C., Chan, E.Y., Chang, R.C., Che, C.M., Chen, C.C., Chen, G.C., Chen, G.Q., Chen, M., Chen, Q., Chen, S.S., Chen, W., Chen, X., Chen, X., Chen, X., Chen, Y.G., Chen, Y., Chen, Y.J., Chen, Z., Cheng, A., Cheng, C.H., Cheng, Y., Cheong, H., Cheong, J.H., Cherry, S., Chess-Williams, R., Cheung, Z.H., Chevet, E., Chiang, H.L., Chiarelli, R., Chiba, T., Chin, L.S., Chiou, S.H., Chisari, F.V., Cho, C.H., Cho, D.H., Choi, A.M., Choi, D., Choi, K.S., Choi, M.E., Chouaib, S., Choubey, D., Choubey, V., Chu, C.T., Chuang, T.H., Chueh, S.H., Chun, T., Chwae, Y.J., Chye, M.L., Ciarcia, R., Ciriolo, M.R., Clague, M.J., Clark, R.S., Clarke, P.G., Clarke, R., Codogno, P., Coller, H.A., Colombo, M.I., Comincini, S., Condello, M., Condorelli, F., Cookson, M.R., Coombs, G.H., Coppens, I., Corbalan, R., Cossart, P., Costelli, P., Costes, S., Coto-Montes, A., Couve, E., Coxon, F.P., Cregg, J.M., Crespo, J.L., Cronje, M.J., Cuervo, A.M., Cullen, J.J., Czaja, M.J., D'Amelio, M., Darfeuille-Michaud, A., Davids, L.M., Davies, F.E., De Felici, M., de Groot, J.F., de Haan, C.A., De Martino, L., De Milito, A., De Tata, V., Debnath, J., Degterey, A., Dehay, B., Delbridge, L.M., Demarchi, F., Deng, Y.Z., Dengjel, J., Dent, P., Denton, D., Deretic, V., Desai, S.D., Devenish, R.J., Di Gioacchino, M., Di Paolo, G., Di Pietro, C., Diaz-Araya, G., Diaz-Laviada, I., Diaz-Meco, M.T., Diaz-Nido, J., Dikic, I., Dinesh-Kumar, S.P., Ding, W.X., Distelhorst, C.W., Diwan, A., Djavaheri-Mergny, M., Dokudovskaya, S., Dong, Z., Dorsey, F.C., Dosenko, V., Dowling, J.J., Doxsey, S., Dreux, M., Drew, M.E., Duan, Q., Duchosal, M.A., Duff, K., Dugail, I., Durbeej, M., Duszenko, M., Edelstein, C.L., Edinger, A.L., Egea, G., Eichinger, L., Eissa, N.T., Ekmekcioglu, S., El-Deiry, W.S., Elazar, Z., Elgendy, M., Ellerby, L.M., Eng, K.E., Engelbrecht, A.M., Engelender, S., Erenpreisa, J., Escalante, R., Esclatine, A., Eskelinen, E.L., Espert, L., Espina, V., Fan, H., Fan, J., Fan, Q.W., Fan, Z., Fang, S., Fang, Y., Fanto, M., Fanzani, A., Farkas, T., Farre, J.C., Faure, M., Fechheimer, M., Feng, C.G., Feng, J., Feng, Q., Feng, Y., Fesus, L., Feuer, R., Figueiredo-Pereira, M.E., Fimia, G.M., Fingar, D.C., Finkbeiner, S., Finkel, T., Finley, K.D., Fiorito, F., Fisher, E.A., Fisher, P.B., Flajolet, M., Florez-McClure, M.L., Florio, S., Fon, E.A., Fornai, F., Fortunato, F., Fotedar, R., Fowler, D.H., Fox, H.S., Franco, R., Frankel, L.B., Fransen, M., Fuentes, J.M., Fueyo, J., Fujii, J., Fujisaki, K., Fujita, E., Fukuda, M., Furukawa, R.H., Gaestel, M., Gailly, P., Gajewska, M., Galliot, B., Galy, V., Ganesh, S., Ganetzky, B., Ganley, I.G., Gao, F.B., Gao, G.F., Gao, J., Garcia, L., Garcia-Manero, G., Garcia-Marcos, M., Garmyn, M., Gartel, A.L., Gatti, E., Gautel, M., Gawriluk, T.R., Gegg, M.E., Geng, J., Germain, M., Gestwicki, J.E., Gewirtz, D.A., Ghavami, S., Ghosh, P., Giammarioli, A.M., Giatromanolaki, A.N., Gibson, S.B., Gilkerson, R.W., Ginger, M.L., Ginsberg, H.N., Golab, J., Goligorsky, M.S., Golstein, P., Gomez-Manzano, C., Goncu, E., Gongora, C., Gonzalez, C.D., Gonzalez, R., Gonzalez-Estevez, C., Gonzalez-Polo, R.A., Gonzalez-Rey, E., Gorbunov, N.V., Gorski, S., Goruppi, S., Gottlieb, R.A., Gozuacik, D., Granato, G.E., Grant, G.D., Green, K.N., Gregorc, A., Gros, F., Grose, C., Grunt, T.W., Gual, P., Guan, J.L., Guan, K.L., Guichard, S.M., Gukovskaya, A.S., Gukovsky, I., Gunst, J., Gustafsson, A.B., Halayko, A.J., Hale, A.N., Halonen, S.K., Hamasaki, M., Han, F., Han, T., Hancock, M.K., Hansen, M.,

Harada, H., Harada, M., Hardt, S.E., Harper, J.W., Harris, A.L., Harris, J., Harris, S.D., Hashimoto, M., Haspel, J.A., Hayashi, S., Hazelhurst, L.A., He, C., He, Y.W., Hebert, M.J., Heidenreich, K.A., Helfrich, M.H., Helgason, G.V., Henske, E.P., Herman, B., Herman, P.K., Hetz, C., Hilfiker, S., Hill, J.A., Hocking, L.J., Hofman, P., Hofmann, T.G., Hohfeld, J., Holyoake, T.L., Hong, M.H., Hood, D.A., Hotamisligil, G.S., Houwerzijl, E.J., Hoyer-Hansen, M., Hu, B., Hu, C.A., Hu, H.M., Hua, Y., Huang, C., Huang, J., Huang, S., Huang, W.P., Huber, T.B., Huh, W.K., Hung, T.H., Hupp, T.R., Hur, G.M., Hurley, J.B., Hussain, S.N., Hussey, P.J., Hwang, J.J., Hwang, S., Ichihara, A., Ilkhanizadeh, S., Inoki, K., Into, T., Iovane, V., Iovanna, J.L., Ip, N.Y., Isaka, Y., Ishida, H., Isidoro, C., Isobe, K., Iwasaki, A., Izquierdo, M., Izumi, Y., Jaakkola, P.M., Jaattela, M., Jackson, G.R., Jackson, W.T., Janji, B., Jendrach, M., Jeon, J.H., Jeung, E.B., Jiang, H., Jiang, H., Jiang, J.X., Jiang, M., Jiang, Q., Jiang, X., Jiang, X., Jimenez, A., Jin, M., Jin, S., Joe, C.O., Johansen, T., Johnson, D.E., Johnson, G.V., Jones, N.L., Joseph, B., Joseph, S.K., Joubert, A.M., Juhasz, G., Juillerat-Jeanneret, L., Jung, C.H., Jung, Y.K., Kaarniranta, K., Kaasik, A., Kabuta, T., Kadowaki, M., Kagedal, K., Kamada, Y., Kaminskyy, V.O., Kampinga, H.H., Kanamori, H., Kang, C., Kang, K.B., Kang, K.I., Kang, R., Kang, Y.A., Kanki, T., Kanneganti, T.D., Kanno, H., Kanthasamy, A.G., Kanthasamy, A., Karantza, V., Kaushal, G.P., Kaushik, S., Kawazoe, Y., Ke, P.Y., Kehrl, J.H., Kelekar, A., Kerkhoff, C., Kessel, D.H., Khalil, H., Kiel, J.A., Kiger, A.A., Kihara, A., Kim, D.R., Kim, D.H., Kim, D.H., Kim, E.K., Kim, H.R., Kim, J.S., Kim, J.H., Kim, J.C., Kim, J.K., Kim, P.K., Kim, S.W., Kim, Y.S., Kim, Y., Kimchi, A., Kimmelman, A.C., King, J.S., Kinsella, T.J., Kirkin, V., Kirshenbaum, L.A., Kitamoto, K., Kitazato, K., Klein, L., Klimecki, W.T., Klucken, J., Knecht, E., Ko, B.C., Koch, J.C., Koga, H., Koh, J.Y., Koh, Y.H., Koike, M., Komatsu, M., Kominami, E., Kong, H.J., Kong, W.J., Korolchuk, V.I., Kotake, Y., Koukourakis, M.I., Kouri Flores, J.B., Kovacs, A.L., Kraft, C., Krainc, D., Kramer, H., Kretz-Remy, C., Krichevsky, A.M., Kroemer, G., Kruger, R., Krut, O., Ktistakis, N.T., Kuan, C.Y., Kucharczyk, R., Kumar, A., Kumar, R., Kumar, S., Kundu, M., Kung, H.J., Kurz, T., Kwon, H.J., La Spada, A.R., Lafont, F., Lamark, T., Landry, J., Lane, J.D., Lapaquette, P., Laporte, J.F., Laszlo, L., Lavandero, S., Lavoie, J.N., Layfield, R., Lazo, P.A., Le, W., Le Cam, L., Ledbetter, D.J., Lee, A.J., Lee, B.W., Lee, G.M., Lee, J., Lee, J.H., Lee, M., Lee, M.S., Lee, S.H., Leeuwenburgh, C., Legembre, P., Legouis, R., Lehmann, M., Lei, H.Y., Lei, Q.Y., Leib, D.A., Leiro, J., Lemasters, J.J., Lemoine, A., Lesniak, M.S., Lev, D., Levenson, V.V., Levine, B., Levy, E., Li, F., Li, J.L., Li, L., Li, S., Li, W., Li, X.J., Li, Y.B., Li, Y.P., Liang, C., Liang, Q., Liao, Y.F., Liberski, P.P., Lieberman, A., Lim, H.J., Lim, K.L., Lim, K., Lin, C.F., Lin, F.C., Lin, J., Lin, J.D., Lin, K., Lin, W.W., Lin, W.C., Lin, Y.L., Linden, R., Lingor, P., Lippincott-Schwartz, J., Lisanti, M.P., Liton, P.B., Liu, B., Liu, C.F., Liu, K., Liu, L., Liu, Q.A., Liu, W., Liu, Y.C., Liu, Y., Lockshin, R.A., Lok, C.N., Lonial, S., Loos, B., Lopez-Berestein, G., Lopez-Otin, C., Lossi, L., Lotze, M.T., Low, P., Lu, B., Lu, B., Lu, Z., Luciano, F., Lukacs, N.W., Lund, A.H., Lynch-Day, M.A., Ma, Y., Macian, F., MacKeigan, J.P., Macleod, K.F., Madeo, F., Maiuri, L., Maiuri, M.C., Malagoli, D., Malicdan, M.C., Malorni, W., Man, N., Mandelkow, E.M., Manon, S., Manov, I., Mao, K., Mao, X., Mao, Z., Marambaud, P., Marazziti, D., Marcel, Y.L., Marchbank, K., Marchetti, P., Marciniak, S.J.,

Marcondes, M., Mardi, M., Marfe, G., Marino, G., Markaki, M., Marten, M.R., Martin, S.J., Martinand-Mari, C., Martinet, W., Martinez-Vicente, M., Masini, M., Matarrese, P., Matsuo, S., Matteoni, R., Mayer, A., Mazure, N.M., McConkey, D.J., McConnell, M.J., McDermott, C., McDonald, C., McInerney, G.M., McKenna, S.L., McLaughlin, B., McLean, P.J., McMaster, C.R., McQuibban, G.A., Meijer, A.J., Meisler, M.H., Melendez, A., Melia, T.J., Melino, G., Mena, M.A., Menendez, J.A., Menna-Barreto, R.F., Menon, M.B., Menzies, F.M., Mercer, C.A., Merighi, A., Merry, D.E., Meschini, S., Meyer, C.G., Meyer, T.F., Miao, C.Y., Miao, J.Y., Michels, P.A., Michiels, C., Mijaljica, D., Milojkovic, A., Minucci, S., Miracco, C., Miranti, C.K., Mitroulis, I., Miyazawa, K., Mizushima, N., Mograbi, B., Mohseni, S., Molero, X., Mollereau, B., Mollinedo, F., Momoi, T., Monastyrska, I., Monick, M.M. Monteiro, M.J., Moore, M.N., Mora, R., Moreau, K., Moreira, P.I., Moriyasu, Y., Moscat, J., Mostowy, S., Mottram, J.C., Motyl, T., Moussa, C.E., Muller, S., Muller, S., Munger, K., Munz, C., Murphy, L.O., Murphy, M.E., Musaro, A., Mysorekar, I., Nagata, E., Nagata, K., Nahimana, A., Nair, U., Nakagawa, T., Nakahira, K., Nakano, H., Nakatogawa, H., Nanjundan, M., Naqvi, N.I., Narendra, D.P., Narita, M., Navarro, M., Nawrocki, S.T., Nazarko, T.Y., Nemchenko, A., Netea, M.G., Neufeld, T.P., Ney, P.A., Nezis, I.P., Nguyen, H.P., Nie, D., Nishino, I., Nislow, C., Nixon, R.A., Noda, T., Noegel, A.A., Nogalska, A., Noguchi, S., Notterpek, L., Novak, I., Nozaki, T., Nukina, N., Nurnberger, T., Nyfeler, B., Obara, K., Oberley, T.D., Oddo, S., Ogawa, M., Ohashi, T., Okamoto, K., Oleinick, N.L., Oliver, F.J., Olsen, L.J., Olsson, S., Opota, O., Osborne, T.F., Ostrander, G.K., Otsu, K., Ou, J.H., Ouimet, M., Overholtzer, M., Ozpolat, B., Paganetti, P., Pagnini, U., Pallet, N., Palmer, G.E., Palumbo, C., Pan, T., Panaretakis, T., Pandey, U.B., Papackova, Z., Papassideri, I., Paris, I., Park, J., Park, O.K., Parys, J.B., Parzych, K.R., Patschan, S., Patterson, C., Pattingre, S., Pawelek, J.M., Peng, J., Perlmutter, D.H., Perrotta, I., Perry, G., Pervaiz, S., Peter, M., Peters, G.J., Petersen, M., Petrovski, G., Phang, J.M., Piacentini, M., Pierre, P., Pierrefite-Carle, V., Pierron, G., Pinkas-Kramarski, R., Piras, A., Piri, N., Platanias, L.C., Poggeler, S., Poirot, M., Poletti, A., Pous, C., Pozuelo-Rubio, M., Praetorius-Ibba, M., Prasad, A., Prescott, M., Priault, M., Produit-Zengaffinen, N., Progulske-Fox, A., Proikas-Cezanne, T., Przedborski, S., Przyklenk, K., Puertollano, R., Puval, J., Qian, S.B., Qin, L., Qin, Z.H., Quaggin, S.E., Raben, N., Rabinowich, H., Rabkin, S.W., Rahman, I., Rami, A., Ramm, G., Randall, G., Randow, F., Rao, V.A., Rathmell, J.C., Ravikumar, B., Ray, S.K., Reed, B.H., Reed, J.C., Reggiori, F., Regnier-Vigouroux, A., Reichert, A.S., Reiners, J.J., Jr., Reiter, R.J., Ren, J., Revuelta, J.L., Rhodes, C.J., Ritis, K., Rizzo, E., Robbins, J., Roberge, M., Roca, H., Roccheri, M.C., Rocchi, S., Rodemann, H.P., Rodriguez de Cordoba, S., Rohrer, B., Roninson, I.B., Rosen, K., Rost-Roszkowska, M.M., Rouis, M., Rouschop, K.M., Rovetta, F., Rubin, B.P., Rubinsztein, D.C., Ruckdeschel, K., Rucker, E.B., 3rd, Rudich, A., Rudolf, E., Ruiz-Opazo, N., Russo, R., Rusten, T.E., Ryan, K.M., Ryter, S.W., Sabatini, D.M., Sadoshima, J., Saha, T., Saitoh, T., Sakagami, H., Sakai, Y., Salekdeh, G.H., Salomoni, P., Salvaterra, P.M., Salvesen, G., Salvioli, R., Sanchez, A.M., Sanchez-Alcazar, J.A., Sanchez-Prieto, R., Sandri, M., Sankar, U., Sansanwal, P., Santambrogio, L., Saran, S., Sarkar, S., Sarwal, M., Sasakawa, C., Sasnauskiene, A., Sass, M., Sato, K., Sato, M., Schapira, A.H., Scharl, M., Schatzl, H.M., Scheper, W., Schiaffino, S., Schneider, C.,

Schneider, M.E., Schneider-Stock, R., Schoenlein, P.V., Schorderet, D.F., Schuller, C., Schwartz, G.K., Scorrano, L., Sealy, L., Seglen, P.O., Segura-Aguilar, J., Seiliez, I., Seleverstov, O., Sell, C., Seo, J.B., Separovic, D., Setaluri, V., Setoguchi, T., Settembre, C., Shacka, J.J., Shanmugam, M., Shapiro, I.M., Shaulian, E., Shaw, R.J., Shelhamer, J.H., Shen, H.M., Shen, W.C., Sheng, Z.H., Shi, Y., Shibuya, K., Shidoji, Y., Shieh, J.J., Shih, C.M., Shimada, Y., Shimizu, S., Shintani, T., Shirihai, O.S., Shore, G.C., Sibirny, A.A., Sidhu, S.B., Sikorska, B., Silva-Zacarin, E.C., Simmons, A., Simon, A.K., Simon, H.U., Simone, C., Simonsen, A., Sinclair, D.A., Singh, R., Sinha, D., Sinicrope, F.A., Sirko, A., Siu, P.M., Sivridis, E., Skop, V., Skulachev, V.P., Slack, R.S., Smaili, S.S., Smith, D.R., Soengas, M.S., Soldati, T., Song, X., Sood, A.K., Soong, T.W., Sotgia, F., Spector, S.A., Spies, C.D., Springer, W., Srinivasula, S.M., Stefanis, L., Steffan, J.S., Stendel, R., Stenmark, H., Stephanou, A., Stern, S.T., Sternberg, C., Stork, B., Stralfors, P., Subauste, C.S., Sui, X., Sulzer, D., Sun, J., Sun, S.Y., Sun, Z.J., Sung, J.J., Suzuki, K., Suzuki, T., Swanson, M.S., Swanton, C., Sweeney, S.T., Sy, L.K., Szabadkai, G., Tabas, I., Taegtmeyer, H., Tafani, M., Takacs-Vellai, K., Takano, Y., Takegawa, K., Takemura, G., Takeshita, F., Talbot, N.J., Tan, K.S., Tanaka, K., Tanaka, K., Tang, D., Tang, D., Tanida, I., Tannous, B.A., Tavernarakis, N., Taylor, G.S., Taylor, G.A., Taylor, J.P., Terada, L.S., Terman, A., Tettamanti, G., Thevissen, K., Thompson, C.B., Thorburn, A., Thumm, M., Tian, F., Tian, Y., Tocchini-Valentini, G., Tolkovsky, A.M., Tomino, Y., Tonges, L., Tooze, S.A., Tournier, C., Tower, J., Towns, R., Trajkovic, V., Travassos, L.H., Tsai, T.F., Tschan, M.P., Tsubata, T., Tsung, A., Turk, B., Turner, L.S., Tyagi, S.C., Uchiyama, Y., Ueno, T., Umekawa, M., Umemiya-Shirafuji, R., Unni, V.K., Vaccaro, M.I., Valente, E.M., Van den Berghe, G., van der Klei, I.J., van Doorn, W., van Dyk, L.F., van Egmond, M., van Grunsven, L.A., Vandenabeele, P., Vandenberghe, W.P., Vanhorebeek, I., Vaquero, E.C., Velasco, G., Vellai, T., Vicencio, J.M., Vierstra, R.D., Vila, M., Vindis, C., Viola, G., Viscomi, M.T., Voitsekhovskaja, O.V., von Haefen, C., Votruba, M., Wada, K., Wade-Martins, R., Walker, C.L., Walsh, C.M., Walter, J., Wan, X.B., Wang, A., Wang, C., Wang, D., Wang, F., Wang, F., Wang, G., Wang, H., Wang, H.G., Wang, H.D., Wang, J., Wang, K., Wang, M., Wang, R.C., Wang, X., Wang, X., Wang, Y.J., Wang, Y., Wang, Z., Wang, Z.C., Wang, Z., Wansink, D.G., Ward, D.M., Watada, H., Waters, S.L., Webster, P., Wei, L., Weihl, C.C., Weiss, W.A., Welford, S.M., Wen, L.P., Whitehouse, C.A., Whitton, J.L., Whitworth, A.J., Wileman, T., Wiley, J.W., Wilkinson, S., Willbold, D., Williams, R.L., Williamson, P.R., Wouters, B.G., Wu, C., Wu, D.C., Wu, W.K., Wyttenbach, A., Xavier, R.J., Xi, Z., Xia, P., Xiao, G., Xie, Z., Xie, Z., Xu, D.Z., Xu, J., Xu, L., Xu, X., Yamamoto, A., Yamamoto, A., Yamashina, S., Yamashita, M., Yan, X., Yanagida, M., Yang, D.S., Yang, E., Yang, J.M., Yang, S.Y., Yang, W., Yang, W.Y., Yang, Z., Yao, M.C., Yao, T.P., Yeganeh, B., Yen, W.L., Yin, J.J., Yin, X.M., Yoo, O.J., Yoon, G., Yoon, S.Y., Yorimitsu, T., Yoshikawa, Y., Yoshimori, T., Yoshimoto, K., You, H.J., Youle, R.J., Younes, A., Yu, L., Yu, L., Yu, S.W., Yu, W.H., Yuan, Z.M., Yue, Z., Yun, C.H., Yuzaki, M., Zabirnyk, O., Silva-Zacarin, E., Zacks, D., Zacksenhaus, E., Zaffaroni, N., Zakeri, Z., Zeh, H.J., 3rd, Zeitlin, S.O., Zhang, H., Zhang, H.L., Zhang, J., Zhang, J.P., Zhang, L., Zhang, L., Zhang, M.Y., Zhang, X.D., Zhao, M., Zhao, Y.F., Zhao, Y., Zhao, Z.J., Zheng, X., Zhivotovsky, B., Zhong, Q., Zhou, C.Z., Zhu, C.,

- Zhu, W.G., Zhu, X.F., Zhu, X., Zhu, Y., Zoladek, T., Zong, W.X., Zorzano, A., Zschocke, J., and Zuckerbraun, B. (2012). Guidelines for the use and interpretation of assays for monitoring autophagy. Autophagy 8, 445-544.
- Li, X., Moellering, E.R., Liu, B., Johnny, C., Fedewa, M., Sears, B.B., Kuo, M.H., and Benning, C. (2012). A galactoglycerolipid lipase is required for triacylglycerol accumulation and survival following nitrogen deprivation in Chlamydomonas reinhardtii. The Plant cell **24**, 4670-4686.
- **Liu, B., and Benning, C.** (2013). Lipid metabolism in microalgae distinguishes itself. Current opinion in biotechnology **24,** 300-309.
- Mason, C.B., Bricker, T.M., and Moroney, J.V. (2006). A rapid method for chloroplast isolation from the green alga Chlamydomonas reinhardtii. Nature protocols 1, 2227-2230.
- Miller, R., Wu, G., Deshpande, R.R., Vieler, A., Gartner, K., Li, X., Moellering, E.R., Zauner, S., Cornish, A.J., Liu, B., Bullard, B., Sears, B.B., Kuo, M.H., Hegg, E.L., Shachar-Hill, Y., Shiu, S.H., and Benning, C. (2010). Changes in transcript abundance in Chlamydomonas reinhardtii following nitrogen deprivation predict diversion of metabolism. Plant physiology 154, 1737-1752.
- **Moellering, E.R., and Benning, C.** (2010). RNA interference silencing of a major lipid droplet protein affects lipid droplet size in Chlamydomonas reinhardtii. Eukaryotic cell **9,** 97-106.
- **Neupert, J., Karcher, D., and Bock, R.** (2009). Generation of Chlamydomonas strains that efficiently express nuclear transgenes. The Plant journal: for cell and molecular biology **57,** 1140-1150.
- Newman, S.M., Boynton, J.E., Gillham, N.W., Randolph-Anderson, B.L., Johnson, A.M., and Harris, E.H. (1990). Transformation of chloroplast ribosomal RNA genes in Chlamydomonas: molecular and genetic characterization of integration events. Genetics 126, 875-888.
- Nguyen, H.M., Cuine, S., Beyly-Adriano, A., Legeret, B., Billon, E., Auroy, P., Beisson, F., Peltier, G., and Li-Beisson, Y. (2013). The green microalga Chlamydomonas reinhardtii has a single omega-3 fatty acid desaturase that localizes to the chloroplast and impacts both plastidic and extraplastidic membrane lipids. Plant physiology **163**, 914-928.
- Nguyen, H.M., Baudet, M., Cuine, S., Adriano, J.M., Barthe, D., Billon, E., Bruley, C., Beisson, F., Peltier, G., Ferro, M., and Li-Beisson, Y. (2011). Proteomic profiling of oil bodies isolated from the unicellular green microalga Chlamydomonas reinhardtii: with focus on proteins involved in lipid metabolism. Proteomics 11, 4266-4273.
- Olson, B.J., Oberholzer, M., Li, Y., Zones, J.M., Kohli, H.S., Bisova, K., Fang, S.C., Meisenhelder, J., Hunter, T., and Umen, J.G. (2010). Regulation of the Chlamydomonas cell cycle by a stable, chromatin-associated retinoblastoma tumor suppressor complex. The Plant cell 22, 3331-3347.

- **Perez-Perez, M.E., Florencio, F.J., and Crespo, J.L.** (2010). Inhibition of target of rapamycin signaling and stress activate autophagy in Chlamydomonas reinhardtii. Plant physiology **152,** 1874-1888.
- Punta, M., Coggill, P.C., Eberhardt, R.Y., Mistry, J., Tate, J., Boursnell, C., Pang, N., Forslund, K., Ceric, G., Clements, J., Heger, A., Holm, L., Sonnhammer, E.L., Eddy, S.R., Bateman, A., and Finn, R.D. (2012). The Pfam protein families database. Nucleic acids research 40, D290-301.
- Rossak, M., Schafer, A., Xu, N., Gage, D.A., and Benning, C. (1997). Accumulation of sulfoquinovosyl-1-O-dihydroxyacetone in a sulfolipid-deficient mutant of Rhodobacter sphaeroides inactivated in sqdC. Archives of biochemistry and biophysics **340**, 219-230.
- **Sadasivam, S., and DeCaprio, J.A.** (2013). The DREAM complex: master coordinator of cell cycle-dependent gene expression. Nature reviews. Cancer **13**, 585-595.
- Sato, M., Murata, Y., Mizusawa, M., Iwahashi, H., and Oka, S.-i. (2004). A simple and rapid dual fluorescence viability assay for microalgae. Microbiol. Cult. Coll. 20, 53-59.
- **Schmit, F., Cremer, S., and Gaubatz, S.** (2009). LIN54 is an essential core subunit of the DREAM/LINC complex that binds to the cdc2 promoter in a sequence-specific manner. The FEBS journal **276**, 5703-5716.
- Schmollinger, S., Muhlhaus, T., Boyle, N.R., Blaby, I.K., Casero, D., Mettler, T., Moseley, J.L., Kropat, J., Sommer, F., Strenkert, D., Hemme, D., Pellegrini, M., Grossman, A.R., Stitt, M., Schroda, M., and Merchant, S.S. (2014). Nitrogen-Sparing Mechanisms in Chlamydomonas Affect the Transcriptome, the Proteome, and Photosynthetic Metabolism. The Plant cell 26, 1410-1435.
- Sugihara, T., Wadhwa, R., Kaul, S.C., and Mitsui, Y. (1999). A novel testis-specific metallothionein-like protein, tesmin, is an early marker of male germ cell differentiation. Genomics 57, 130-136.
- **Tabuchi, T.M., Deplancke, B., Osato, N., Zhu, L.J., Barrasa, M.I., Harrison, M.M., Horvitz, H.R., Walhout, A.J., and Hagstrom, K.A.** (2011). Chromosome-biased binding and gene regulation by the Caenorhabditis elegans DRM complex. PLoS genetics **7**, e1002074.
- Tan, G., Gao, Y., Shi, M., Zhang, X., He, S., Chen, Z., and An, C. (2005). SiteFinding-PCR: a simple and efficient PCR method for chromosome walking. Nucleic acids research 33, e122.
- Valcourt, J.R., Lemons, J.M., Haley, E.M., Kojima, M., Demuren, O.O., and Coller, H.A. (2012). Staying alive: metabolic adaptations to quiescence. Cell cycle 11, 1680-1696.
- Winck, F., Kwasniewski, M., Wienkoop, S., and Mueller-Roeber, B. (2011). An optimized method for the isolation of nuclei from Chlamydomonas reinhardtii. J Phycol 47, 333-340.

- Wittig, I., Braun, H.P., and Schagger, H. (2006). Blue native PAGE. Nature protocols 1, 418-428.
- **Young, M.D., Wakefield, M.J., Smyth, G.K., and Oshlack, A.** (2010). Gene ontology analysis for RNA-seq: accounting for selection bias. Genome biology **11,** R14.

CHAPTER 3

Comparative Transcriptomic Analysis of Nitrogen Resupply-induced Modifications in a

Chlamydomonas Quiescence-exit Mutant

ABSTRACT

In response to environmental cues such as nutrient deprivation, cells can temporary cease divisions and enter a reversible state of quiescence. The regulatory processes by which photosynthetic organisms preserve the reversibility are largely unknown. Therefore, I used *Chlamydomonas reinhardtii* as a reference model and conducted comparative transcriptomics of *cht7*, a mutant slow to resume growth from quiescence. My data uncover transcriptional programs unique to the exit of quiescence induced by N deprivation, and the CHT7 regulon including tetrapyrrole pathway and peroxisomal redox homeostasis, which potentially interplays with the cAMP-PKA pathway. Focusing on lipid metabolism for detailed analysis, I found that the metabolite state is closely associated with the way transcripts are regulated. And in some cases, e.g. monogalactosyldiacylglycerol and fatty acid syntheses, the transcription is subjected to a feedback control by metabolite levels. These data provide rich resources for future investigation of any biological process in the context of cellular quiescence.

INTRODUCTION

The ability of cells to temporarily halt divisions is essential for survival during adverse conditions, particularly for unicellular organisms, and for the maintenance of tissue homeostasis in multicellular organisms. This non-dividing state is called quiescence, and is distinguished from senescence or terminal differentiation by its reversibility (Gray et al., 2004; Coller, 2011). Yeast offers a well-studied example of quiescence for unicellular eukaryotes: upon reaching stationary phase, yeast cells cease proliferation due to the exhaustion of the main carbon source or specific nutrients such as nitrogen (N) (Gasch et al., 2000). Growth typically resumes in fresh medium. The reversibility of quiescence in mammalian cells often requires cues other than the availability of nutrients. Examples are T lymphocytes that become activated to mount an immune response when exposed to antigens, or dermal fibroblasts that are activated during wound healing (Valcourt et al., 2012). In Chlamydomonas reinhardtii, a unicellular microalga on which this study is based, N deprivation-induced cell cycle arrest has all the hallmarks of quiescence including reversibility, change in metabolism, reduced transcription and translation, reduced synthesis of rRNA and ribosomal proteins, and activation of autophagy (Miller et al., 2010; Goodson et al., 2011; Schmollinger et al., 2014). In facing quiescence, a plethora of metabolic adjustments has to take place to meet the changing demands (Gray et al., 2004; Valcourt et al., 2012). For example, because quiescent cells cannot dilute out reactive oxygen species (ROS) and replace damaged protein or other macromolecules by rapid synthesis, they require specialized ROS-dissipating mechanisms to maintain redox homeostasis, such as catalase and superoxide dismutase. Autophagy in most conditions is reduced to a very low level, but drastically elevated during quiescence, which allows degradation and recycling of cellular components. For photosynthetic organisms, there is an additional challenge, that is, to quench energy passing through photosynthetic electron transport chain in a way that it can be restored momentarily when conditions improve. Beyond transcriptional and translational modifications, such as down-regulation of photosynthetic genes or degradation of light-harvesting complexes, lipid metabolism is also an important contributor. Shortly following N deprivation, acetate typically provided in the medium under laboratory conditions to Chlamydomonas is no longer incorporated into biomass through the glyoxylate cycle and gluconeogenesis; instead acetate is directly funneled into biosynthesis of fatty acids and triacylglycerols (TAGs) (Miller et al., 2010; Boyle et al., 2012). This process relieves the overreduction of photosynthetic electron transport chain, which otherwise produces harmful ROS and subsequent cell death (Li et al., 2012b). Meanwhile, chloroplast thylakoid lipids, especially monogalactosyldiacylglycerol (MGDG), undergo major turnover hence contributing to the dismantling of the structural base of the photosynthetic membrane.

The discovery of CHT7 in Chlamydomonas expands the landscape of quiescence research. It demonstrates that the exit of quiescence is a highly controlled process, not just a passive response to nutrient availability (Figure 3.1) (Tsai et al., 2014). I am thus interested to understand the transcriptional modifications in response to quiescence exit, and ask whether programmed responses unique to quiescence exit exist. In addition, while it is evident that CHT7 acts as a repressor of cellular quiescence, and is hypothesized to ensure the reversibility by resuppressing quiescence, I wondered whether CHT7 has additional, more direct impacts on quiescence exit. Therefore in this study, I undertook comparative transcriptomics spanning the entire quiescence cycle of *cht7* and its parental line (PL). Although I place an emphasis on lipid metabolism when describing the data, the overall datasets provide rich resources for exploration in any biological process in the context of quiescence.

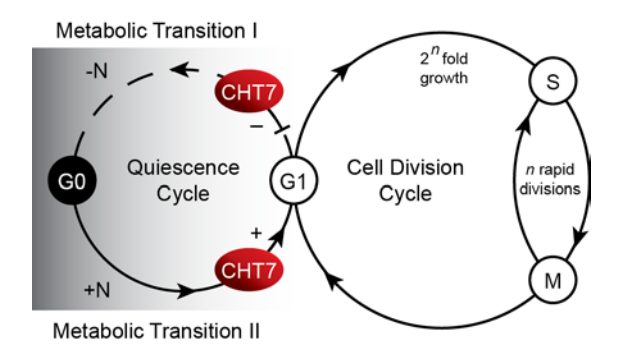


Figure 3.1. Cell Cycle and Proposed Functions for CHT7 in Quiescence. The cell division cycle with G1, S, G2, and M phases, and the quiescence cycle (G0) are depicted. CHT7 is proposed to play distinct roles at quiescence entry (- repression) and exit (+ stimulation) as discussed in the text. -N, N deprivation, +N, N resupply.

MATERIALS AND METHODS

Strains and Growth Conditions

Chlamydomonas reinhardtii cell wall-less strain dw15 (cw15, nit1, mt⁺) was obtained from A. Grossman and is referred to as the wild-type (with regard to *CHT7*) parental line (PL) throughout. 21gr (wild-type mt⁺; the parental line of *mat3-4*) was obtained from the Chlamydomonas Resource Center (http://www.chlamycollection.org). Complemented strains of *cht7* and the *MLDP* RNAi lines were generated as described in previous work (Moellering and Benning, 2010; Tsai et al., 2014). Cells were grown in Tris-acetate-phosphate (TAP) medium (Harris, 1989), under continuous light (70 to 80 μmol m⁻² s⁻¹) at 22°C or ambient room temperature (~22°C) for solid media, which contained 0.8% agar (Phytoblend (Caisson Labs), North Logan, UT). To induce N deprivation, mid-log phase cells grown in TAP were collected by centrifugation (1500 g, 4°C, 2 min), washed twice with TAP-N (NH₄Cl omitted from TAP), and resuspended in TAP-N at 0.3 OD550. N resupply was done by refeeding 1% culture volume of 1 M NH₄Cl (100x) to the N-deprived culture. In some experiments, Protein Kinase A Inhibitor (P9115, Sigma-Aldrich) was added to the culture along with N resupply. The cell concentration of cultures was determined using a Z2 Coulter Counter (Beckman).

Illumina RNA Sequencing and Bioinformatics

As described in (Tsai et al., 2014).

Metabolite Measurements

Chlorophylls were extracted from fresh cell pellets using 80% acetone, and concentrations were calculated from the absorbance values at 647 and 664 nm according to (Zieger and Egle, 1965).

For the TBARS assay 5 mL of culture was centrifuged and analyzed immediately. Cell pellets were resuspended in 1 mL of thiobarbituric acid/trichloroacetic acid solution (0.3 and 3.9% respectively) and heated at 95°C for 15 min. The solution alone was also heated to serve as the blank for spectrophotometric measurements. Samples and blank were measured after no further gas bubbles were released. TBARS were determined by absorbance at 532 and 600 nm as previously described (Baroli et al., 2003). The extinction coefficient used was 155 mM⁻¹ cm⁻¹. Quantification of cellular cyclic AMP (cAMP) was conducted using Cyclic AMP Competitive ELISA kit (Thermo Scientific) according to manufacturer instruction. The concentration of cells in all assays was monitored by Z2 Coulter Counter.

Fatty Acid and Lipid Analysis

For lipid analysis extraction, TLC of neutral and polar lipids, fatty acid methyl ester (FAME) preparation, and gas–liquid chromatography were conducted as previously described in (Moellering and Benning, 2010). Cell pellets were extracted into methanol and chloroform (2:1 vol/vol, for neutral lipids) or methanol, chloroform, and 88% formic acid (2:1:0.1 vol/vol/vol, for polar lipids). To the extract, 0.5 volume of 0.9% KCL (neutral lipids) or 1 M KCl and 0.2 M H₃PO₄ (polar lipids) was added and mixed, followed by phase separation at low-speed centrifugation. For TAG quantification, lipids were resolved by TLC on Silica G60 plates (EMD Chemicals, Gibbstown, NJ) developed in petroleum ether-diethyl ether-acetic acid (80:20:1 by volume). Polar lipids were separated on the same plate using chloroform-methanol-acetic acid-distilled water (75:13:9:3 by volume) as solvent. After visualization by brief iodine staining, FAME of each lipid or total cellular lipid was processed and quantified by gas chromatography as previously described (Rossak et al., 1997). Staining with α-naphtol and Dragendorff reagent

was used for the detection of galactoglycerolipids and diacylglyceryl-trimethylhomoserine (DGTS) (Benning et al., 1995).

Standard RNA Techniques

To produce cDNA templates used for qPCR, total RNA was purified using the RNeasy plant mini kit (Qiagen) including the on-column DNase digestion, and then subjected to reverse transcription using Superscript III reverse transcriptase (Life Technologies). qPCR was performed on an ABI Prism 7000 (Applied Biosystems, Grand Island, NY) using the SYBR green PCR master mix (Life Technologies) with an equivalent cDNA template and 0.25 μM of each primer. The amount of cDNA input was optimized after serial dilutions. In all qPCR experiments, expression of the target gene was normalized to the endogenous reference gene CBLP, a gene commonly used for normalization in *C. reinhardtii* (Allen et al., 2007), using the cycle threshold (CT) 2^{-ΔΔCT} method. All experiments were done using at least two biological replicates and each reaction was run with technical replicates. qPCR procedures and analysis followed the MIQE guidelines (Bustin et al., 2009). For quantification, Trizol reagent (Life Technologies) was used for RNA isolation and the concentration of RNA was measured using a NanoDrop instrument (Thermo Scientific).

RESULTS

Transcriptomes of Parental Line during different N regimes

Previously, we conducted RNA-Seq experiments on the *cht7* mutant and the parental line (PL) grown in N-replete (mid-log phase of a culture in standard Tris-acetate phosphate (TAP) medium) and N-deprived (48 h in TAP lacking N) conditions, and found that the transcriptional program characteristic for quiescence was partially induced in the absence of CHT7, suggesting CHT7 as a repressor of cellular quiescence (Tsai et al., 2014). Here I show the global transcript profiles of *cht7* and PL in two additional conditions of N availability: 6 and 12 h of N resupply following 48 h of N deprivation (designated NR6 and NR12, respectively; Figure 3.2). These time points were chosen to reflect the metabolic and physiological contexts. For instance, both the regeneration of chlorophyll and turnover of TAGs restarted at NR6 (see below), and at NR12 cell division resumed. Importantly, the NR6 and NR12 RNAs were harvested, prepared, and sequenced in parallel with the samples for the N-replete and N-deprived data sets and, thus, can be directly compared. In each of the experiments, three replicates were taken independently to allow statistically sound analyses.

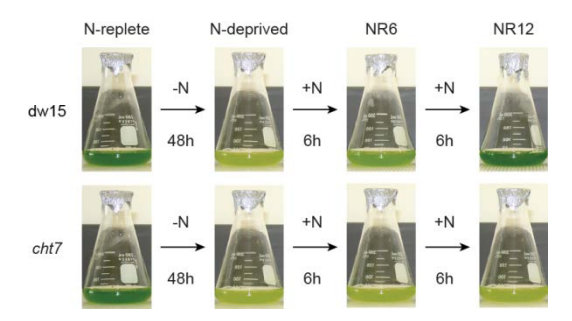


Figure 3.2. Experimental Design of RNA-Seq Experiments. Parental line (*dw15*) and *cht7* cells grown to mid-log phase in N-replete medium were sampled (N-replete) before being deprived of N (-N); cells were sampled after 48 h following N deprivation (N-deprived) and resupplied with N (+N) and sampled at 6 (NR6) and 12 h (NR12).

One key objective of this investigation was to understand the molecular changes that facilitate cells to exit and regrow from the N deprivation-induced quiescence. Towards this goal, transcripts of the NR6 PL or NR12 PL were compared with those of the N-deprived PL (for complete data set see Online Supplemental Data Set 4). Previously we showed that when PL cells transited from N-replete to N-deprived condition, 2647 genes were up-regulated and 3346 down-regulated (Tsai et al., 2014). We found that in response to N resupply these genes reversed their expression in a time-dependent manner and can be categorized according to three different stages, i.e. early, mid, and late (Figure 3.3A). Taking the genes for which expression was upregulated during N deprivation as an example, 1405 of them reversed at least two-fold ($\log 2 \le -1$ with a p value of < 0.05) at NR6 and were defined as early-reverse (1309 of the 1405 retained at least two-fold reversion at NR12); another 519 genes reversed not until NR12 and were defined as mid-reverse; 723 genes had not reversed by NR12 and were assumed to reverse at later time and were defined as late-reverse. Likewise, 1208 (1136 retained at least two-fold reversion at NR12), 991 and 1147 genes of those down-regulated during N deprivation are defined as early, mid and late-reverse, respectively (Online Supplemental Data Set 5). Selected metabolic pathways are discussed in detail in the later result sections.

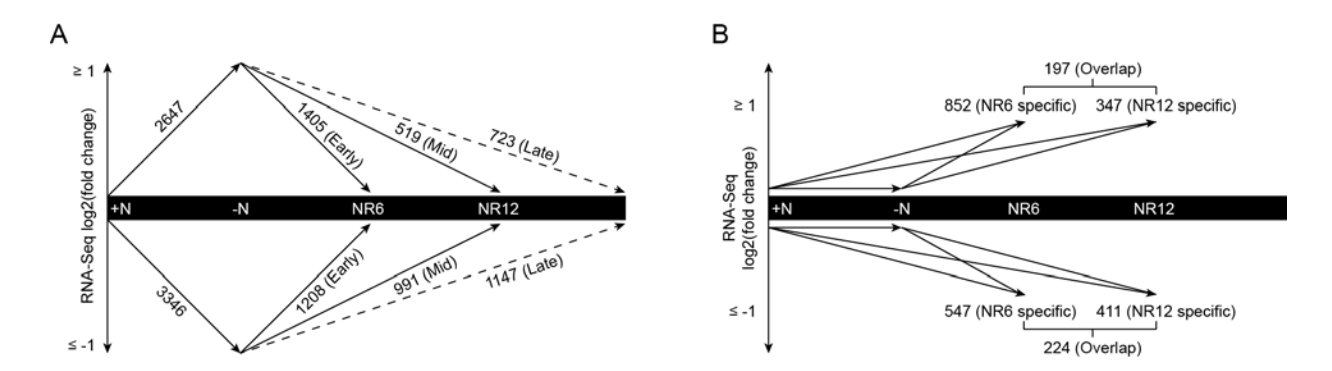


Figure 3.3. Summary Scheme of Transcriptomic Analyses in the Parental Line. (A) Early, Mid, and Late-reverse gene groups in the parental line. Numbers represent transcript changes by

Figure 3.3 (cont'd)

the N status using a 2-fold cutoff ($\log 2 = 1$) and a p value of < 0.05. +N, N-replete; -N, N-deprived; NR6 and NR12, 6 and 12 h of N resupply. Dashed line means the numbers shown are indirectly based on extrapolation of s , the RNA-Seq data. (B) NR-specific gene groups in the parental line. Numbers represent the transcripts whose abundance did not vary in the -N over +N RNA-Seq comparison (-1 < $\log 2$ < 1), but changed over 2-fold with a p value of < 0.05) in the NR over +N and NR over -N comparison.

The regrowth delay of *cht7* suggests the existence of a specific exit program that governs the quiescence exit. I therefore asked whether there are transcriptional responses specific to N resupply (NR-specific). To be classified as a NR-specific gene, its relative RNA abundance must not vary when shifting from N-replete to N-deprived condition (less than two-fold), but is either up or down-regulated in both the NR versus N-replete and the NR versus N-deprived transcriptomes (using a 2-fold cutoff and a p value of < 0.05, Figure 3.3B). It should be noted that NR-specific regulation means the transcripts are differentially regulated only when exposed to N resupply, but this does not necessarily mean they are only expressed during the period of N resupply. Given these criteria, 852 (NR6-specific) and 347 (NR12-specific) genes were specifically up-regulated after 6 and 12 h of N resupply, respectively, among which 197 genes overlapped. For genes specifically down-regulated during N resupply, 547 (NR6-specific) and 411 (NR12-specific), 224 overlapped (Online Supplemental Data Set 6). The events of NRspecific regulation were more frequent soon after N was refed (NR6). The overlaps (197 and 224) were judged to be the most robust set of NR-specific genes. Selected metabolic pathways are discussed in detail in the later result sections. It is important to note that the NR-reverse and NRspecific gene groups are mutually exclusive, enabling me to better dissect the responses in the phase of quiescence exit.

Comparative Transcriptomics of *cht7* and the Parental Line following N-resupply

CHT7 encodes a putative transcription factor and without it, quiescent cells show delayed regrowth. It would not be unexpected to see differences in transcript abundance between cells that undergo orderly progression and cells that fail to do so. Therefore, to distill meaningful dysregulation in cht7 when PL cells would be exiting quiescence, I adopted the strategy described previously for similar purposes (Gonzalez-Ballester et al., 2010; Castruita et al., 2011). Transcripts of the PL after 6 h and 12 h of N resupply were compared with those of N-deprived PL (Figure 3.4 A and B, blue circles); transcripts of the PL after 6 h and 12 h of N resupply were compared with those from cht7 (Figure 3.4 A and B, yellow circles). It is useful to know that the blue circles in Figure 3.4A contain all the early-reverse and NR6-specific genes mentioned above and the blue circles in Figure 3.4B contain all the mid-reverse and NR12-specific genes. While most transcripts responsive to N resupply in the PL were readjusted normally in cht7 (Figure 3.4) A and B, blue circles outside the overlap), a specific group did not respond in cht7 and remained at expression levels that were similar to those of N-deprived PL cells (Figure 3.4 A and B, overlap between blue and yellow circles; See Online Supplemental Data Set 7 for complete information). I hypothesize that these overlapping genes constitute the core of the CHT7 regulon during quiescence exit that is required for resuming cell growth, whereas the changes in expression of other genes (yellow circles outside the overlap) are secondary or compensatory effects due to the impaired growth resulting from the loss of CHT7. Moreover, 446 of the 1293 NR6 overlapping genes (594 plus 699) and 164 of the 1176 NR12 overlapping genes (639 plus 537) are NR-specific (Online Supplemental Data Set 7), arguing that CHT7 impacts quiescence exit in ways that are distinct from ordinary cell proliferation.

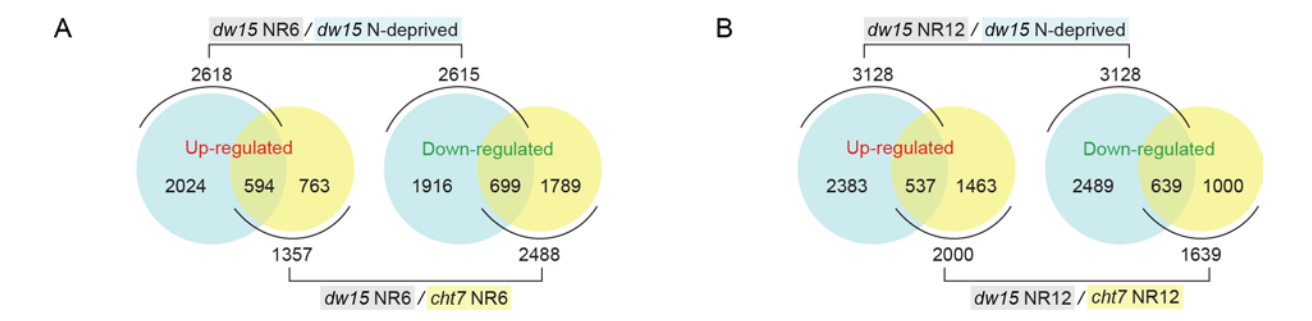


Figure 3.4. Comparative Transcriptomics during Quiescence Exit. (A, B) Global gene expression analysis of the parental line (*dw15*) and *cht7* following N resupply. Large blue circles: total number of genes changed in expression in a comparison of *dw15* after 48 h of N deprivation followed by 6 h (NR6) or 12 h (NR12) of N resupply and *dw15* N-deprived for 48 h. Small circles: total number of genes changed in expression in a comparison of *dw15* NR6 and *cht7* NR6 and *dw15* NR12 and *cht7* NR12.

Closer examination of the full data sets provided striking examples in support of this hypothesis, namely genes encoding enzymes involved in the tetrapyrrole pathway (chlorophyll synthesis, in the NR6 and NR12 overlaps) and peroxisomal redox homeostasis (mainly in the NR12 overlaps). At 6 and 12 h following N resupply, nearly every gene of tetrapyrrole biosynthesis tended to show lower transcript levels in *cht7* compared to PL following N resupply (Figure 3.5A, included here were genes that fall below the 2-fold threshold; Online Supplemental Data Set 8). These genes did not greatly differ in expression between cht7 and the PL in Nreplete condition; hence, I conclude that they are specifically misregulated in cht7 in response to the signals that should cause the cells to exit quiescence. The RNA-Seq data were confirmed for representative genes by quantitative PCR (qPCR) including cht7 complemented lines in this analysis (Figure 3.6A). These changes in transcript abundance were corroborated at the metabolite level. Shortly after 6 h following N resupply, the cellular chlorophyll content of the PL and complementation lines increased; it decreased after 12 h, likely because cells were dividing (Figure 3.5C). In contrast, the chlorophyll cell content of cht7 did not increase during the entire observation period. Genes encoding enzymes maintaining redox homeostasis during high demand of fatty acid β-oxidation were down-regulated in *cht7* following N resupply (Figures 3.5B and 3.6B; Online Supplemental Data Set 8). Among these were catalase (CAT1 and CAT2), ascorbate peroxidase (APX1 and APX2) and monodehydroascorbate reductase (MDAR1) which are responsible for detoxifying ROS generated within peroxisomes as a byproduct of β-oxidation (Eastmond, 2007). Consistently, thiobarbituric acid reactive substances (TBARS), the cellular metabolites reflecting damage caused by ROS, accumulated in *cht7* following N resupply (Figure 3.5D). Intriguingly, Arabidopsis homologues of HPR1, MAS1, MDH2, MDH4, MDAR1 and PXN1 (all misregulated in NR12 *cht7*) have defects in seed oil breakdown and seedling establishment, reminiscent of the *cht7* mutant phenotypes (Graham, 2008; Theodoulou and Eastmond, 2012).

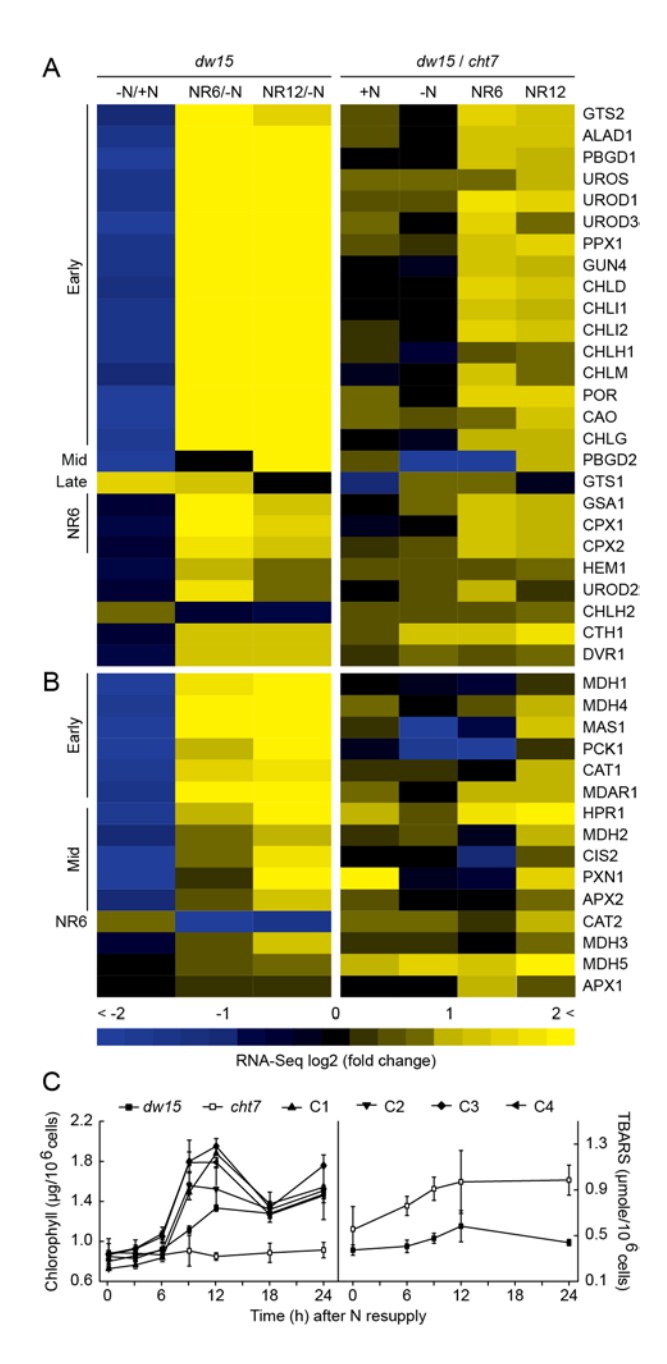


Figure 3.5. Changes in Gene Expression and Metabolite of Tetrapyrrole Pathway and Peroxisomal Redox Homeostasis. (A, B) Overview of expression of genes involved in the tetrapyrrole pathway (A) and in peroxisomal redox homeostasis (B). RNA-Seq comparisons of *dw15* at different N status and the comparisons between *dw15* and *cht7* at each N status are shown in the heatmap. +N, N-replete; -N, N-deprived; NR6 and NR12, 6 and 12 h of N resupply. Early, Mid, Late, NR6 or NR12 is indicated on the left of the heatmap for the gene whose response to N resupply has been classified. (C) Left panel: total cellular chlorophyll content. C1-C4 individual complemented lines. Right panel: cellular TBARS content. For all quantitative data, averages (n=3) and standard deviation are indicated.

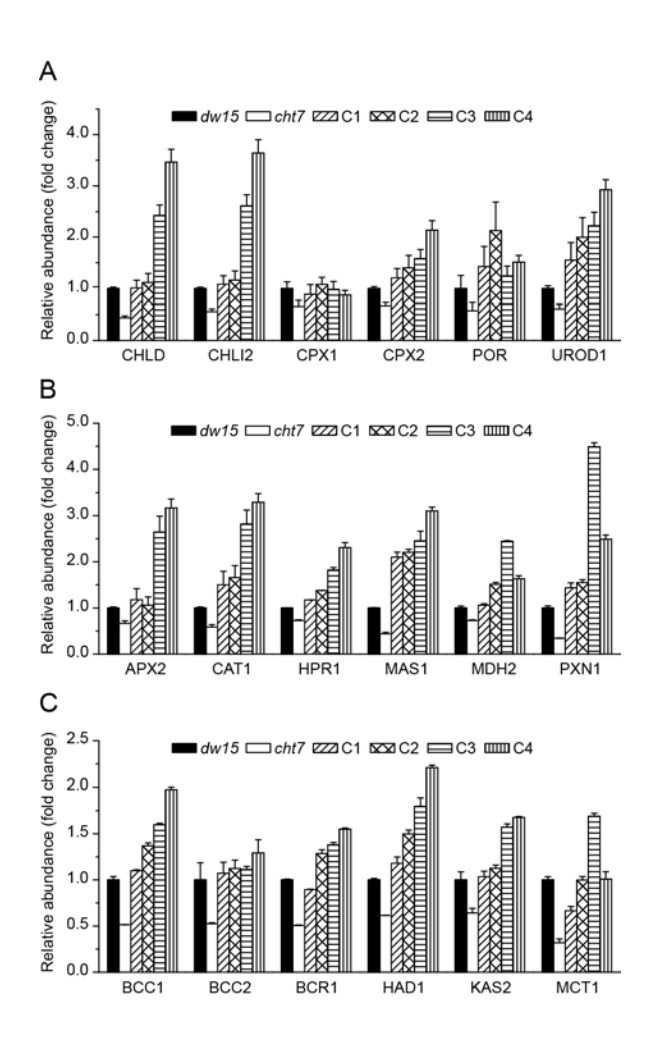


Figure 3.6. Confirmation of Transcript Changes at Quiescence Exit. (A, B, C) qPCR analysis of selected transcripts of genes encoding enzymes of the tetrapyrrole pathway at 6 h of N resupply (A), of genes involved in peroxisomal redox homeostasis at 12 h of N resupply (B), and of genes involved in fatty acid synthesis at 12 h of N resupply (C) (*dw15*, parental line; *cht7* mutant; C1-4, complemented *cht7* mutant lines).

Metabolite Analyses Confirm the Effect of Transcriptional Changes on Lipid Metabolism

Upon N deprivation, changes in TAG metabolism are reflected in the way genes in lipid metabolic pathways are regulated (Miller et al., 2010; Blaby et al., 2013; Schmollinger et al., 2014). Genes encoding 3-ketoacyl-ACP synthase (KAS1), stearoyl-ACP-Δ9-desaturase (FAB2) – the key enzyme for the signature TAG fatty acid oleate (18:1Δ9), acyl-ACP-thioesterase (FAT1) and long-chain acyl-CoA synthetase (LACS1) were upregulated, implying

elevated export of de novo synthesized fatty acids from chloroplast to where TAGs are made. Phosphatidate phosphatase (PAP), which increases the DAG pool through the Kennedy pathway, and the putative DAG acyltransferase (e.g. DGTT1) also showed increased transcript levels. All of the above genes reversed their expression in response to N resupply (Online Supplemental Data Set 9). Interestingly, the two long-chain acyl-CoA synthetase isoforms (LACS1 and LACS2) behaved just in the opposite. LACS2 transcripts decreased when N-deprived and increased when N was resupplied, which paralleled the need of β-oxidation, and thus likely to catalyze the activation of fatty acids for resulting from TAG breakdown for β-oxidation. In contrast, some modifications only occur upon N resupply, that is, NR-specific. Betaine lipid synthase (BTA1) synthesizes the diacylglyceryl-trimethylhomoserine (DGTS), a major lipid component presumed to take the role of PC in extraplastidic membranes in Chlamydomonas (Riekhof et al., 2005). Transcript levels of BTA1 remained constant when entering N deprivation, but increased approximately 4 fold after 6 h and 12 h of N resupply, a typical NR-specific gene. DGTT4 is one of the five putative DAG acyltransferases; however its association with TAG production has been unclear. I found a near 4-fold increase of DGTT4 RNAs after 6 h and 12 h of N resupply – the time when TAGs were being hydrolyzed – which could suggest a need to detoxify excessive free fatty acids by redirecting some back to TAGs, or that DGTT4 was to transfer acyl groups from TAG to other lipids (e.g. MGDG).

N status also has an impact on membrane lipids. The relative fraction of the thylakoid lipid MGDG to total membrane lipids in PL was reduced following N deprivation, and restored following N resupply (Figure 3.7C). Digalactosyldiacylglycerol (DGDG) on the other hand, was more abundant when N is absent (Figure 3.7C) in accord with the upregulation of DGDG synthase (DGD1). The increase of DGTS following N deprivation was small but statistically

significant; however unlike DGDG which gradually returned to its initial level when the condition was reversed, the elevated amount of DGTS was retained throughout the observation period (Figure 3.7C), consistent with the NR-specific upregulation of BTA1 mRNA levels. The significance of the increase in DGDG and DGTS when TAGs are built is perhaps related to LD formation as discussed later. No statistically significant changes were observed for phosphatidylethanolamine (PE), phosphatidylglycerol (PG), phosphatidylinositol (PI) and sulfoquinovosyldiacylglycerol (SQDG) (Figure 3.8A).

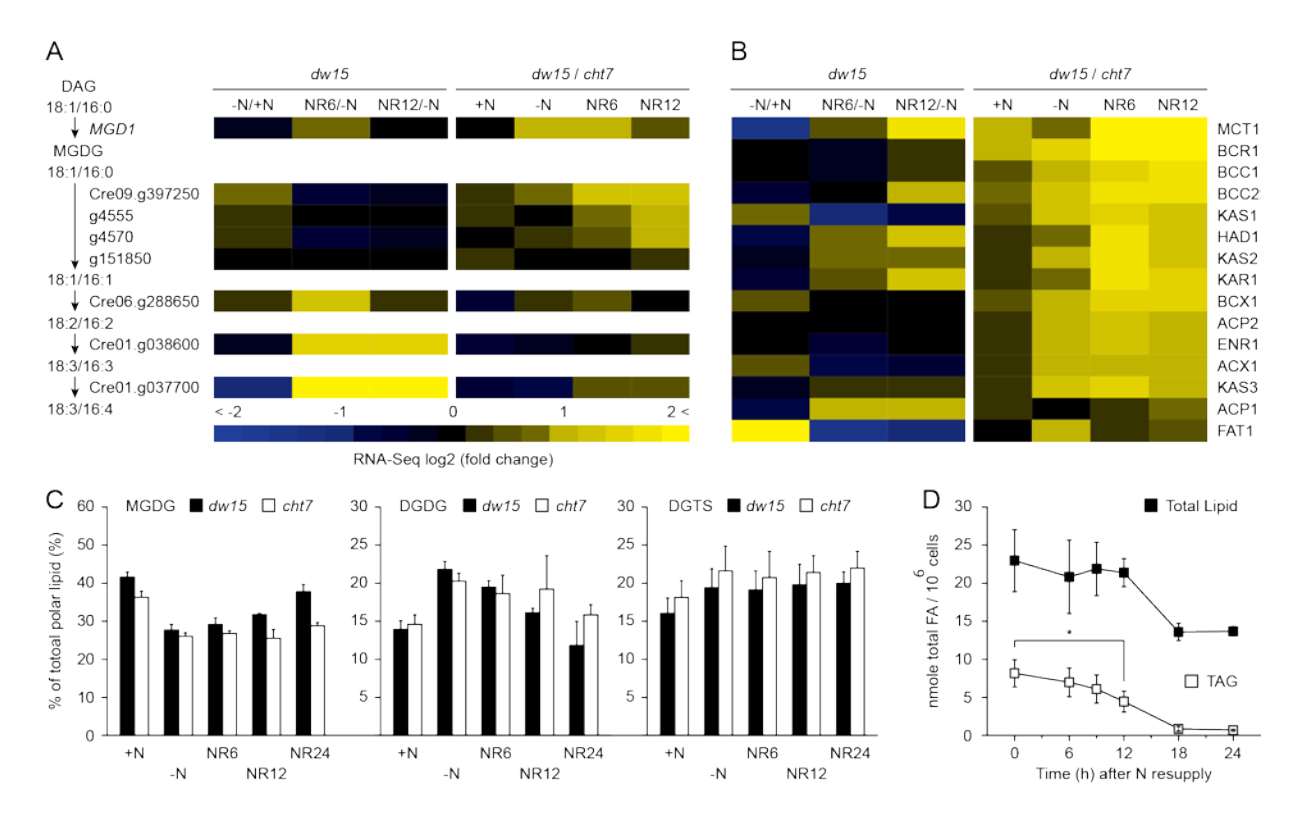


Figure 3.7. Changes in Gene Expression and Metabolite Levels Related to MGDG and Fatty Acid Syntheses. (A, B) Overview of expression of genes expression involved in MGDG (A) and in fatty acid (B) syntheses. RNA-Seq comparisons of *dw15* at different N status and the comparisons between *dw15* and *cht7* at each N status are shown in the heatmap. Arrows indicate the sequence of reactants and products of the catalyzed reactions for each enzyme encoded by the gene as indicated. +N, N-replete; -N, N-deprived; NR6 and NR12, 6 and 12 h of N resupply. 18:1/16:0 indicates the fatty acid (FA) at the sn-1/sn-2 position of DAG (diacylglycerol) or MGDG (monogalactosyldiacylglycerol). (C) Polar lipid content (depicted as the ratio of each polar lipid FAs over total polar lipid FAs) in the presence (+N, N-replete) or absence (-N, N-deprived) of N or following N resupply at times indicated (h). DGDG, digalactosyldiacylglycerol; DGTS, diacylglyceryl-trimethylhomoserine. Averages (n=4) and standard deviation are indicated.

Figure 3.7 (cont'd)

(D) Per cell FA content for total lipid and TAG following N resupply in *dw15*. Averages (n=3) and standard deviation are indicated.

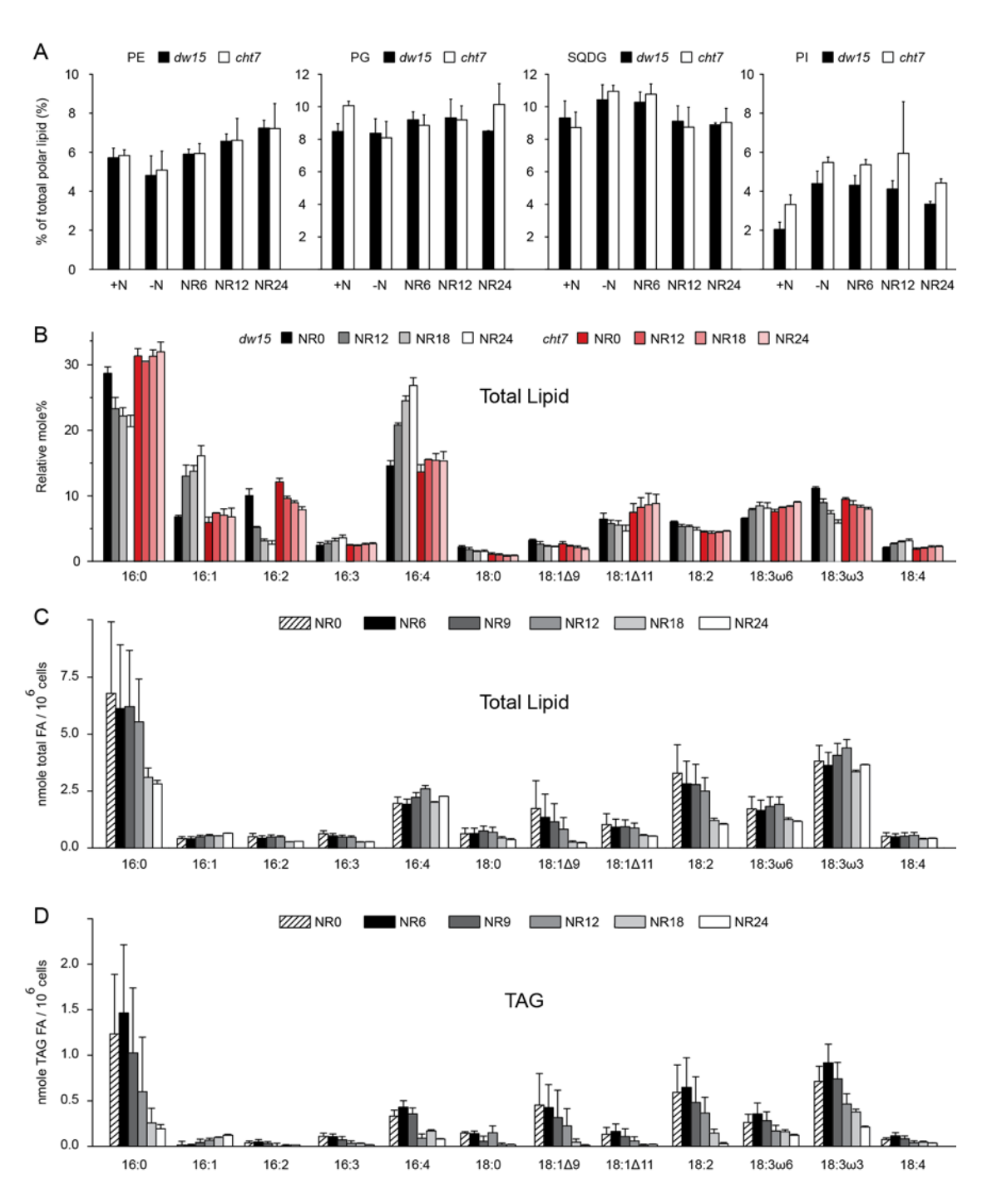


Figure 3.8. Detailed Lipid Analysis at Quiescence Exit. (A) Quantification of polar lipids in *dw15* and *cht7* grown at different N status (+N, N-replete; -N, N-deprived; NR, N-resupplied) for

Figure 3.8 (cont'd)

the times (h) indicated, including phosphatidylethanolamine (PE), phosphatidylglycerol (PG), sulfoquinovosyldiacylglycerol (SQDG) and phosphatidylinositol (PI). The y-axis is depicted as ratio of each polar lipid fatty acids (FAs) over total polar FAs. (B) Relative fatty acid composition of *dw15* and *cht7* following N resupply (NR) at times indicated (h). (C, D) Relative fatty acid composition of *dw15* of total lipids (C) and of TAGs (D) following N resupply at times indicated (h).

Fatty acid profiles of total lipids remained almost unchanged in cht7 after N resupply, while in the PL, 16:4 and 18:3\omega3 fatty acids increased over time in parallel to increases in MGDG content (Figure 3.8B). 16:4 and 18:3ω3 are the major fatty acids of the MGDG (Giroud et al., 1988). Not surprisingly, among all the membrane lipids cht7 was not able to readjust MGDG in response to N resupply (Figures 3.7C and 3.8A). I found that MGD1 encoding the MGDG synthase, three genes for MGDG palmitate-delta7-desaturase (Cre09.g397250, g4555 and g4570), and virtually every gene involved in fatty acid synthesis were misregulated in cht7 (Figures 3.7 A-B and 3.6C). Nevertheless, these genes might not be under the direct control of CHT7 since they were not present in the NR6 or NR12 overlap groups (Figure 3.4 A and B; Online Supplemental Data Sets 7 and 9), except for *HAD1*, *KAR1* and *MCT1* but only in NR12. TAG degradation started soon after 6 h of N resupply in almost a linear fashion; however, the total lipid content per cell did not vary noticeably by 12 h of N resupply (Figure 3.7D), implicating that the fatty acids removed from TAGs were not sent to peroxisomes for β -oxidation, but probably to the chloroplast for rebuilding of MGDG, the predominant lipid of photosynthetic membranes. Indeed, 16:4 and 18:3\omega3 fatty acids were not being degraded after N is resupplied and had been stored in TAGs during N deprivation (Figure 3.8 C and D). Therefore we hypothesize that the transcription of MGDG and fatty acid synthesis is subjected to a feedback control by metabolite levels. In cht7 following N resupply, the low 16:4 and 18:3\omega3 levels (as free fatty acids or in DAGs) and the high overall fatty acid levels (in TAGs) created a negative

feedback that does not allow upregulation of genes for MGDG and fatty acid syntheses, respectively. Moreover, MGDG desaturation was also part of the NR-specific responses, as the genes encoding the enzymes that catalyze the second and third double bonds on the *sn*-1 and *sn*-2 position of MGDG were especially up-regulated following N resupply (Cre06.g288650 and Cre01.g038600, Figure 3.7A; Online Supplemental Data Set 9), suggesting that the demand for MGDG in exiting quiescence was higher than that for ordinary growth.

Two Classes of Lipases Affect TAG Accumulation in opposite ways

Lipases are a subclass of acyl hydrolases that deesterify carboxylic esters. Traditionally, they are referred to as class 3 lipases when involved in the hydrolysis of TAG, with a serine protease triad forming the catalytic center (Brady et al., 1990; Winkler et al., 1990). Since it has become clear that during N deprivation membrane lipid turnover is an alternative route for fatty acids channeled into TAGs (Li et al., 2012b), lipases can actually affect TAG accumulation in opposite ways. However, it is a challenge to distinguish them. There are 131 proteins predicted to be lipases, phospholipases, or patatin-like proteins based on the GXSXG motif common to hydrolases (Online Supplemental Data Set 8), and biochemical validation often comes with surprises. PGD1, the galactoglyceride lipase responsible for half of the TAG production, was purported to be a TAG lipase based on in silico annotation (Li et al., 2012b). Although LIP1 is a class 3 lipase, it can act on polar lipids in addition to its involvement in TAG turnover (Li et al., 2012a). Through integrated pairwise comparison, I was able to filter and classify lipases according to the gene expression patterns. As TAGs increase during N deprivation and decrease following N resupply, I expected genes encoding lipases involved in TAG turnover (e.g. LIP1) to be down-regulated during N deprivation (Figure 3.9, -N/+N), and up-regulated following N

resupply (Figure 3.9, NR6/-N or NR12/-N), and genes encoding lipases assisting TAG production (e.g. PGD1) to behave in the opposite way. Thus I narrowed down the number of potential functional lipases to 9 (TAG turnover, Figure 3.9 upper panel) and 23 (TAG production, Figure 3.9 middle panel), including LIP1 and PGD1 in their expected class. We also included 2 (TAG turnover) and 6 (TAG production) NR-specific lipase candidates whose abundance might be critical for TAGs when N is again available. Transcript profiling of candidate genes for peroxisomal β-oxidation (e.g. 3-oxoacyl-CoA thiolase (ATO1) and acyl-CoA oxidase) is in tune with TAG turnover under these conditions, with the exception of enoyl-CoA oxidase/isomerase (ECH1) which is particularly important for degradation of unsaturated fatty acids (Goepfert et al., 2008). A primary phenotype of cht7 is the compromised hydrolysis of TAGs, after which the mutant is named. After 6 h of N resupply, among the genes of two classes of lipases, Cre17.g707300, Cre06.g265850, Cre03.g195200 and Cre03.g152800 (possibly TAG-reducing) and PGD1, g9707 and Cre03.g174900 (possibly TAG-enhancing) were misregulated in cht7 and behaved in a way that would hinder the degradation and promote the accumulation of TAGs, making them promising candidates for reverse genetic studies (Figure 3.9 and Online Supplemental Data Set 8). These seven genes are also among the NR6 overlaps mentioned above.

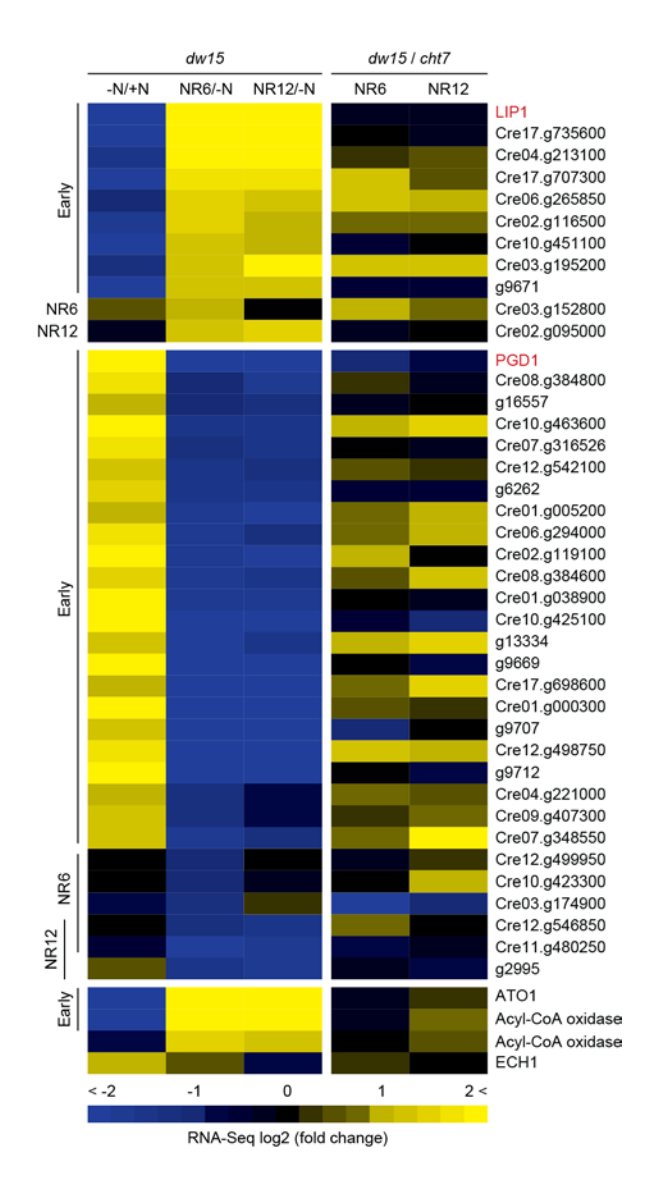


Figure 3.9. Changes in Gene Expression of Putative Lipases and β**-oxidation.** Transcript profiles of genes encoding lipases potentially involved in the degradation of TAGs (upper panel) or in the production TAGs (middle panel), and of the genes involved in β-oxidation (lower panel). RNA-Seq comparisons of dw15 between at N status and the comparisons between dw15 and cht7 at each N status are shown in the heatmap. +N, N-replete; -N, N-deprived; NR6 and NR12, 6 and 12 h of N resupply. Early, Mid, Late, NR6 or NR12 is indicated on the left of the heatmap for the gene whose response to N resupply has been classified.

The cAMP-Dependent Protein Kinase A Pathway Is Involved in Quiescence Exit

I also explored signaling cascades that may impact TAG metabolism. In adipocytes, adenylyl cyclase and protein kinase A (PKA) act as transducers between hormone signals and lipolytic responses (Guo et al., 2009). Upon activation, adenylyl cyclase converts ATP to cyclic AMP

(cAMP) and binding of cAMP to the regulatory domains of PKA activates the enzyme and leads to the phosphorylation of the respective targets, e.g. hormone sensitive lipase and perilipin. Adenylyl and guanylyl cyclases form one of the largest enzyme families in the Chlamydomonas genome (Merchant et al., 2007), and discrimination based solely on primary sequences is difficult. At a glance, many of the adenylyl cyclase candidates were differentially regulated by N status and in the cht7 background (Online Supplemental Data Set 10). A cAMP specific ELISA assay showed that concentrations of cAMP positively correlate with the activation of TAG breakdown (Figure 3.10A). I therefore intended to clarify the involvement of PKA in the lipolysis in Chlamydomonas. A 20-amino acid fragment of the naturally occurring protein kinase inhibitor (PKI) has been shown to bind to the catalytic domain of PKA (Knighton et al., 1991). A derivative of this fragment has been used in the study of protein kinases in flagellar assembly in Chlamydomonas (Howard et al., 1994). When applied simultaneously with N refeeding, PKI blocked lipolysis in the PL in a dosage-dependent manner (Figure 3.10B). 10 µM of PKI caused chlorosis indicative of cell death, thus none of the TAGs in the PL or cht7 being degraded even at 24 h of N resupply. Fatty acid profiles of cells treated with PKI resembled those of cht7 (Figure 3.11). Importantly, within the nontoxic range the TAG contents of *cht7* were not affected by PKI. PKI treatment also mimicked the regrowth defect of cht7 in the PL (Figure 3.10C). Phosphodiesterases are the enzyme counteracting adenylyl cyclase by breaking cAMP into AMP. Stimulating the activity of phosphodiesterase attenuates cAMP-mediated lipolysis (Botion and Green, 1999). We curated potential adenylyl cyclases and phosphodiesterases whose expression profile matched the fluctuation of cAMP (Figure 3.10D; Online Supplemental Data Set 10), with the intent to provide possible candidates for reverse genetic studies, such as Cre13.g607150, Cre05.g237800, Cre02.g080550 and g11603 considering their regulation in cht7. The remainder of the enzymes (in Online Supplemental Data Set 10 but not listed in Figure 3.10A) might be responsible for cyclic GMP signaling.

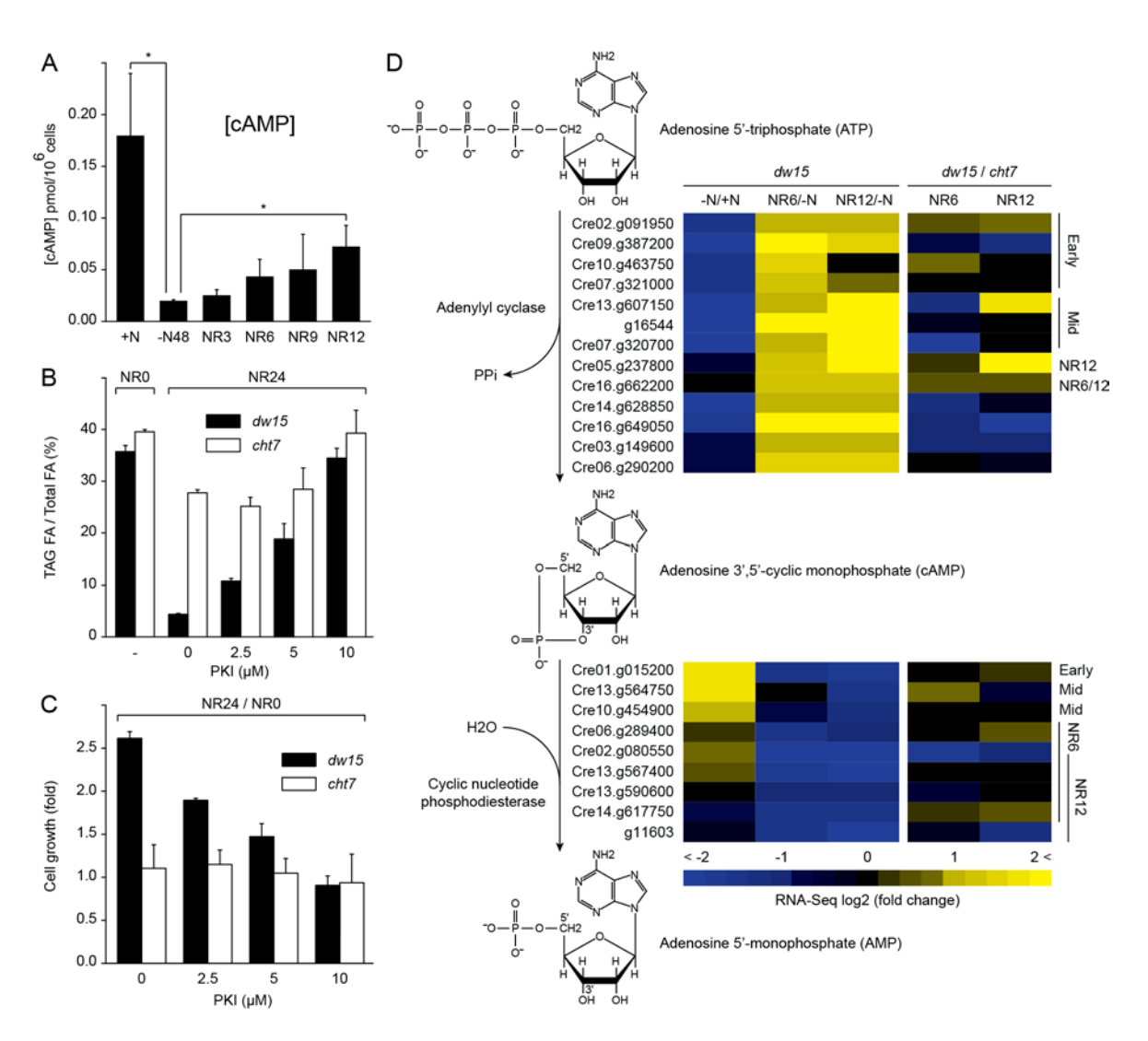


Figure 3.10. Possible Role o cAMP-PKA Signaling in Quiescence Exit and Transcript Profiles of Related Genes. (A) ELISA assay to quantify the cellular content of cAMP in dw15. +N, N-replete; -N, N-deprived; NR, N resupply at times indicated (h). Asterisks indicate a statistically significant difference (unpaired t-test, p < 0.05). (B) Efficacy of TAG degradation in the presence of the inhibitor PKI . TAG contents (depicted as ratio of TAG fatty acids (FA) over total FAs) right before N resupply (NR) are shown under NR0 (equivalent to -N, N-deprived for 48 h). TAG contents after 24 h of N resupply with and without PKI treatment are shown under NR24. (C) Regrowth during PKI treatment is shown as fold increase by comparing the cell number counted at 24 h of N resupply to that counted right before N resupply with and without PKI treatment. (D) Transcript profiles of genes encoding putative adenylyl cyclase and phosphodiesterase. RNA-Seq comparisons of dw15 at different N status and the comparisons

Figure 3.10 (cont'd)

between *dw15* and *cht7* at each N status are shown in the heatmap. +N, N-replete; -N, N-deprived; NR6 and NR12, 6 and 12 h of N resupply. Early, Mid, Late, NR6 or NR12 is indicated on the left of the heatmap for the gene whose response to N resupply has been classified. For all quantitative data, averages (n=3) and standard deviation are indicated.

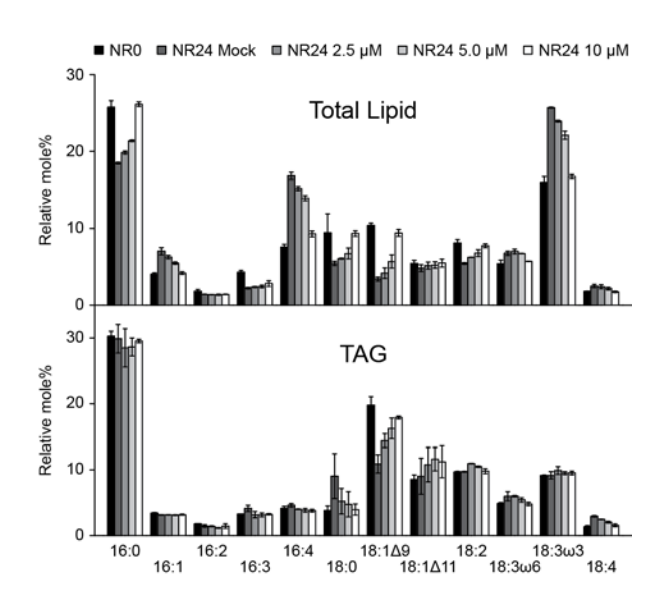


Figure 3.11. Fatty Acid Profiles of PKI-Treated Samples. Relative fatty acid composition of total lipids (upper panel) and of TAGs (lower panel) in dw15. After 48 h of N deprivation, cells were sampled right before N resupply (NR0) and at 24 h of N resupply with and without PKI treatment (μ M).

DISCUSSION

N deprivation is as an effective approach to induce TAG accumulation in microalgae, attracting interest from public and private sectors due to the potential in creating a renewable energy source (Hu et al., 2008). From a biology standpoint, the reversible cessation of growth provides a facile experimental system to study cellular quiescence. Chlamydomonas offers perspectives beyond yeast in studying quiescence because, apart from the unique features related to photosynthesis, the underlying regulatory processes in this green alga utilize a Retinoblastoma (RB) tumor suppressor homologue and CXC domain proteins such as CHT7 and thus more closely resemble regulation in mammalian cells (Armbrust et al., 1995; Burkhart and Sage, 2008; Sadasivam and DeCaprio, 2013). Yeast cells possess neither RB nor CXC domain proteins. Cellular responses to N deprivation have been studied on multiple omic levels, including transcripts, proteins, and metabolites, drawing an integrated picture of N sparing mechanisms (Miller et al., 2010; Blaby et al., 2013; Schmollinger et al., 2014; Wase et al., 2014). In contrast, the research on quiescence exit or the means that triggers it (i.e. N resupply) has not yet been studied; in part due to the misconception that quiescence exit might simply be the reverse of entry. In this work, global transcriptomic analysis uncovered a subset of genes whose expression only fluctuated during N resupply (e.g. BTA1 and DGTT4), as a first entry point to explore the unique aspects of quiescence exit. Metabolite levels are usually lower in quiescent cells than newly divided ones because of a higher catabolic and lower anabolic rate, for example, chlorophylls (Gray et al., 2004; Schmollinger et al., 2014). It is natural to imagine the regrowth out of quiescence demands more than ordinary cell proliferation does. NR-specific genes were dispersed in diverse pathways with genes that reverted expression pattern in response to N resupply. I discussed many

examples, such as BTA1 in DGTS synthesis and MGDG desaturation, to show that NR-specific responses are important to boost the rapid resumption of growth.

The CHT7 regulon and possible influence of cAMP-PKA signaling

NR overlaps (Figure 3.4 A and B) highlight programs of genes most likely responsible for—not only responsive to—quiescence exit and at the same time under the control of CHT7. I hypothesize that when cells receive signals to exit quiescence, CHT7 governs these programs that affect metabolic pathways necessary for the resumption of growth. The discussed examples of misregulated pathways, i.e., tetrapyrrole pathway and peroxisomal redox homeostasis, represent just a fraction of genes affected in their expression by CHT7. Particularly important is that these metabolic pathways misregulated in *cht7* during N resupply were normal during N-replete growth. As such CHT7 may play distinct roles in repressing transcriptional programs prior to quiescence entry and in adjusting transcriptional networks during the exit from quiescence. Whether the control of CHT7 on these genes is direct or indirect remains to be answered through further analysis, e.g. chromatin immunoprecipitation followed by sequencing of fragments bound to CH7 or its complex.

My finding of cAMP-PKA signaling being potentially involved in lipolysis and quiescence exit in Chlamydomonas was a logical prediction based on the current knowledge in adipocytes and in yeast quiescence cells. However, none of the two classic examples of PKA phosphorylation in lipolysis, hormone sensitive lipase and perilipin, has apparent homologues encoded in the *C. reinhardtii* genome (Yeaman, 1990; Marcinkiewicz et al., 2006). Even so it does not rule out the existence of unknown PKA targets that can modulate lipolysis. Another possibility is that the cAMP-PKA signaling pathway controls upstream aspects of quiescence,

and the inhibition of TAG turnover by PKI treatment is a secondary effect. It drew my attention when PKI treatment did not exacerbate the TAG phenotype in cht7, which strongly suggests that the CHT7 and cAMP-PKA pathways converge at some point, at least in the regulation of TAG turnover. In yeast, cAMP-PKA singling, like CHT7 in Chlamydomonas, prevents the entry into quiescence. Mutants of adenylyl cyclase fail to proliferate and display phenotypes superficially similar to quiescence (van Aelst et al., 1991). On the contrary, constitutive activation of PKA causes premature cell death when entering quiescence, indicative of the necessity to deactivate the negative regulators of quiescence to ensure a proper entry (Uno et al., 1984; Shin et al., 1987). Downregulation of CHT7 activity in quiescent cells might as well be necessary in Chlamydomonas. In addition, reactivation of the cAMP-PKA pathway is critical for successful exit from quiescence in yeast. Yeast mutants unable to raise a transient cAMP level when fresh nutrients are again available show extended delay in resuming growth (Jiang et al., 1998). Pharmacological and biochemical approaches have uncovered the existence of PKA catalytic subunits in Chlamydomonas even though respective genes are still missing (Howard et al., 1994). Future studies of a possible CHT7-cAMP-PKA interplay may shed light on the complex network underlying quiescence control. At present, whether the Chlamydomonas cAMP-PKA pathway directly controls lipolysis, which in turn affects quiescence exit or vise versa remains unclear, but either way it points to unique opportunities to unravel questions concerning LD biology and cellular quiescence.

REFERENCES

REFERENCES

- Allen, M.D., Kropat, J., Tottey, S., Del Campo, J.A., and Merchant, S.S. (2007). Manganese deficiency in Chlamydomonas results in loss of photosystem II and MnSOD function, sensitivity to peroxides, and secondary phosphorus and iron deficiency. Plant physiology **143**, 263-277.
- **Armbrust, E.V., Ibrahim, A., and Goodenough, U.W.** (1995). A mating type-linked mutation that disrupts the uniparental inheritance of chloroplast DNA also disrupts cell-size control in Chlamydomonas. Molecular biology of the cell **6**, 1807-1818.
- **Baroli, I., Do, A.D., Yamane, T., and Niyogi, K.K.** (2003). Zeaxanthin accumulation in the absence of a functional xanthophyll cycle protects Chlamydomonas reinhardtii from photooxidative stress. The Plant cell **15,** 992-1008.
- **Benning, C., Huang, Z.H., and Gage, D.A.** (1995). Accumulation of a novel glycolipid and a betaine lipid in cells of Rhodobacter sphaeroides grown under phosphate limitation. Archives of biochemistry and biophysics **317**, 103-111.
- Blaby, I.K., Glaesener, A.G., Mettler, T., Fitz-Gibbon, S.T., Gallaher, S.D., Liu, B., Boyle, N.R., Kropat, J., Stitt, M., Johnson, S., Benning, C., Pellegrini, M., Casero, D., and Merchant, S.S. (2013). Systems-level analysis of nitrogen starvation-induced modifications of carbon metabolism in a Chlamydomonas reinhardtii starchless mutant. The Plant cell **25**, 4305-4323.
- **Botion, L.M., and Green, A.** (1999). Long-term regulation of lipolysis and hormone-sensitive lipase by insulin and glucose. Diabetes **48,** 1691-1697.
- Boyle, N.R., Page, M.D., Liu, B., Blaby, I.K., Casero, D., Kropat, J., Cokus, S.J., Hong-Hermesdorf, A., Shaw, J., Karpowicz, S.J., Gallaher, S.D., Johnson, S., Benning, C., Pellegrini, M., Grossman, A., and Merchant, S.S. (2012). Three acyltransferases and nitrogen-responsive regulator are implicated in nitrogen starvation-induced triacylglycerol accumulation in Chlamydomonas. The Journal of biological chemistry 287, 15811-15825.
- Brady, L., Brzozowski, A.M., Derewenda, Z.S., Dodson, E., Dodson, G., Tolley, S., Turkenburg, J.P., Christiansen, L., Huge-Jensen, B., Norskov, L., and et al. (1990). A serine protease triad forms the catalytic centre of a triacylglycerol lipase. Nature 343, 767-770.
- **Burkhart, D.L., and Sage, J.** (2008). Cellular mechanisms of tumour suppression by the retinoblastoma gene. Nature reviews. Cancer **8,** 671-682.

- Bustin, S.A., Benes, V., Garson, J.A., Hellemans, J., Huggett, J., Kubista, M., Mueller, R., Nolan, T., Pfaffl, M.W., Shipley, G.L., Vandesompele, J., and Wittwer, C.T. (2009). The MIQE guidelines: minimum information for publication of quantitative real-time PCR experiments. Clinical chemistry 55, 611-622.
- Castruita, M., Casero, D., Karpowicz, S.J., Kropat, J., Vieler, A., Hsieh, S.I., Yan, W., Cokus, S., Loo, J.A., Benning, C., Pellegrini, M., and Merchant, S.S. (2011). Systems biology approach in Chlamydomonas reveals connections between copper nutrition and multiple metabolic steps. The Plant cell 23, 1273-1292.
- Coller, H.A. (2011). Cell biology. The essence of quiescence. Science 334, 1074-1075.
- **Eastmond, P.J.** (2007). MONODEHYROASCORBATE REDUCTASE4 is required for seed storage oil hydrolysis and postgerminative growth in Arabidopsis. The Plant cell **19**, 1376-1387.
- Gasch, A.P., Spellman, P.T., Kao, C.M., Carmel-Harel, O., Eisen, M.B., Storz, G., Botstein, D., and Brown, P.O. (2000). Genomic expression programs in the response of yeast cells to environmental changes. Molecular biology of the cell 11, 4241-4257.
- **Giroud, C., Gerber, A., and Eichenberger, W.** (1988). Lipids of Chlamydomonas reinhardtii Analysis of molecular species and intracellular site(s) of biosynthesis. Plant Cell Physiol. **29**, 587-595.
- Goepfert, S., Vidoudez, C., Tellgren-Roth, C., Delessert, S., Hiltunen, J.K., and Poirier, Y. (2008). Peroxisomal Delta(3),Delta(2)-enoyl CoA isomerases and evolution of cytosolic paralogues in embryophytes. The Plant journal: for cell and molecular biology **56**, 728-742.
- Gonzalez-Ballester, D., Casero, D., Cokus, S., Pellegrini, M., Merchant, S.S., and Grossman, A.R. (2010). RNA-seq analysis of sulfur-deprived Chlamydomonas cells reveals aspects of acclimation critical for cell survival. The Plant cell **22**, 2058-2084.
- Goodson, C., Roth, R., Wang, Z.T., and Goodenough, U. (2011). Structural correlates of cytoplasmic and chloroplast lipid body synthesis in Chlamydomonas reinhardtii and stimulation of lipid body production with acetate boost. Eukaryotic cell 10, 1592-1606.
- **Graham, I.A.** (2008). Seed storage oil mobilization. Annual review of plant biology **59**, 115-142.
- Gray, J.V., Petsko, G.A., Johnston, G.C., Ringe, D., Singer, R.A., and Werner-Washburne, M. (2004). "Sleeping beauty": quiescence in Saccharomyces cerevisiae. Microbiology and molecular biology reviews: MMBR 68, 187-206.
- Guo, Y., Cordes, K.R., Farese, R.V., Jr., and Walther, T.C. (2009). Lipid droplets at a glance. Journal of cell science 122, 749-752.
- **Harris, E.H.** (1989). Chlamydomonas Sourcebook. (New York: Academic Press: New York: Academic Press).

- Howard, D.R., Habermacher, G., Glass, D.B., Smith, E.F., and Sale, W.S. (1994). Regulation of Chlamydomonas flagellar dynein by an axonemal protein kinase. The Journal of cell biology 127, 1683-1692.
- Hu, Q., Sommerfeld, M., Jarvis, E., Ghirardi, M., Posewitz, M., Seibert, M., and Darzins, A. (2008). Microalgal triacylglycerols as feedstocks for biofuel production: perspectives and advances. The Plant journal: for cell and molecular biology **54**, 621-639.
- **Jiang, Y., Davis, C., and Broach, J.R.** (1998). Efficient transition to growth on fermentable carbon sources in Saccharomyces cerevisiae requires signaling through the Ras pathway. The EMBO journal **17**, 6942-6951.
- Knighton, D.R., Zheng, J.H., Ten Eyck, L.F., Xuong, N.H., Taylor, S.S., and Sowadski, J.M. (1991). Structure of a peptide inhibitor bound to the catalytic subunit of cyclic adenosine monophosphate-dependent protein kinase. Science 253, 414-420.
- **Li, X., Benning, C., and Kuo, M.H.** (2012a). Rapid triacylglycerol turnover in Chlamydomonas reinhardtii requires a lipase with broad substrate specificity. Eukaryotic cell **11,** 1451-1462.
- Li, X., Moellering, E.R., Liu, B., Johnny, C., Fedewa, M., Sears, B.B., Kuo, M.H., and Benning, C. (2012b). A galactoglycerolipid lipase is required for triacylglycerol accumulation and survival following nitrogen deprivation in Chlamydomonas reinhardtii. The Plant cell **24**, 4670-4686.
- Marcinkiewicz, A., Gauthier, D., Garcia, A., and Brasaemle, D.L. (2006). The phosphorylation of serine 492 of perilipin a directs lipid droplet fragmentation and dispersion. The Journal of biological chemistry 281, 11901-11909.
- Merchant, S.S., Prochnik, S.E., Vallon, O., Harris, E.H., Karpowicz, S.J., Witman, G.B., Terry, A., Salamov, A., Fritz-Laylin, L.K., Marechal-Drouard, L., Marshall, W.F., Qu, L.H., Nelson, D.R., Sanderfoot, A.A., Spalding, M.H., Kapitonov, V.V., Ren, Q., Ferris, P., Lindquist, E., Shapiro, H., Lucas, S.M., Grimwood, J., Schmutz, J., Cardol, P., Cerutti, H., Chanfreau, G., Chen, C.L., Cognat, V., Croft, M.T., Dent, R., Dutcher, S., Fernandez, E., Fukuzawa, H., Gonzalez-Ballester, D., Gonzalez-Halphen, D., Hallmann, A., Hanikenne, M., Hippler, M., Inwood, W., Jabbari, K., Kalanon, M., Kuras, R., Lefebvre, P.A., Lemaire, S.D., Lobanov, A.V., Lohr, M., Manuell, A., Meier, I., Mets, L., Mittag, M., Mittelmeier, T., Moroney, J.V., Moseley, J., Napoli, C., Nedelcu, A.M., Niyogi, K., Novoselov, S.V., Paulsen, I.T., Pazour, G., Purton, S., Ral, J.P., Riano-Pachon, D.M., Riekhof, W., Rymarquis, L., Schroda, M., Stern, D., Umen, J., Willows, R., Wilson, N., Zimmer, S.L., Allmer, J., Balk, J., Bisova, K., Chen, C.J., Elias, M., Gendler, K., Hauser, C., Lamb, M.R., Ledford, H., Long, J.C., Minagawa, J., Page, M.D., Pan, J., Pootakham, W., Roje, S., Rose, A., Stahlberg, E., Terauchi, A.M., Yang, P., Ball, S., Bowler, C., Dieckmann, C.L., Gladyshev, V.N., Green, P., Jorgensen, R., Mayfield, S., Mueller-Roeber, B., Rajamani, S., Sayre, R.T., Brokstein, P., Dubchak, I., Goodstein, D., Hornick, L., Huang, Y.W., Jhaveri, J., Luo, Y., Martinez, D., Ngau, W.C., Otillar, B., Poliakov,

- A., Porter, A., Szajkowski, L., Werner, G., Zhou, K., Grigoriev, I.V., Rokhsar, D.S., and Grossman, A.R. (2007). The Chlamydomonas genome reveals the evolution of key animal and plant functions. Science 318, 245-250.
- Miller, R., Wu, G., Deshpande, R.R., Vieler, A., Gartner, K., Li, X., Moellering, E.R., Zauner, S., Cornish, A.J., Liu, B., Bullard, B., Sears, B.B., Kuo, M.H., Hegg, E.L., Shachar-Hill, Y., Shiu, S.H., and Benning, C. (2010). Changes in transcript abundance in Chlamydomonas reinhardtii following nitrogen deprivation predict diversion of metabolism. Plant physiology 154, 1737-1752.
- **Moellering, E.R., and Benning, C.** (2010). RNA interference silencing of a major lipid droplet protein affects lipid droplet size in Chlamydomonas reinhardtii. Eukaryotic cell **9,** 97-106.
- **Riekhof, W.R., Sears, B.B., and Benning, C.** (2005). Annotation of genes involved in glycerolipid biosynthesis in Chlamydomonas reinhardtii: discovery of the betaine lipid synthase BTA1Cr. Eukaryotic cell **4,** 242-252.
- Rossak, M., Schafer, A., Xu, N., Gage, D.A., and Benning, C. (1997). Accumulation of sulfoquinovosyl-1-O-dihydroxyacetone in a sulfolipid-deficient mutant of Rhodobacter sphaeroides inactivated in sqdC. Archives of biochemistry and biophysics **340**, 219-230.
- **Sadasivam, S., and DeCaprio, J.A.** (2013). The DREAM complex: master coordinator of cell cycle-dependent gene expression. Nature reviews. Cancer **13**, 585-595.
- Schmollinger, S., Muhlhaus, T., Boyle, N.R., Blaby, I.K., Casero, D., Mettler, T., Moseley, J.L., Kropat, J., Sommer, F., Strenkert, D., Hemme, D., Pellegrini, M., Grossman, A.R., Stitt, M., Schroda, M., and Merchant, S.S. (2014). Nitrogen-Sparing Mechanisms in Chlamydomonas Affect the Transcriptome, the Proteome, and Photosynthetic Metabolism. The Plant cell **26**, 1410-1435.
- Shin, D.Y., Matsumoto, K., Iida, H., Uno, I., and Ishikawa, T. (1987). Heat shock response of Saccharomyces cerevisiae mutants altered in cyclic AMP-dependent protein phosphorylation. Molecular and cellular biology 7, 244-250.
- **Theodoulou, F.L., and Eastmond, P.J.** (2012). Seed storage oil catabolism: a story of give and take. Current opinion in plant biology **15**, 322-328.
- **Tsai, C.H., Warakanont, J., Takeuchi, T., Sears, B.B., Moellering, E.R., and Benning, C.** (2014). The protein Compromised Hydrolysis of Triacylglycerols 7 (CHT7) acts as a repressor of cellular quiescence in Chlamydomonas. Proceedings of the National Academy of Sciences of the United States of America **111**, 15833-15838.
- Uno, I., Matsumoto, K., Adachi, K., and Ishikawa, T. (1984). Characterization of cyclic AMP-requiring yeast mutants altered in the catalytic subunit of protein kinase. The Journal of biological chemistry **259**, 12508-12513.
- Valcourt, J.R., Lemons, J.M., Haley, E.M., Kojima, M., Demuren, O.O., and Coller, H.A. (2012). Staying alive: metabolic adaptations to quiescence. Cell cycle 11, 1680-1696.

- van Aelst, L., Jans, A.W., and Thevelein, J.M. (1991). Involvement of the CDC25 gene product in the signal transmission pathway of the glucose-induced RAS-mediated cAMP signal in the yeast Saccharomyces cerevisiae. Journal of general microbiology **137**, 341-349.
- Wase, N., Black, P.N., Stanley, B.A., and DiRusso, C.C. (2014). Integrated quantitative analysis of nitrogen stress response in Chlamydomonas reinhardtii using metabolite and protein profiling. Journal of proteome research 13, 1373-1396.
- Winkler, F.K., D'Arcy, A., and Hunziker, W. (1990). Structure of human pancreatic lipase. Nature 343, 771-774.
- **Yeaman, S.J.** (1990). Hormone-sensitive lipase--a multipurpose enzyme in lipid metabolism. Biochimica et biophysica acta **1052**, 128-132.
- **Zieger, R., and Egle, K.** (1965). Zur quantitativen Analyse der Chloroplasten pigmente. I. Kritische Überprüfung der spektralphotometrischen Chlorophyllbestimmung. Beitr. Biol. Pflanz. **41,** 11-37.

CHAPTER 4	
The Role of Lipid Droplet in Coordinating Lipid Dynamics to Ensure the Reversib	oility of
Cellular Quiescence in Chlamydomonas ¹	
contributed to the data shown in all of the figures. Krzysztof Zienkiewicz also made sign ontribution to Figures 4.4C, 4,7 D, E, and F.	gnifican

ABSTRACT

ABSTRACT

Lipid droplets (LDs) are unique among organelles for their hydrophobic core which allows the storage of neutral lipids. They are also known as hubs for lipid metabolism and temporary shelters for protein under stress conditions. The fate of LD is closely tied to the state of quiescence in unicellular organisms. However, whether or how LDs influence quiescence is largely unknown. Here, I provide evidence that LDs coordinate critical responses for quiescence. These comprise a possible deacylation/reacylation cycle that exchanges the polyunsaturated acyl groups of LD surface lipids with *de novo* synthesized saturated ones; providing temporary shelter for refugee proteins; and being in close proximity to the chloroplast outer envelope to allow protein and lipid trafficking between the two organelles during quiescence exit. The mature LD requires stabilization by a proteinaceous coating. Failure to maintain an optimized surface areato-volume ratio of LD compromises the efficacy of triacylglycerol turnover, and disturbs the timely progression out of quiescence.

INTRODUCTION

TAGs synthesized during quiescence are stored in lipid droplets (LDs), the dynamic organelles found ubiquitously across species and cell types. Long perceived as inert, lipid droplets are now known to have many cellular functions (Martin and Parton, 2006; Walther and Farese, 2012). Such recognition comes from LD proteomes and biochemical evidence. The localization of a long chain acyl-CoA synthetase (ACSL3), two phosphocholine cytidylyltransferase isoforms (CCT1 and CCT2), and a diacylglycerol acyltransferase (DGAT2) to LDs in animals suggests local synthesis of phosphotidylcholine (PC) and TAG needed for LD growth (Fujimoto et al., 2007; Guo et al., 2008; Kuerschner et al., 2008). Activities of ACSL3 and CCT1 associated with LDs are experimentally verified (Fujimoto et al., 2007; Krahmer et al., 2011). Proteomic studies in Chlamydomonas also portray LDs as a hub for lipid synthesis, acyl exchange, lipid signaling and trafficking (Moellering and Benning, 2010; Nguyen et al., 2011). Under stress conditions (e.g. heat shock or endoplasmic reticulum (ER) stress) or certain developmental stages (e.g. Drosophila embryos or viral infection), LDs recruit seemingly unrelated proteins from other cellular compartments, hypothetically for temporary sheltering and to proteins sequestered when not needed, or as a way to transport proteins (Welte, 2007). It is a common belief that LDs in eukaryotes emerge from the ER. However, recent studies in Chlamydomonas proposed that the ER and chloroplast are both involved in LD biogenesis. Evidence shows that LDs are invariably cytosolic but snuggled into the folds of the chloroplast envelope, forming numerous punctate associations with the outer envelope, and that nearly all the diacylglycerols (DAGs) acylated into TAGs in LDs are derived from the chloroplast (Fan et al., 2011; Goodson et al., 2011).

The mutant phenotype of *cht7* shows that LD formation as well as its degradation is tightly linked to the state of quiescence (Tsai et al., 2014). However, whether or how LDs

contribute to the entry, maintenance, and exit of quiescence has not yet been addressed. In this study, I conducted functional analysis of LDs using biochemical, genetic, microscopic and proteomic approaches. The detailed characterization of LDs may transform our thinking about mechanisms responsible for the reversibility of quiescence.

MATERIALS AND METHODS

Strains and Growth Conditions

As described in Chapter 2.

Fatty Acid and Lipid Analysis

As described in Chapter 2.

Lipid Droplet Isolation, HDN-PAGE, and Co-immunoprecipitation

Cells grown in 400 mL of N-deprived or 800 mL of N-resupplied cultures were spun down and resuspended in 10 mL of isolation buffer (50 mM HEPES pH 7.5, 5 mM KCl, 5 mM MgCl₂, 0.5 mM sucrose, 1 mM phenylmethylsulfonylfluoride (PMSF), 1 mM 2,2'-dipyridyl, and 1X protease inhibitor cocktail Roche), and lysed by sonication on ice with 10 s on/off cycle for 2 min. The homogenate was overlaid with 25 mL of floating buffer 1 (isolation buffer with only 0.1 M sucrose) and centrifuged in swing bucket at 23,000 g for 30 min. Lipid droplets floating on top of the overlay buffer were collected using a Potter S homogenizer. Lipid droplets were then solubilized in 200 µL of floating buffer 2 (isolation buffer without sucrose), and mixed 1:1 with 2X HDN sample buffer (200 mM Tris-HCl pH 8.0, 1 M 6-aminocapronic acid, 20 % glycerol, 10 mM dithiothreitol, 2 μM PMSF) supplemented with 0.5 or 1% n-Dodecyl-β-D-maltopyranoside (DDM). The mixture was incubated on ice for 20 min followed by centrifugation at 20,000g for 10 min at 4°C. The aqueous phase was carefully transferred to a new tube to avoid the contamination from the lipid layer on top and the precipitates, and then run on 4-14% histidine deoxycholate native gels as described (Kikuchi et al., 2006; Ladig et al., 2011). Electrophoresis was done at 50 V for an hour, and then switched to 30 V overnight at 4°C. The gels were

denatured and either subjected directly to immunobloting, or run in a second dimension on denaturing SDS-PAGE before immunobloting. In all cases of the study, the RC DC Protein Assay Kit (Bio-Rad) was adopted for protein quantification.

For immunoblot analysis SDS-PAGE gels were blotted onto polyvinylidene fluoride (PVDF) membranes in transfer buffer (25 mM Tris, 192 mM Gly, and 10% methanol) for 60 min at 100V. Membranes were blocked for 60 min in TBST (50 mM Tris, 150 mM NaCl, 0.05 % (v/v) Tween 20, pH 7.6) with 5% nonfat dry milk, and probed with primary antibodies overnight at 4°C. The primary antibodies were used at 1:1000 dilutions, except for mouse anti-atubulin (1:10,000). Goat anti-mouse or anti-rabbit secondary antibodies coupled to horseradish peroxidase were used at 1:10000 dilution and incubated with blots at room temperature for 30 min. Blots were then washed six times with TBST at room temperature for 10 min each. Antigen was detected by chemiluminescence (Bio-Rad Clarity Western ECL substrate) using a chargecoupled device (CCD) imaging system. Anti-MLDP was generated as described (Tsai et al., 2014). Anti-NAB1 was a gift from Krishna K. Niyogi, Department of Plant and Microbial Biology, Berkeley, CA. To generate antibodies against Chlamydomonas TGD2, the full length coding sequence of TGD2 was amplified using total cDNA as the template, and inserted into the expression vector pET28B(+) (Novagen). Construct was introduced into E. coli BL21 (DE3). Recombinant proteins (6xHis-TGD2) were purified using Ni-NTA agarose (Qiagen) and separated by SDS-PAGE to examine the purity. Few other proteins were co-purified with 6xHis MLDP. Roughly 2 mg of each protein was sent for antibody production in rabbits by Cocalico Biologicals, Inc.

For Co-immunoprecipitation (CoIP) experiments, 1.2 L N-deprived or 2.4 L N-resupplied cultures were centrifuged. Cell pellets were washed twice in phosphate-buffered saline pH 7.2

(PBS), resuspended in PBS with protease inhibitor (P9599, Sigma-Aldrich) and phosphatase inhibitor (Thermo Scientific) at a concentration of 10⁹ cells/mL, and then crosslinked on ice with 1 mM freshly prepared DSP (Dithiobissuccinimidyl propionate, Pierce). To quench the crosslinking, 1 M Tris-HCL pH 7.5 was added to a final concentration of 100 mM and incubated on ice for 15 min. Cells were then snap frozen in liquid nitrogen and stored at -80°C until use. Lipid droplets were isolated as described above, but instead of dissolving in the floating buffer 2, they were washed in 500 μL of washing buffer (same as isolation buffer but with 150 mM KCl). The suspension was overlaid with 1 mL of floating buffer 1 and centrifuged at 20,000 g for 15 min at 4°C. The washing was repeated three times until no green pellet was seen after centrifugation. LDs were then solubilized in 400 µL of floating buffer added with 1% DDM. After incubating on ice for 20 min, insoluble materials and the lipid layer were separated by centrifugation at 20,000 g for 10 min at 4°C. The supernatant was divided into two portions, one incubated with 100 μL Dynabeads Protein A (Life Technologies) coupled with 10 µg of purified MLDP IgG, and the other with Dynabeads coupled with MLDP prebleed as negative control. Incubation was carried out overnight at 4°C with gentle rotation. Dynabeads were collected magnetically and washed with PBS supplemented with 100 mM NaCl and 1 mM PMSF. The washing was repeated three times and finished by an additional wash using PBS only. Proteins were eluted with nonreducing sodium dodecyl sulfate (SDS) sample buffer by incubating at room temperature for 15 min. Before being processed for mass spectrometry, DSP was cleaved by boiling in the presence of 5% β-mercaptoethanol. CoIP elutes were separated by SDS-PAGE but shortly after the samples had entered the gel, the gel bands were excised. Gel bands were digested in-gel according to (Shevchenko et al., 1996) with modifications. Briefly, gel bands were dehydrated using 100% acetonitrile and incubated with 10 mM dithiothreitol in 100 mM ammonium bicarbonate, pH~8, at 56°C for 45min, dehydrated again and incubated in the dark with 50 mM iodoacetamide in 100 mM ammonium bicarbonate for 20min. Gel bands were then washed with ammonium bicarbonate and dehydrated again. Sequencing grade modified Trypsin was prepared to 0.01ug/μL in 50mM ammonium bicarbonate and ~50 μL of this was added to each gel band so that the gel was completely submerged. Bands were then incubated at 37°C overnight. Peptides were extracted from the gel by water bath sonication in a solution of 60% ACN/1% TCA and vacuum dried to $\sim 2 \mu L$. Peptides were then re-suspended in 2% acetonitrile/0.1% TFA to 25 μL . From this, 5 µL were automatically injected by a Thermo (www.thermo.com) EASYnLC 1000 onto a Thermo Acclaim PepMap RSLC 0.075mm x 150mm C18 column and eluted over 120min with a gradient of 2% B to 30% B in 109 min, ramping to 100% B at 110 min and held at 100% B for the duration of the run (Buffer A = 99.9% Water/0.1% Formic Acid, Buffer B = 99.9% Acetonitrile/0.1% Formic Acid). Sample injection order was randomized to avoid bias. Eluted peptides were sprayed into a ThermoFisher Q-Exactive mass spectrometer (www.thermo.com) using a FlexSpray spray ion source. Survey scans were taken in the Orbi trap (35000 resolution, determined at m/z 200) and the top ten ions in each survey scan are then subjected to automatic higher energy collision induced dissociation (HCD) with fragment spectra acquired at 17,500 resolution. The resulting MS/MS spectra are converted to peak lists using Mascot Distiller, v2.4.3.3 (www.matrixscience.com) and searched against all protein entries in the C. reinhardtii v5.3.1, protein database (downloaded from www.phytozome.net) and appended with common laboratory contaminants (downloaded from www.thegpm.org, cRAP project) using the Mascot searching algorithm, v 2.4. The Mascot output was then analyzed using Scaffold Q+S, v4.3.0 (www.proteomesoftware.com) to probabilistically validate protein identifications. Assignments validated using the Scaffold 1% FDR filter (protein threshold) and 95% confidence filter (peptide threshold) are considered true. Variable modifications of Oxidation of Methionine and of DSP cleavable x-linker were adjusted accordingly.

Immunofluorescence, Confocal, and Transmission Electronic Microscopy

For immunofluorescence, cells were fixed in a mixture of 4% (w/v) paraformaldehyde and 0.15 M sucrose in PBS (pH 7.4) for 1 h at room temperature. After two washes in phosphate-buffered saline (PBS) buffer, cells were permeabilized by incubation in 0.01% Triton-X100 in PBS for 5 min. at room temperature and washed twice in PBS. Samples of 200 µl of volume were transferred into sterile Eppendorrf tubes and blocked with a solution containing 1% (w/v) BSA in PBS (pH 7.2) for 1 h. Then, samples were incubated with primary antibodies: 1) mouse antiαtubulin (T6074, Sigma-Aldrich) diluted 1:50 in PBS buffer, pH 7.2, containing 1% (w/v) BSA or 2) rabbit anti-MLDP diluted 1:50 in PBS buffer, pH 7.2, containing 1% (w/v) BSA or 3) mixture of both antibodies, overnight at 4 °C on rotary shaker. Anti-mouse IgG conjugated with Alexa Fluor 405 (Molecular Probes) or anti-rabbit IgG conjugated with Alexa Fluor 488 (Molecular Probes) or a mixture of both diluted 1:200 in PBS buffer (pH 7.2) were used as the secondary antibodies. In order to visualize LDs, just before examination, aliquots (100 µl) of cell suspension were mixed with 10 µl of a solution of 0.1 mg ml-1 Nile Red (Sigma-Aldrich) in acetone or with 1 µl of 1 mM solution of Bodipy 665/676 in DMSO. Samples were then washed with PBS, re-suspended in ProLong Gold anti-fade reagent (Invitrogen) and observed with a Spectral-based Olympus FluoView 1000 confocal laser scanning microscope (Olympus, Japan) using a combination of: 1) a diode 405 nm laser for Alexa Fluor 405 signal detection, 2) an argon (488 nm) laser for Alexa Fluor 488 signal or Nile Red staining visualization, or 3) solid state (633 nm) laser for Bodipy 665/676 detection. Chloroplast autofluorescence was excited by using solid state (556 nm) laser. Z-series images were collected and processed with the Olympus FluoView FV1000 confocal microscope software (Olympus, Japan). Negative controls were treated as above, but the primary antibody was omitted. For the observation other than immunofluorescence such as counting LD number and size in the *MLDP* RNAi lines, live cells were used without fixation. For electron microscopy, centrifuged cell pellets were processed as previously described (Harris, 1989), and transmission electron micrographs were captured using a JEOL100 CXII instrument (Japan Electron Optics Laboratories, Tokyo, Japan).

RESULTS

Transmission Electronic Microscopy Reveals Two Stages of LD Mobilization

N deprivation led to drastic changes in cellular ultra-structures in Chlamydomonas, such as vacuolization, replacing of stacked thylakoids by starch granules, and the accumulation of LDs (Figures 4.1A and 4.2 A-C). On the other hand, ultra-structures of Chlamydomonas during quiescence exit have not been explored in detail. To fill this gap, transmission electron micrographs were taken over a time course of N resupply and showed that, initially, while LDs decreased in size they remained connected with the chloroplast outer envelope (Figures 4.1 B, D and 4.2 D-F). Later on, two types of LDs were visible with usually the larger ones still making contact with the chloroplast and the smaller ones moving toward the vacuoles (Figures 4.2 G-I and 4.3 A-I), in accordance with the finding that interaction of oil bodies with vacuoles contributes to the degradation of storage lipids in seeds (Poxleitner et al., 2006). Completion of LD degradation is not necessary for the cell cycle to proceed as LDs were found in newly produced daughter cells (Figures 4.1C and 4.2 J-L).

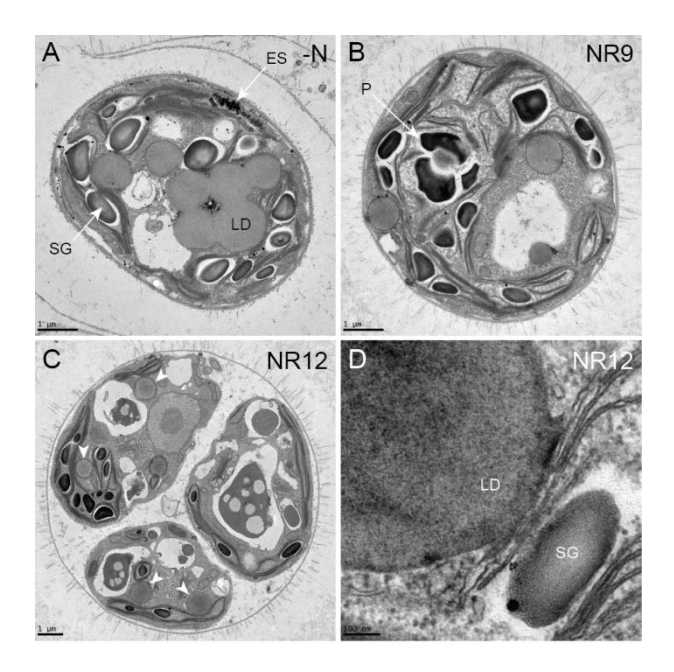


Figure 4.1. Ultrastructure of Cells during Quiescence Exit. (A-C) Transmission electron micrographs of a representative 21gr cell grown in N deprivation (-N) for 48 h (A) and representative cells resupplied with N (NR) and grown for r 9 (B) and 12 h (C). (D) Close contact of lipid droplet (LD) with chloroplast the outer envelope during early stage of LD mobilization is shown. Scale bars are indicated. ES, eyespot; P, pyranoid; S, starch granules.

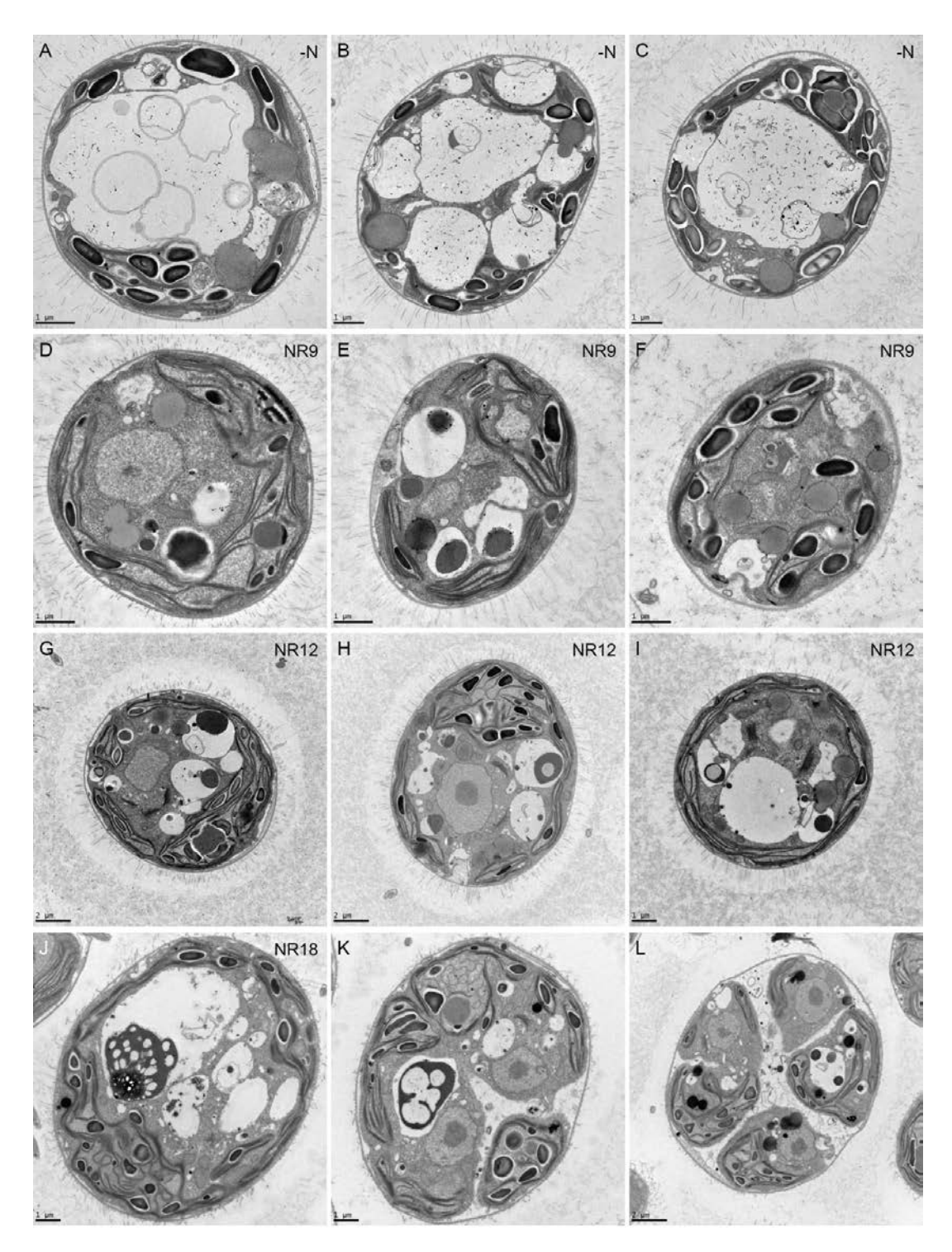


Figure 4.2. Ultrastructure of Cells during Quiescence Exit. (A-L) Transmission electron micrographs of a representative 21gr cell grown in N deprivation (-N) for 48 h (A-C) and representative cells N-resupplied (NR) for 9 (D-F), 12 h (G-I) and 18 h (J-L). Scale bars are indicated.

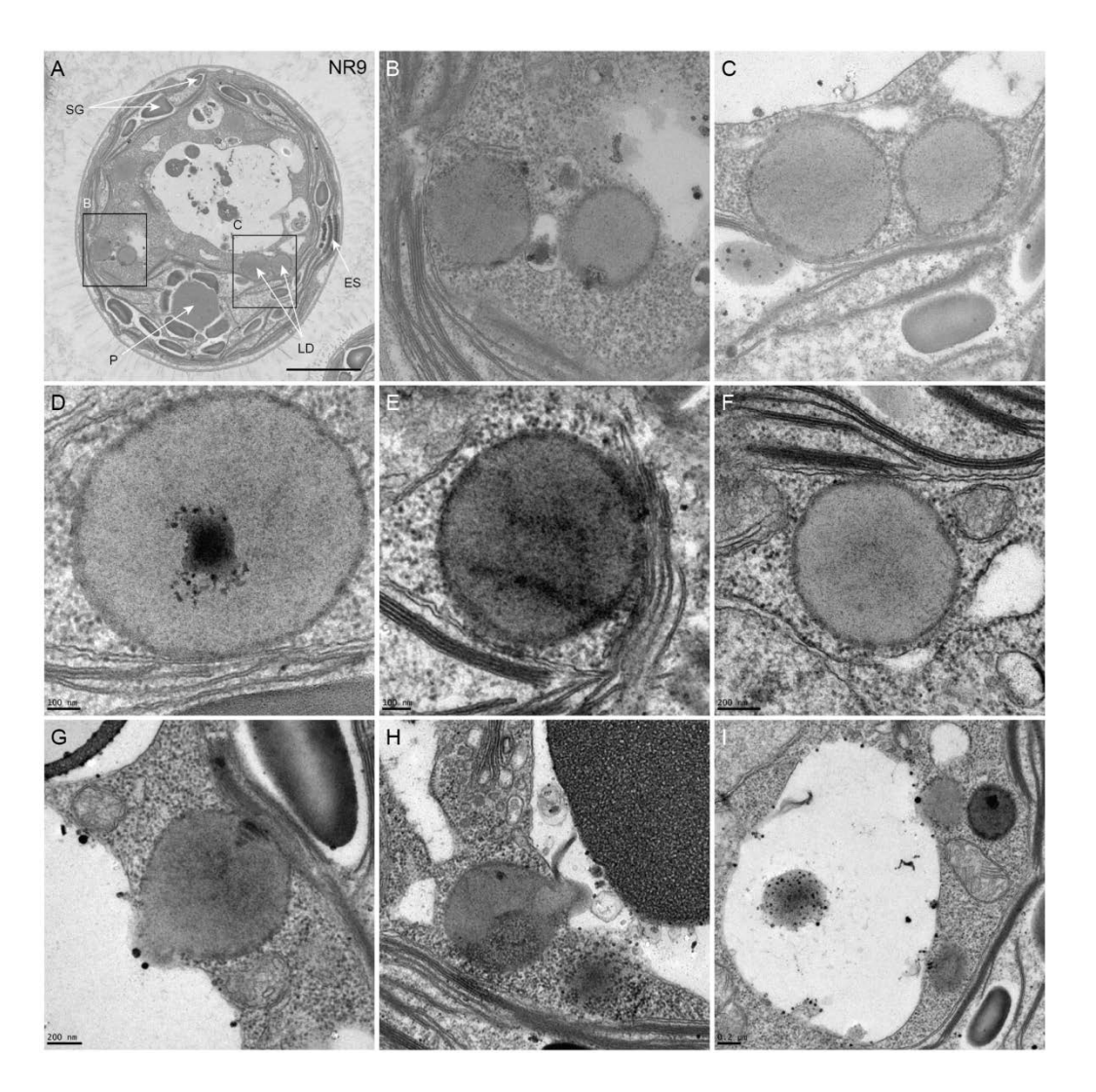


Figure 4.3. Ultrastructure of Cells during Quiescence Exit. (A-C) Transmission electron micrographs of a representative 21gr cell grown following N deprivation for 48 h followed by 9 h of N resupply (A), at higher magnification in (B, C). LD, lipid droplet; ES, eyespot; P, pyranoid; S, starch granules. (D-F) Electron micrographs of LD-chloroplast contacts in cells fixed at 12 h of N resupply. (G-I) Electron micrographs showing smaller LDs detaching from the chloroplast and moving towards the vacuole. Scale bars are indicated.

MLDP Recruits Different Sets of Proteins to LDs

Previously we showed that the reduction of MLDP – the major lipid droplet protein in Chlamydomonas – increases LD size without affecting TAG content (Moellering and Benning, 2010). In addition, its abundance is linked to the status of quiescence (Tsai et al., 2014). This protein could provide a unique entry for a more in-depth study of the role of LDs in cellular

quiescence. MLDP abundance decreased following N resupply as shown before (Figure 4.4A) (Tsai et al., 2014). It was highly enriched in the fraction containing of LDs, and much less in the ER fractions (Figure 4.4B). BIP was used as an ER marker. I used indirect immuno-fluorescence to probe the localization of MLDP in fixed N-deprived cells. Signals of MLDP predominantly formed a ring-like structure around LDs (Figure 4.4C), which is typical of proteins located on the LD surface (Welte, 2007). They could also be detected in the cytosol albeit to a lesser extent, and seemingly in a reticulate pattern. Notably, the distribution of MLDP was not evenly around LDs but often polarized on one side or on multiple spots, and the larger the LDs the more concentrated the MLDP. We think that in Chlamydomonas the coating with scaffold proteins – at least in the case of MLDP – is a separate process carried out after LDs have been formed.

Many of the enzymes identified in LD proteomes possess neither amphipathic helices nor hydrophobic spans (Walther and Farese, 2012). I hypothesized that in Chlamydomonas these proteins associate with LDs by protein-protein interactions, e.g. with LD-bound protein, such as MLDP. LDs isolated from cells deprived of N for 48h were solubilized and complexes were fractionated by histidine and deoxycholate-based native PAGE (HDN-PAGE) (Ladig et al., 2011). Immunoblots recognized MLDP in five distinct complexes of between 66 to 480 kDa with no detection of the MLDP monomer (~28 kDa) (Figure 4.4D). A gel slice from the first dimension was excised and the proteins therein were separated by SDS-PAGE in the second dimension. The 2D SDS-PAGE confirmed the identity of these immunoreactive proteins to be MLDP (Figure 4.4E). While the change in MLDP abundance was modest at 9 h of N resupply (Figure 4.4A), the difference in complex formation was great – only the complex of the lowest molecular mass was detected (Figure 4.4D). To characterize the protein components in these MLDP complexes, I performed co-immunoprecipitation (Co-IP) in combination with LC-

MS/MS. Dynabeads coupled with MLDP antibodies were incubated with LDs isolated from cells exposed to 48 h of N deprivation (-N LDs) or 48 h of N deprivation followed by 9 h of N resupply (NR9 LDs). As a negative control, Dynabeads coupled with MLDP prebleed were used. Although in total 817 (-N LDs) and 349 (NR9 LDs) proteins were found, quantitative information was only obtained for 188 (-N LDs) and 25 (NR9 LDs) distinct protein sets by requiring that at least two peptides of each protein were repeatedly quantified in all three replicates and that the ratio of total spectrum count between the experiments and the negative control using MLDP prebleed was less than that for MLDP (Online Supplemental Data Set 11). In theory, this approach allowed us to identify proteins that localized to LDs through the interaction with MLDP. Compared with two recently reported Chlamydomonas LD proteomes (Moellering and Benning, 2010; Nguyen et al., 2011), our experiments uncovered 97 newly identified LD proteins (Figure 4.4F). Examples are MGD1 and LIP1. It is likely that MGD1is sheltered by association with LDs from proteolysis and, thus is readily available without transcription and translation as N is resupplied, to resynthesize the MGDG degraded during N deprivation without delay. LIP1 is a TAG-reducing lipase. Being constitutively on LDs shows that LIP1-mediated lipolysis is not controlled by a translocation event that moves the enzyme from the cytosol to LDs, but requires activation of activity, as has been shown for the yeast TAG lipase Tgl4 (Kurat et al., 2009). 28 proteins were found in all three data sets (Figure 4.4F), including those involved in lipid metabolism such as BTA1, LCS1, a phosphoinositide phosphatase (TEF21), a phospholipase D (Cre13.g591900), a glycosyl hydrolase with similarity to the galactolipid:galactolipid galactosyltransferase SFR2 of Arabidopsis, although this activity has not been shown to exist in Chlamydomonas) and a cyclopropane-fatty-acyl-phospholipid synthase (CFA2). On the contrary, only 25 proteins were identified by MLDP CoIP with the LDs

isolated following N resupply (Figure 4.4G; Online Supplemental Data Set 11), in accord with the finding that only one type of MLDP complexes was detected by HDN-PAGE under this condition. 11 of the 25 proteins were identified in both CoIP experiments, some of which may constitute the core of MLDP complexes, such as BTA1 and β-tubulin (TUB1).

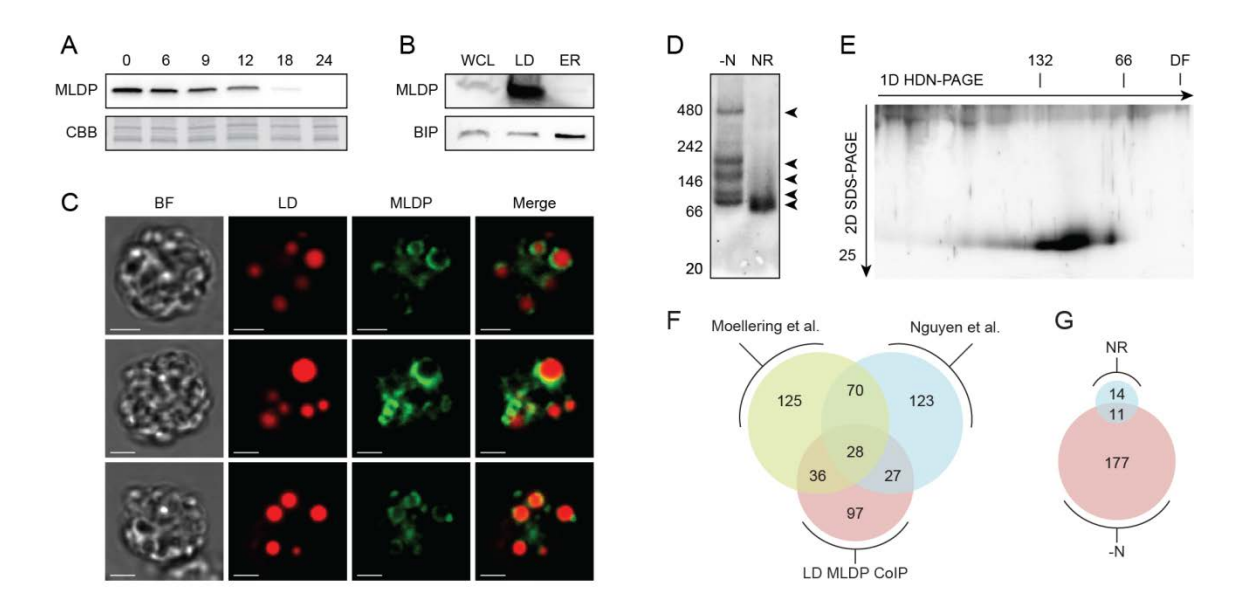


Figure 4.4. Lipid Droplet Localization and MLDP Complex Formation. (A) Immunoblot of MLDP in *dw15* following N resupply (NR) at times indicated (h). Coomassie Brilliant Blue (CBB) staining shows equal protein loading. (B) Relative abundance of MLDP in different cell fractions is shown by immunobloting. WCL, whole cell lysate; LD, lipid droplet; ER, endoplasmic reticulum. BIP is used as an ER marker. Equal amounts of protein were loaded. (C) Immunofluorescence detection of MLDP during N deprivation. BF, bright field. Scale bars in each panel represent 2 μm. (D) LDs isolated at 48 h of N deprivation (-N) and 9 h of N resupply (NR) were fractionated by HDN-PAGE and detected by MLDP immunoblot. Arrows indicate each MLDP complex identified. (E) Proteins of –N LDs were separated by HDN-PAGE in the first dimension (on the top) and then SDS-PAGE in the second dimension (on the left), and detected by MLDP immunoblot. (F) Overlapping proteins between the data sets of Moellering et al., of Nguyen et al., and of the LD MLDP-CoIP conducted with the LDs harvested at 48 h of N deprivation. (G) Overlapping proteins between the data sets of the LD MLDP-CoIP conducted with the LDs harvested at 48 h of N deprivation (-N) and at 9 h of N resupply (NR).

MLDP Is Indispensible for α-tubulin Association with LDs

Interaction with MLDP might be important for the stability or the sequestration of its associated protein partners. Given the limited number of tools developed for Chlamydomonas, I decided to

focus on two representative examples of the CoIP results. These are α-tubulin (TUA1), which like β-tubulin is the major component of microtubules, and the presumed ortholog of TGD2, a protein involved in ER-chloroplast lipid trafficking (Awai et al., 2006). In fact, α-tubulin is one of the 28 proteins found in all three data sets, whereas TGD2 is present in two of the data sets but not in the one generated by Moellering et al. I first verified the association of α-tubulin and TGD2 with lipid droplets by subcellular fractionation, with respective negative controls to judge the purity of lipid droplets. α-tubulin is universally known as cytosolic; therefore the Chlamydomonas cytosolic marker NAB1 (for putative nucleic acid binding protein) was used as a negative control (Mussgnug et al., 2005). Although not more enriched than whole cell lysates, α-tubulin was seen in the LD fractions while NAB1 was not (Figure 4.5A). As in Arabidopsis (Awai et al., 2006), Chlamydomonas TGD2 was presumed to be on the inner envelope of chloroplasts at least during regular growth. However, upon N deprivation it was strongly enriched in the LD fraction, but not another chloroplast inner envelope protein, Tic40. Early on we suppressed MLDP by RNA interference (RNAi) and showed the effect on LD size in multiple independent lines (Moellering and Benning, 2010). Here, when MLDP is reduced, α tubulin and TGD2 were not affected on the whole cell level (Figure 4.5B). Strikingly, α-tubulin virtually disappeared from the LDs isolated from MLDP RNAi lines (Figure 4.5C). It appears that MLDP is required for α-tubulin association with LDs, and perhaps also for mediating the physical interaction between microtubules and LDs. TGD2, on the other hand, persisted on LDs regardless of MLDP. Perhaps MLDP was helpful but not required for the relocation of TGD2, or the level of MLDP was not low enough to have an impact. I also examined the protein levels of MLDP, α-tubulin, and TGD2 in the LDs fraction when cells were exiting quiescence. Recall that within the first 9 h of N resupply, MLDP only slightly altered its abundance on whole cell level

(Figure 4.4A). It was similar for MLDP in the LDs fraction (Figure 4.5D). Protein abundance of α-tubulin (modestly) and TGD2 (strongly) decreased in LDs in response to N resupply. TGD2 may have been relocated back to chloroplast, perhaps due to the close contact during the early stage of LD degradation (Figure 4.1D).

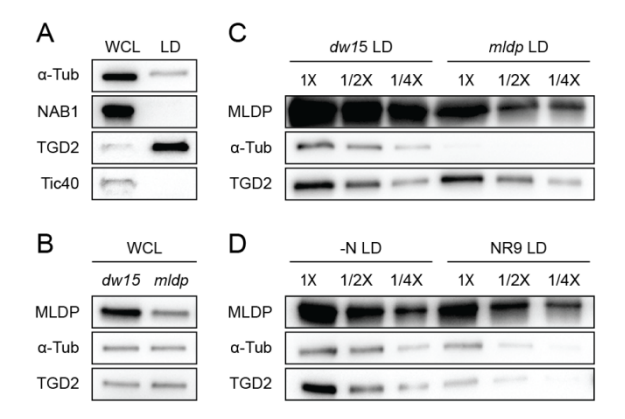


Figure 4.5. Lipid Droplet Protein Quantification in the *MLDP* **RNAi Lines.** (A) Immunoblot detection of cytosolic proteins α-tubulin (α-tub) and NAB1, and putative chloroplast inner envelope proteins TGD2 and Tic40. WCL, whole cell lysate; LD, lipid droplet. Equal amounts of protein were loaded. (B) MLDP, α-tubulin, and TGD2 abundance in the whole cell lysates of dw15 and MLDP RNAi lines (mldp). Equal amounts of protein were loaded. (C) Protein abundance in the LD fractions. 1X, 1/2X and 1/4X represent the serial dilutions of protein loading, and are equal in dw15 and MLDP RNAi lines. (D) Comparison of protein abundance in the –N (48 h of N deprivation) and NR9 (9h of N resupply) LDs. All data shown here are representative of three or four independent biological replicates.

The Surface of Lipid Droplet Has Unique Lipid and Fatty Acid Composition

By and large, LDs consist of a neutral lipid core surrounded by a phospholipid monolayer (Tauchi-Sato et al., 2002). While it is true for yeast and animals, it might be different in Chlamydomonas since the commonly most abundant phospholipid, PC, is missing. I was therefore interested in characterizing the polar lipid fractions of LDs. Lipid species from total cells or LDs were separated by thin layer chromatography (TLC) plate (Figure 4.6A and B). DGDG and DGTS appeared to be most abundant among polar lipids associated with LDs, confirmed by quantitative analysis using gas chromatography (Online Supplemental Table 1).

These data explained the increase of DGTS and especially DGDG during N deprivation (Figure 5C), as LDs grow in size and number so does the demand for surface lipids. Under closer examination, phospholipids all together (i.e. PE, PG and PI) only accounted for less than 25% of LD surface lipids, contrasting to ~25% of DGTS, and more than 50% of galactolipids which could only originate from the chloroplast. Surprisingly, the fatty acid spectrum of LD surface lipids was very different from that of whole cells, generally more enriched in saturated fatty acids (~70% for lipid droplets versus ~40% for whole cells). This finding strongly suggested that these polar lipids were bona fide LD lipids. The abundance of DGDG dropped in half (~32% to ~16%) after 9 h of N resupply, implying a regulated lipid trafficking happened on the surface of LD or a targeted degradation of DGDG.

To my surprise, two additional lipid species were seen chromatographingly close to DGTS and DGDG in fractions from the LDs of the RNAi lines (Figure 4.6 B). Since they were not detected in the total cell fractions, this effect was LD-specific. We deduced that these lipids could be different molecular species of DGTS and DGDG, according to their responses to Dragendorff reagent which reacts with tertiary amines of DGTS, and to α-naphthol which binds to sugar group such as galactose of DGDG (Figure 4.6C) (Benning et al., 1995). Also, the combined amount of the original and putative DGTS in the RNAi lines (~26%) was comparable to the DGTS in the PL (~24%), so was for DGDG (~35% in RNAi lines versus ~32% in the PL). The difference in migration could result from the difference in fatty acid composition. Lipids with more saturated fatty acids are slightly less hydrophobic and thus migrate slower on TLC plate compared to the same species of lipid carrying more unsaturated fatty acids. Indeed, in the RNAi lines, saturated fatty acids were ~90% in the putative DGTS and ~92% in the putative DGDG, whereas the original DGTS and DGDG contained ~78% and ~69% of saturated fatty

acids, respectively. Overall, the surface of LDs isolated from RNAi lines was even more enriched in saturated fatty acids (~88%). Collectively, these results suggest that MLDP affects the lipid composition at the surface of lipid droplets.

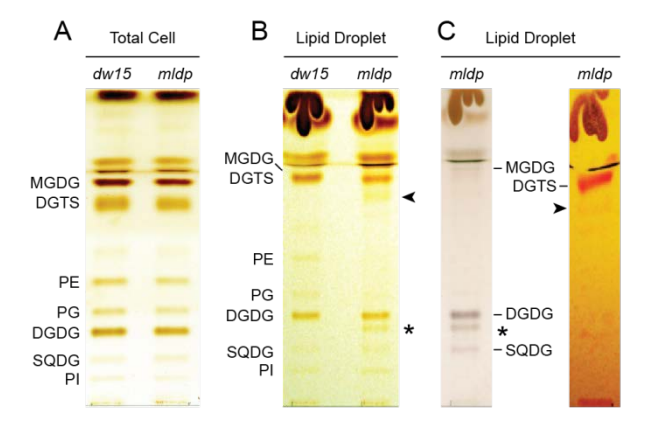


Figure 4.6. Lipid Profiles of Lipid Droplet Surface Membrane. (A) Whole cell lipids of dw15 and MLDP RNAi lines (mldp) were separated by thin layer chromatography (TLC). MGDG, monogalactosyldiacylglycerol; DGTS, diacylglyceryl-trimethylhomoserine; PE, phosphatidylethanolamine; PG, phosphatidylglycerol; DGDG, digalactosyldiacylglycerol; SQDG, sulfoquinovosyldiacylglycerol; PI, phosphatidylinositol. (B) Lipids of lipid droplets were separated by TLC. Arrow and asterisk indicate additional lipids from the mldp lipid droplets. (C) Lipids separated by TLC were stained by α-naphthol (left panel) Dragendorff reagent (right panel). (A), (B) and (C) are not from the same TLC plate, except left panel of (C) is the same plate as in (B).

Proper Surface Area of Lipid Droplet Ensures Orderly Progression out of Quiescence

Fortuitously I observed that *MLDP* RNAi lines did not grow in fresh medium if inoculated from plates over three weeks old, whereas regular strains can be stored for months under the same conditions, implying a defect in quiescence exit. To follow up, we transferred cells in the midlog phase to liquid medium without N, and waited for various times before adding N back. Cell biomass based on optical density and cell concentration were monitored at 0 and 24 h of N resupply. The regrowth of PL gradually slowed down over the longer period of N deprivation, and RNAi lines began to lag further behind after being incubated in N-free medium for 6 days (Figure 4.7A and B). TAGs continued to accumulate in the PL and RNAi lines and finally

saturated at day 6 of N deprivation. The delayed turnover of TAGs in the PL after prolonged N deprivation correlated with the slower regrowth, and starting from the samples being deprived for 4 days, RNAi lines exhibited a lipolysis defect even though it did not yet affect regrowth (Figure 4.7C). Knowing that the reduction of MLDP causes morphological changes of LDs, we examined the dynamics of LD formation in the PL and RNAi lines. As reported before, after 2 days of N deprivation RNAi lines had fewer LDs but larger in size (Figure 4.7D and E). At day 4, LDs in the PL grew to near the size of LD in RNAi lines at day 2 but decreased in number, indicating LD fusions. A critical observation was made on day 6. In the PL there was no obvious increase of large LDs (1 µm up in diameter), but numerous small ones (1 µm down in diameter) were formed, positing that large LDs had grown to their maximal capacity and new LDs were needed to accommodate the incoming TAGs. On the contrary, LDs in the RNAi lines continued to enlarge. By day 8, small LDs were no longer seen in the PL, indicating that another round of fusion events had occurred. LDs in RNAi lines never ceased to fuse even though after day 6 there was no increase in TAGs, and in some cells the entire cytosol was occupied by a giant droplet (Figure 4.7F). In summary, our data demonstrated that MLDP balanced the surface areaper-volume ratio which is important for metabolizing TAGs, and ensured orderly progression out of quiescence.

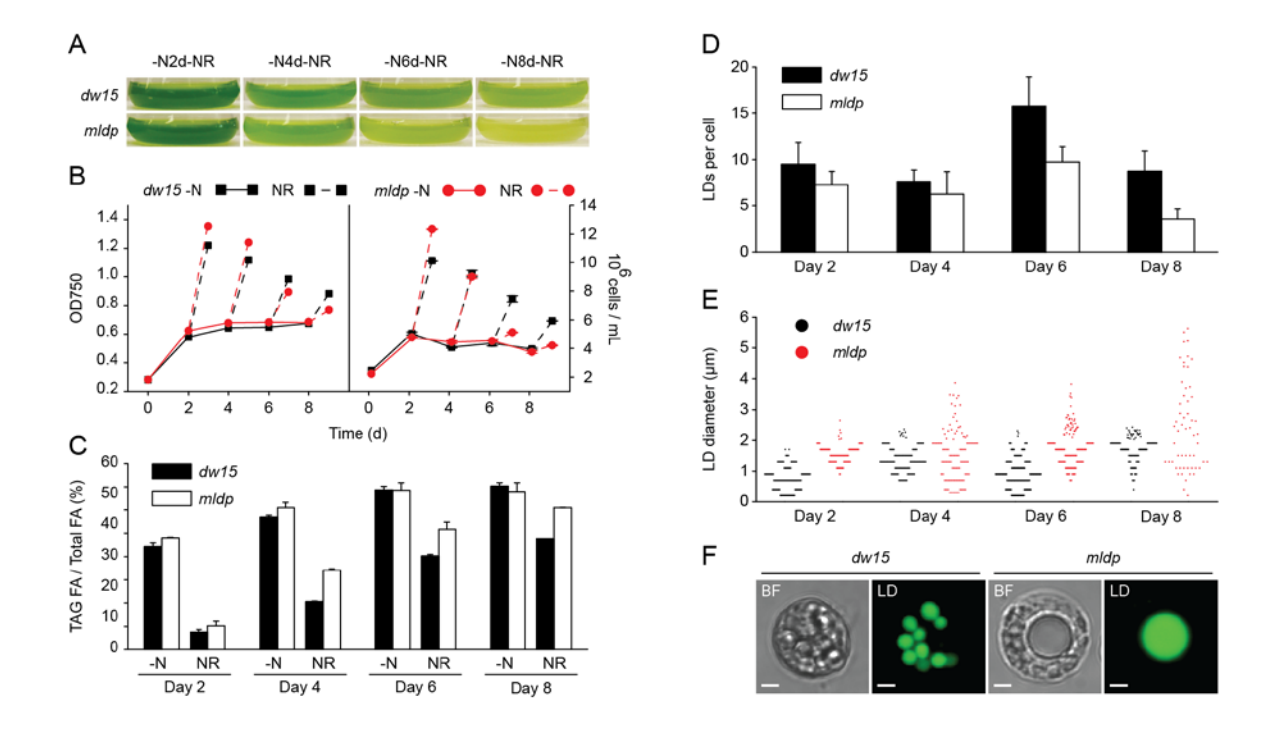


Figure 4.7. Reduction of MLDP Affects Quiescence Exit, TAG Turnover, and Lipid Droplet Homeostasis. (A) Cultures of *dw15* and *MLDP* RNAi lines (*mldp*) at 24 h of N resupply (NR) following N deprivation (-N) as times indicated (d, day). (B) Growth of *dw15* and *mldp* during the course of N deprivation followed by N resupply measured at the times indicated. (C) TAG contents (depicted as ratio of TAG fatty acids (FA) over total FAs) at different days of N deprivation (-N) and at 24 h of N resupply (NR) following N deprivation as times indicated. (D, E) Lipid droplets (LD) of 15 cells for each sample were counted (D) over days of N deprivation as indicated, and their diameter (E) was quantified with imaging software and shown in data point-box plot. (F) BODIPY staining of LDs in representative cells. Scale bars represent 2 μm.

DISCUSSION

The role of lipid droplet in cellular quiescence

Biochemical assays validated some of the inferences based on transcriptional analysis described in Chapter 3. In fact, many key enzymes in lipid metabolic pathways were identified by MLDP CoIP from LDs, the most prominent of which is BTA1. Normal growth of LD requires increasing amount of DGTS in the surface area. It is reasonable to assume that BTA1 is deployed on LDs so that DGTS can be synthesized locally. BTA1 was only upregulated during N resupply, the time when membrane rebuilding is heavily in demand. It is also possible that BTA1 is protected on LDs from active proteolysis, so that during transit out of quiescence it can immediately participate in the restoration of organelles. These hypotheses are not mutually exclusive. LD localization of LACS1 has been observed repeatedly including the study described here. Its possible function can be discussed in view of two conceptual phases. First, fatty acids are synthesized by 3-ketoacyl-ACP synthase in the form of acyl-ACP (acyl carrier protein). To be exported out of chloroplast the ACP moiety must be removed by the activity of acyl-ACP thioesterase, and almost instantly long-chain acyl-CoA synthetase activates the resulting free fatty acids so they can be incorporated into glycolipids. Previously it was thought that fatty acids after being converted to acyl-CoA were transported to the ER where TAG was assembled (Guixe and Babul, 1985). Here I propose a new possibility, namely that activation of fatty acids occurs at the contact sites between chloroplast and LDs after ACP is removed. Second, several putative lipases and acyltransferases are found on LDs including examples from the current work, a lysophosphatidate:acyl-ACP acyltransferase (g9888) and a phospholipid/glycerol acyltransferase (Cre17.g738350), indicative of active deacylation and reacylation. LACS1 may intervene in the processes by turning fatty acids released by lipase into acyl-CoA, which can then be utilized by

the acyltransferase. Theoretically, the proteins isolated by MLDP CoIP from LDs are LD-localized by interacting with MLDP. However, an inevitable pitfall of CoIP experiments is protein contamination through the hydrophobic interaction with bait protein, a fact that needs to be taken into consideration when interpreting the data.

The monolayer surface of LD contained all the polar lipids that can be found in Chlamydomonas. At first, it may seem like contamination, especially with more than 50% of galactolipids whose biosynthesis and distribution are thought to be exclusively with the chloroplast. However, the fatty acid profile differed in every polar lipid when compared between LDs and whole cells. Except for DGTS, there is no indication of possible local synthesis. Therefore, one can only assume that these lipids were transported to LDs from the chloroplast (i.e. MGDG, DGDG, SQDG and PG) and the ER (i.e. PE, PI, PG and perhaps DGTS) where syntheses occur. Despite coming from different sources, these lipids share a common feature which is a higher saturation level than their counterparts in whole cell extracts. This has led me to hypothesize a LD-specialized acyl exchange mechanism that utilizes the de novo-synthesized acyl groups palmitate (16:0) and oleate (18:1 Δ 9) to replace the mature, mostly unsaturated fatty acids from polar lipids, which are then stored in lipid droplets (Figure 4.8). Oleate seemed to be specific for the LD DGDG (Online Supplemental Table 1). It is reminiscent of the deacylation/acylation cycle catalyzed in part by PGD1 during N deprivation, which prefers $18:1\Delta9/16:0$ MGDG but not its mature 18:3/16:4 molecular species (Li et al., 2012). The proposed mechanism can be potentially executed by any of the numerous LD-bound lipases and acyltransferases that have been reported in Chlamydomonas (Moellering and Benning, 2010; Nguyen et al., 2011). The fact that LD surface lipids in MLDP RNAi lines had an even higher saturation rate, to an extent that distinct DGTS and DGDG species were possible separated by

TLC, further confirms the acyl exchange took place on the LDs. This might result from the lower total LD surface area in the RNAi lines, in other words, lower substrate-to-enzyme ratio, and give rise to a high degree of acyl exchange.

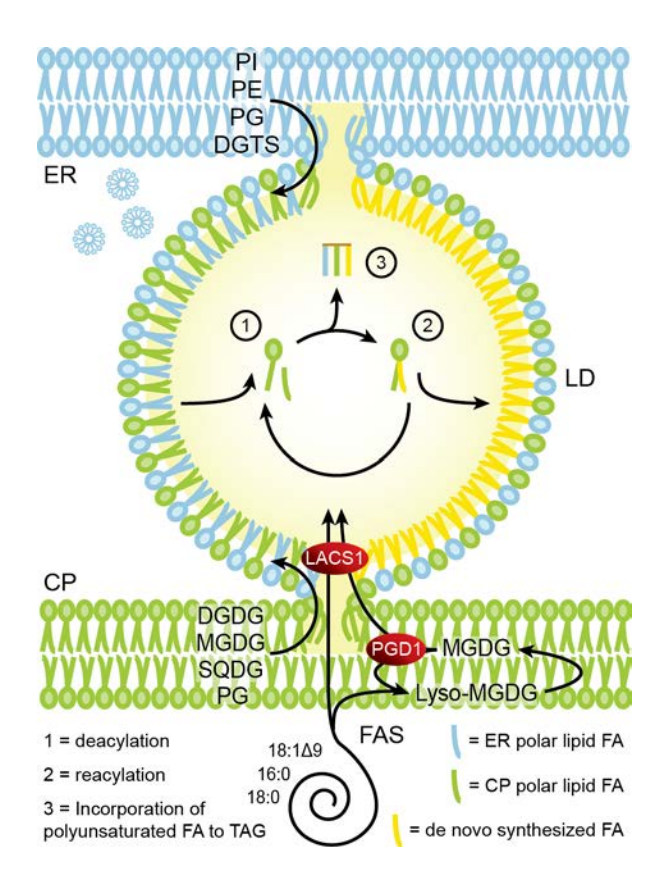


Figure 4.8. A model for lipid droplet-specialized deacylation/reacylation cycle. De novo synthesized fatty acids (FA) (16:0, 18:0, and 18:1 Δ 9) in the form of acyl-ACP are exported from chloroplast either right after fatty acid synthesis (FAS) or after the deacylation/reacylation cycle mediated by PGD1. Acyl-ACP is transformed into acyl-CoA by lipid droplet (LD)-bound LACS1 before it can be incorporated into polar lipids or triacylglycerols (TAGs) on the LD. The ER-originated and chloroplast (CP)-originated polar lipids after transported to LD are subjected to deacylation, following by reacylation using the de novo synthesized FA stored in the LD. The deacylation/reacylation cycle may repeat until both acyl groups have been replaced. The polyunsaturated FA removed during the deacylation is then incorporated into TAG and stored in the LD.

A new model of lipid droplet formation

LD assembly in Chlamydomonas can be divided into two distinct phases (Figure 4.9). TAGs were packed into a hydrophobic compartment in proximity to the chloroplast. Whether this is a

direct budding from chloroplast is not clear at this point, but the close proximity and punctate fusions ought to have physiological relevance, for instance, to allow chloroplast lipids or proteins to diffuse naturally to LDs. When LDs reached a certain size (approximately 0.5 µm in diameter), MLDP proteins would begin to gather around them. This proteinaceous coating is apparently important in determining LD size, because LDs would no longer fuse or enlarge once they have been stabilized by MLDP (approximately 2 µm in diameter). Supposedly, as more TAGs were continuously being made, new rounds of LD formation and stabilization have to occur. How is MLDP transported to LDs? Unique peptides such as sequences that direct proteins to the ER or chloroplast have not been found for LDs in any cell type, despite that hundreds of LD proteins have been identified. Nevertheless we presume microtubule-mediated transport is likely involved (Hirokawa et al., 2009). Microtubules are a component of cytoskeleton, commonly comprised of α and β-tubulin, and they are known for LD fusion as well as LD trafficking by cytoplasmic motor proteins in animal cells (Gross et al., 2000; Bostrom et al., 2005; Shubeita et al., 2008). Both α and β-tubulin were shown to interact with MLDP (Online Supplemental Data Set 11) and have been found in Chlamydomonas LD proteomes (Moellering and Benning, 2010; Nguyen et al., 2011). In my hypothesis, minute droplets or vesicles carrying MLDP are secreted from the ER, and then the droplets are bound to microtubules through MLDP, and transported to the uncoated LDs that are attached to the chloroplast (Figure 4.9). Afterwards fusions occur and release the cargo. Microtubule units remained bound to the mature LDs through MLDP as demonstrated by the example of α-tubulin. In view of this, MLDP functionally resembles a perilipin homolog LSD2 which coordinates LD motion in Drosophila embryos by clustering with another LD protein Klar and the motor protein dynein that move along microtubules towards minus-end (Welte et al., 2005). This model suggests that in Chlamydomonas the main role of the

ER in LD formation is to provide decorated proteins and ER-originated polar lipids, and less in TAGs, consistent with the finding that the reduction of MLDP did not affect the total TAG content stored in the mature LDs.

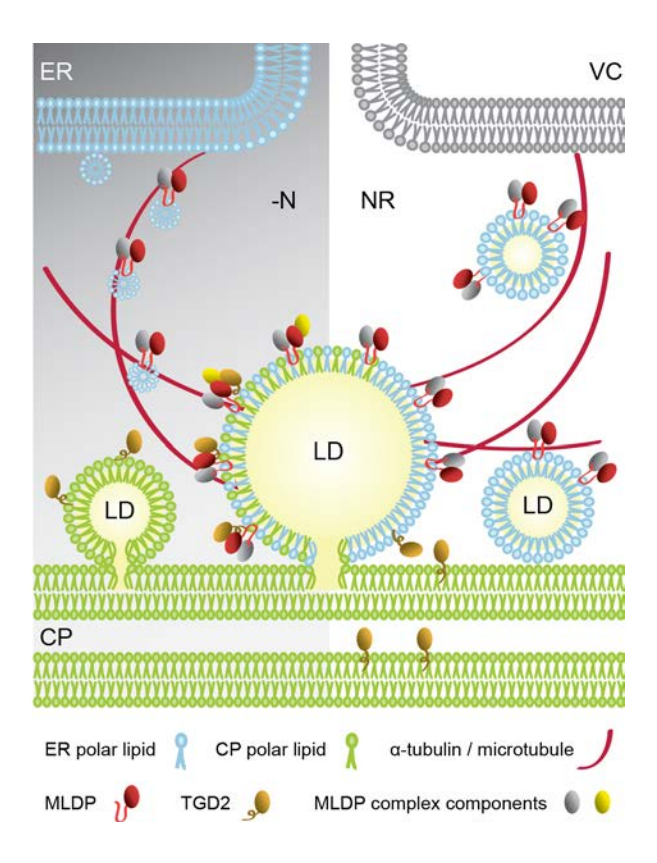


Figure 4.9. A model for lipid droplet formation and deformation. Small lipid droplet evolves from the chloroplast (CP) and thus allows natural diffusion of CP proteins to LD, such as TGD2. As the LD grows, MLDP complexes are transported to LD through microtubule to stabilize the mature LD. The complexity of MLDP complex increases when interacting with proteins preoccupied the LD. Upon N resupply, some proteins dissociate from MLDP complexes and move away from the LD. Small LD detaches from the CP and moves toward vacuole for final turnover.

Is MLDP part of a LD targeting mechanism? MLDP forms multi-order protein complexes on the mature LDs. These complexes or key components of the complexes could have been assembled on the ER, and then moved along microtubules to LDs through the mediation of MLDP. The proteins preexisted on the developing LDs, such as those from the chloroplast, then

interacted with the MLDP complexes after being transported, thus contributing to the complexity of the complexes (Figure 4.9). This might explain why TGD2 did not require MLDP to locate on LD in spite of a possible interaction. Thus far underlying mechanisms for LD protein targeting are poorly understood, with some insights derived from the Arf1/COPI machinery that secures the ER-LD connections for protein trafficking (Wilfling et al., 2014). Future investigation of the transport of MLDP will provide unique insights in photosynthetic cells.

The dynamics of LDs has direct impact on the reversibility of quiescence. TAGs stored in LDs are the main source of energy and membrane building blocks to fuel the regrowth. Therefore, when droplets fail to optimize the surface area-to-volume ratio it not only affects the efficacy of TAG turnover, which is most likely due to the limited accessibility to lipases, but also disturbs the timeliness of quiescence exit, and this situation could become exacerbated if the time in quiescence is extended. Close LD-to-chloroplast proximity was maintained during the first stage of LD mobilization, which might create a conduit for lipids (e.g. DGDG) and proteins (e.g. TGD2) to move back to chloroplast. CHT7 and MLDP appear to represent different classes of effectors for cellular quiescence, according to their respective mutant phenotypes. Once the cells of *cht7* enter quiescence (approximately 12 to 24 h of N deprivation), they are destined to experience severe challenges at the exit (Tsai et al., 2014). On the other hand, a defect in regrowth of the *MLDP* RNAi lines only became obvious in prolonged quiescence. In a sense, the depth of quiescence is manifested by the developmental stage of LDs.

REFERENCES

REFERENCES

- **Awai, K., Xu, C., Tamot, B., and Benning, C.** (2006). A phosphatidic acid-binding protein of the chloroplast inner envelope membrane involved in lipid trafficking. Proceedings of the National Academy of Sciences of the United States of America **103**, 10817-10822.
- **Benning, C., Huang, Z.H., and Gage, D.A.** (1995). Accumulation of a novel glycolipid and a betaine lipid in cells of Rhodobacter sphaeroides grown under phosphate limitation. Archives of biochemistry and biophysics **317**, 103-111.
- Bostrom, P., Rutberg, M., Ericsson, J., Holmdahl, P., Andersson, L., Frohman, M.A., Boren, J., and Olofsson, S.O. (2005). Cytosolic lipid droplets increase in size by microtubule-dependent complex formation. Arteriosclerosis, thrombosis, and vascular biology 25, 1945-1951.
- Fan, J., Andre, C., and Xu, C. (2011). A chloroplast pathway for the de novo biosynthesis of triacylglycerol in Chlamydomonas reinhardtii. FEBS letters **585**, 1985-1991.
- Fujimoto, Y., Itabe, H., Kinoshita, T., Homma, K.J., Onoduka, J., Mori, M., Yamaguchi, S., Makita, M., Higashi, Y., Yamashita, A., and Takano, T. (2007). Involvement of ACSL in local synthesis of neutral lipids in cytoplasmic lipid droplets in human hepatocyte HuH7. Journal of lipid research 48, 1280-1292.
- Goodson, C., Roth, R., Wang, Z.T., and Goodenough, U. (2011). Structural correlates of cytoplasmic and chloroplast lipid body synthesis in Chlamydomonas reinhardtii and stimulation of lipid body production with acetate boost. Eukaryotic cell 10, 1592-1606.
- Gross, S.P., Welte, M.A., Block, S.M., and Wieschaus, E.F. (2000). Dynein-mediated cargo transport in vivo. A switch controls travel distance. The Journal of cell biology **148**, 945-956.
- **Guixe, V., and Babul, J.** (1985). Effect of ATP on phosphofructokinase-2 from Escherichia coli. A mutant enzyme altered in the allosteric site for MgATP. The Journal of biological chemistry **260,** 11001-11005.
- Guo, Y., Walther, T.C., Rao, M., Stuurman, N., Goshima, G., Terayama, K., Wong, J.S., Vale, R.D., Walter, P., and Farese, R.V. (2008). Functional genomic screen reveals genes involved in lipid-droplet formation and utilization. Nature **453**, 657-661.
- **Harris, E.H.** (1989). Chlamydomonas Sourcebook. (New York: Academic Press: New York: Academic Press).
- **Hirokawa, N., Noda, Y., Tanaka, Y., and Niwa, S.** (2009). Kinesin superfamily motor proteins and intracellular transport. Nature reviews. Molecular cell biology **10,** 682-696.

- **Kikuchi, S., Hirohashi, T., and Nakai, M.** (2006). Characterization of the preprotein translocon at the outer envelope membrane of chloroplasts by blue native PAGE. Plant & cell physiology **47**, 363-371.
- Krahmer, N., Guo, Y., Wilfling, F., Hilger, M., Lingrell, S., Heger, K., Newman, H.W., Schmidt-Supprian, M., Vance, D.E., Mann, M., Farese, R.V., Jr., and Walther, T.C. (2011). Phosphatidylcholine synthesis for lipid droplet expansion is mediated by localized activation of CTP:phosphocholine cytidylyltransferase. Cell metabolism 14, 504-515.
- **Kuerschner, L., Moessinger, C., and Thiele, C.** (2008). Imaging of lipid biosynthesis: how a neutral lipid enters lipid droplets. Traffic **9,** 338-352.
- Kurat, C.F., Wolinski, H., Petschnigg, J., Kaluarachchi, S., Andrews, B., Natter, K., and Kohlwein, S.D. (2009). Cdk1/Cdc28-dependent activation of the major triacylglycerol lipase Tgl4 in yeast links lipolysis to cell-cycle progression. Molecular cell **33**, 53-63.
- Ladig, R., Sommer, M.S., Hahn, A., Leisegang, M.S., Papasotiriou, D.G., Ibrahim, M., Elkehal, R., Karas, M., Zickermann, V., Gutensohn, M., Brandt, U., Klosgen, R.B., and Schleiff, E. (2011). A high-definition native polyacrylamide gel electrophoresis system for the analysis of membrane complexes. The Plant journal: for cell and molecular biology 67, 181-194.
- Li, X., Moellering, E.R., Liu, B., Johnny, C., Fedewa, M., Sears, B.B., Kuo, M.H., and Benning, C. (2012). A galactoglycerolipid lipase is required for triacylglycerol accumulation and survival following nitrogen deprivation in Chlamydomonas reinhardtii. The Plant cell **24**, 4670-4686.
- **Martin, S., and Parton, R.G.** (2006). Lipid droplets: a unified view of a dynamic organelle. Nature reviews. Molecular cell biology **7,** 373-378.
- Moellering, E.R., and Benning, C. (2010). RNA interference silencing of a major lipid droplet protein affects lipid droplet size in Chlamydomonas reinhardtii. Eukaryotic cell 9, 97-106.
- Mussgnug, J.H., Wobbe, L., Elles, I., Claus, C., Hamilton, M., Fink, A., Kahmann, U., Kapazoglou, A., Mullineaux, C.W., Hippler, M., Nickelsen, J., Nixon, P.J., and Kruse, O. (2005). NAB1 is an RNA binding protein involved in the light-regulated differential expression of the light-harvesting antenna of Chlamydomonas reinhardtii. The Plant cell 17, 3409-3421.
- Nguyen, H.M., Baudet, M., Cuine, S., Adriano, J.M., Barthe, D., Billon, E., Bruley, C., Beisson, F., Peltier, G., Ferro, M., and Li-Beisson, Y. (2011). Proteomic profiling of oil bodies isolated from the unicellular green microalga Chlamydomonas reinhardtii: with focus on proteins involved in lipid metabolism. Proteomics 11, 4266-4273.
- **Poxleitner, M., Rogers, S.W., Lacey Samuels, A., Browse, J., and Rogers, J.C.** (2006). A role for caleosin in degradation of oil-body storage lipid during seed germination. The Plant journal: for cell and molecular biology **47**, 917-933.

- **Shevchenko, A., Wilm, M., Vorm, O., and Mann, M.** (1996). Mass spectrometric sequencing of proteins silver-stained polyacrylamide gels. Analytical chemistry **68**, 850-858.
- Shubeita, G.T., Tran, S.L., Xu, J., Vershinin, M., Cermelli, S., Cotton, S.L., Welte, M.A., and Gross, S.P. (2008). Consequences of motor copy number on the intracellular transport of kinesin-1-driven lipid droplets. Cell 135, 1098-1107.
- **Tauchi-Sato, K., Ozeki, S., Houjou, T., Taguchi, R., and Fujimoto, T.** (2002). The surface of lipid droplets is a phospholipid monolayer with a unique Fatty Acid composition. The Journal of biological chemistry **277**, 44507-44512.
- **Tsai, C.H., Warakanont, J., Takeuchi, T., Sears, B.B., Moellering, E.R., and Benning, C.** (2014). The protein Compromised Hydrolysis of Triacylglycerols 7 (CHT7) acts as a repressor of cellular quiescence in Chlamydomonas. Proceedings of the National Academy of Sciences of the United States of America **111,** 15833-15838.
- **Walther, T.C., and Farese, R.V., Jr.** (2012). Lipid droplets and cellular lipid metabolism. Annual review of biochemistry **81,** 687-714.
- **Welte, M.A.** (2007). Proteins under new management: lipid droplets deliver. Trends in cell biology **17**, 363-369.
- Welte, M.A., Cermelli, S., Griner, J., Viera, A., Guo, Y., Kim, D.H., Gindhart, J.G., and Gross, S.P. (2005). Regulation of lipid-droplet transport by the perilipin homolog LSD2. Current biology: CB 15, 1266-1275.
- Wilfling, F., Thiam, A.R., Olarte, M.J., Wang, J., Beck, R., Gould, T.J., Allgeyer, E.S., Pincet, F., Bewersdorf, J., Farese, R.V., Jr., and Walther, T.C. (2014). Arf1/COPI machinery acts directly on lipid droplets and enables their connection to the ER for protein targeting. eLife 3, e01607.

CHAPTER 5

Conclusions and Perspectives

Nature is the integration of environmental factors and biological complexity. In response to the dynamic environment all living cells need to make a resolute choice between division and quiescence to ensure the continuity of life; the decision made is then executed through cell cycle determinants and metabolic fluxes. Plants, due to their sessile nature, are inevitably exposed to more biotic and abiotic stresses that drive them to redirect resources from growth and cell division to respective defence mechanisms. However, how plant cells recover from the conditional, temporary cessation of growth/division has never been explored in detail. In this dissertation, I present progress towards the comprehensive understanding of cellular quiescence in photosynthetic eukaryotes, using *Chlamydomonas reinhardtii* as a reference model. Among the principle findings are the discovery of CHT7 as a repressor of cellular quiescence (Chapter 2), the CHT7 regulon and the transcriptional programs unique to N resupply (Chapter 3), and the aspects in which lipid droplets (LD) integrate with cellular metabolism to ensure the orderly progression from quiescence (Chapter 4). In this final chapter, I will discuss the unanswered questions and related future issues.

Regulatory processes by which CHT7 maintains the reversibility of quiescence

Current data point toward a role of CHT7 as a repressor of transcriptional programs associated with quiescence, based on which, I hypothesized that CHT7 secures the orderly and rapid exit from quiescence by resuppressing the induced responses. Nevertheless, comparative transcriptomics of N-resupplied conditions uncover a subset of the CHT7 regulon that differs from the gene regulation CHT7 imposes under normal N-replete growth, e.g. the tetrapyrrole pathway and peroxisomal redox homeostasis. As such, CHT7 may have additional, more direct impacts on quiescence exit. These speculations can only be addressed through the identification

of the *in vivo* chromatin binding sites for CHT7 or CHT7-containing complexes under different growth conditions. Integrative analysis of the transcriptome and chromatin binding data will help distinguish the genes that are primary or secondary targets of CHT7, as well as clarify the potential feedback regulations by metabolite levels.

Potential modification of CHT7 activity during the entry into quiescence

In yeast, the pathways that prevent the entry into quiescence (e.g. cAMP-PKA) must be deactivated during the transition; otherwise cells will not be able to survive (Uno et al., 1984; Shin et al., 1987). Since CHT7 also represses quiescence when cell cycle progresses regularly, it is reasonable to speculate that the activity of CHT7 is curtailed during quiescence. As a matter of fact, CHT7 seems dispensable during quiescence for its mutant remains viable even under extended period of N deprivation. Overexpression of CHT7 during quiescence using promoters responsive to N deprivation, such as that of MLDP or NIT1 (nitrate reductase 1), will help address this issue. The overexpression lines are expected to lose viability during quiescence.

Provided that CHT7 is indeed deactivated during quiescence, the question arises: By what means can this be done? The persistence of CHT7 and CHT7 complexes before, during, and after quiescence suggests that fluctuation of abundance or change of interacting partners likely is not part of the regulatory mechanism to regulate CHT7. Nuclear-cytoplasmic shuttling is neither the case as CHT7 remains in the nucleus throughout the quiescence cycle. A recently published global phosphoproteome of *C. reinhardtii* reports two phosphorylation sites of CHT7 during regular growth condition (Wang et al., 2014). Posttranslational modifications of CHT7 depending on the nutritional status of the cell may modulate its possible DNA binding

preferences. But again, the experimental evidence of posttranslational modification and whether it causes functional impact remain to be addressed.

The regulatory logic underlying the CHT7 and Rb complexes to enable transitions between quiescence and cell division

In Chlamydomonas, a protein complex containing orthologs of DP1, E2F1 and Rb/MAT3 is present in the nucleus throughout the cell cycle (Olson et al., 2010). Two lines of evidence let me hypothesize that CHT7 may be a part of larger regulatory complex that transiently associates with the Rb/MAT3 protein of Chlamydomonas. First, CXC domain proteins have been found in large regulatory protein complexes with Rb in animal cells (Sadasivam and DeCaprio, 2013; van den Heuvel and Dyson, 2008), and second, the mat3 mutant of Chlamydomonas not only shows a cell size defect, but like the cht7 mutant is also slow to respond when resupplied with N following N-deprivation (Armbrust et al., 1995). Precedence is set by the dynamic nature of CXC protein-containing complexes such as the human DREAM/LINC complex. Five proteins, including the CXC domain protein LIN54, form the complex core and remain together throughout the cell cycle (Litovchick et al., 2007). During quiescence, the core binds the Rb-like pocket protein p130, E2F4, and DP to repress cell cycle-dependent gene expression. This association is reversed upon phosphorylation of the core subunit LIN52, hence allowing the core to recruit the transcription factors BMYB and then FOXM1 to promoters with highest activity during the G2/M phases (Sadasivam and DeCaprio, 2013). Thus, multiple CHT7 containing complexes of varying abundance depending on the cellular conditions seem possible and will have to be explored in future to gain a more complete understanding of the function of CHT7.

The Rb/MAT3 protein of Chlamydomonas clearly has functions in addition to CHT7 such as in the control of cell size (Armbrust et al., 1995; Umen and Goodenough, 2001). At this time, no data describing global changes in transcriptional profiles for the *mat3* mutant under different N supply conditions are available that would allow me to compare possible regulatory networks governed by CHT7, Rb/MAT3 or both.

Functional interplay between CHT7 and other quiescence regulators

Recall that contrasting to yeast, rapamycin functions only to slow down, not to completely abolish the growth and division of Chlamydomonas. The *cht7* mutant is more sensitive to rapamycin treatment, judged by the even slower growth in the medium with rapamycin (Tsai et al., 2014), which means that both CHT7 and TOR pathways are negative regulators of quiescence and are not redundant. On the other hand, the cAMP-PKA signaling pathway, to the most part, might be redundant with CHT7 in regulating the exit from quiescence. It is reasonable to hypothesize functional interplay among pathways of CHT7, TOR, cAMP-PKA, and even Rb/MAT3, as illustrated in Figure 5.1. Hints about the role of CHT7 in the regulatory networks of quiescence can be obtained by characterizing the protein components of CHT7 complex. This comparative proteomic analysis should provide direct evidence, whether and to what extent the CHT7 complex shares common components with TOR, cAMP-PKA, and Rb complexes. Arguably, current knowledge does not even begin to accurately portray the multiple flavors of the N deprivation-induced quiescence or quiescence in general, and other key regulators doubtless remain to be uncovered.

Growth and division CHT7 — CHT7 PKA TOR — Rb Acquisition of features of

quiescence (e.g. LD formation)

Figure 5.1. Summary of pathways thought to control transitions between growth/division and quiescence in *Chlamydomonas reinhardtii.* The CHT7 and TOR pathways are thought to repress aspects of quiescence. CHT7, Rb, and PKA signaling are required for orderly transition out of quiescence. CHT7 and PKA pathways may share a certain level of redundancy.

Lipid droplets are important for the survival during quiescence and for the quiescence exit

The three constituents of LD—a TAG core, polar lipid monolayer, and associated proteins—give hints to the multiple roles of LD in cellular quiescence. In response to quiescence, Chlamydomonas cells deposit TAGs into LDs. On the one hand, it likely takes away the acetyl-CoA from TCA cycle so prevent it from producing chemical energy (i.e. ATP and NADH), as a way to restrict cell growth and division. On the other hand, it consumes the reducing power generated from the photosynthetic electron transport chain, which otherwise will cause lethal oxidative damage to the cell (Li et al., 2012). To be used as membrane building blocks in most organelles, polar lipids must undergo several steps of desaturation on their acyl chains. During quiescence, although large portion of polar lipids, thylakoid MGDG in particular, are degraded by autophagy, their polyunsaturated acyl chains are preserved safely. The proposed LDspecialized deacylation/reacylation cycle provides one such mechanism, which removes polyunsaturated fatty acids from the polar lipids imported to the LD and stores them in the TAG core. Supposedly, this process allows rapid reconstruction of organelle lipids without remaking the polyunsaturated fatty acids when conditions reverse. Autophagy also degrades proteins. It has been hypothesized and observed that LDs serve as temporary shelters for proteins under stress

conditions (Welte, 2007). In Chlamydomonas, LDs may function in a similar way, and MLDP may establish LD targeting through protein-protein interaction for proteins unable to anchor themselves on the lipid monolayer. Again, preservation of these proteins might be crucial for the rapid restoration of cellular status during the transit out of quiescence.

Biotechnological applications of cellular quiescence and lipid droplet biology

Microalgae accumulate valuable compounds under conditions adverse to growth. For example, nutrient starvation causes accumulation of TAGs but also induces cellular quiescence, characterized by the reversible cessation of growth. Among other factors, this inverse relationship between biomass productivity and TAG accumulation has long hampered efforts toward the efficient generation of biofuel feedstocks from microalgae. The discovery of a mutant and the corresponding protein CHT7 affecting the orderly transition of algal cells from quiescence to normal growth provides mechanistic insights to address this problem. For example, CHT7 acts as a repressor of cellular quiescence. It might be possible to use CHT7 to lower the expressivity of quiescence in the oil-producing conditions, and thus to engineer a high-biomass-high-oil algal strain. In addition, overexpression of CHT7 in the regular growth condition might delay the entry into stationary phase, and enhance the biomass capacity per growth unit.

LDs can also be readily isolated, thus facilitating harvesting of the desired compound. Knowledge of how complex enzyme arrays can be assembled on LDs allows the design of a synthetic intracellular platform that can produce both known secondary metabolites and novel compounds in unicellular photosynthetic organisms, as well as having the benefit that lipophilic toxic compounds can be sequestered into them and thus rendered harmless to the cell.

REFERENCES

REFERENCES

- **Armbrust, E.V., Ibrahim, A., and Goodenough, U.W.** (1995). A mating type-linked mutation that disrupts the uniparental inheritance of chloroplast DNA also disrupts cell-size control in Chlamydomonas. Molecular biology of the cell **6**, 1807-1818.
- Li, X., Moellering, E.R., Liu, B., Johnny, C., Fedewa, M., Sears, B.B., Kuo, M.H., and Benning, C. (2012). A galactoglycerolipid lipase is required for triacylglycerol accumulation and survival following nitrogen deprivation in Chlamydomonas reinhardtii. The Plant cell **24**, 4670-4686.
- Litovchick, L., Sadasivam, S., Florens, L., Zhu, X., Swanson, S.K., Velmurugan, S., Chen, R., Washburn, M.P., Liu, X.S., and DeCaprio, J.A. (2007). Evolutionarily conserved multisubunit RBL2/p130 and E2F4 protein complex represses human cell cycle-dependent genes in quiescence. Molecular cell **26**, 539-551.
- Olson, B.J., Oberholzer, M., Li, Y., Zones, J.M., Kohli, H.S., Bisova, K., Fang, S.C., Meisenhelder, J., Hunter, T., and Umen, J.G. (2010). Regulation of the Chlamydomonas cell cycle by a stable, chromatin-associated retinoblastoma tumor suppressor complex. The Plant cell 22, 3331-3347.
- **Sadasivam, S., and DeCaprio, J.A.** (2013). The DREAM complex: master coordinator of cell cycle-dependent gene expression. Nature reviews. Cancer **13**, 585-595.
- Shin, D.Y., Matsumoto, K., Iida, H., Uno, I., and Ishikawa, T. (1987). Heat shock response of Saccharomyces cerevisiae mutants altered in cyclic AMP-dependent protein phosphorylation. Molecular and cellular biology **7**, 244-250.
- **Tsai, C.H., Warakanont, J., Takeuchi, T., Sears, B.B., Moellering, E.R., and Benning, C.** (2014). The protein Compromised Hydrolysis of Triacylglycerols 7 (CHT7) acts as a repressor of cellular quiescence in Chlamydomonas. Proceedings of the National Academy of Sciences of the United States of America **111,** 15833-15838.
- Uno, I., Matsumoto, K., Adachi, K., and Ishikawa, T. (1984). Characterization of cyclic AMP-requiring yeast mutants altered in the catalytic subunit of protein kinase. The Journal of biological chemistry **259**, 12508-12513.
- van den Heuvel, S., and Dyson, N.J. (2008). Conserved functions of the pRB and E2F families. Nature reviews Molecular cell biology 9, 713-724.
- Wang, H., Gau, B., Slade, W.O., Juergens, M., Li, P., and Hicks, L.M. (2014). The global phosphoproteome of Chlamydomonas reinhardtii reveals complex organellar phosphorylation in the flagella and thylakoid membrane. Molecular & cellular proteomics: MCP 13, 2337-2353.

Welte, M.A. (2007). Proteins under new management: lipid droplets deliver. Trends in cell biology **17**, 363-369.